AUTOPHAGY: CIRCADIAN REGULATION AND ROLE IN NON-ALCOHOLIC FATTY LIVER DISEASE

by

Di Ma

A dissertation submitted in partial fulfillment
of the requirements for the degree of
Doctor of Philosophy
(Cell and Developmental Biology)
in the University of Michigan
2013

Doctoral committee:

Associate Professor Jiandie D. Lin, Chair
Assistant Professor Diane C. Fingar
Assistant Professor Ken Inoki
Professor Daniel J. Klionsky
Professor Alan R. Saltiel

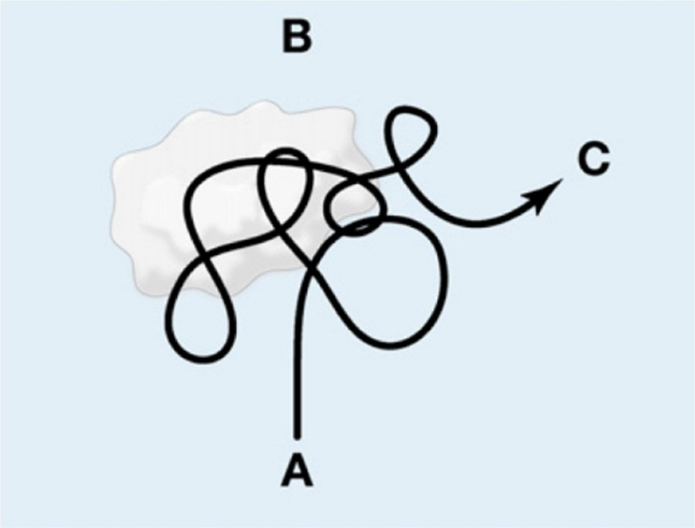

Figure reprinted from *How to choose a good scientific problem* by Dr. Uri Alon

2013

DEDICATION

To my parents and my husband,

for their unconditional love.

ACKNOWLEDGEMENTS

I would like to give my special thanks to my mentor Jiandie Lin and senior research staff Siming Li. Thank you for all your care and mentoring. In retrospect, joining Lin Lab is the second-best decision I have made in my life, with my marriage to Wenfeng being the best decision. In the past five years, I have been given enormous attention and resource to work on the projects that interest me. Besides science, I learnt to be open-minded and started to understand that when you set out from A to find B, most of time you may not find B, but a good researcher will find C. Moreover, your concern to my future career development is touching and rare. Sometimes, I feel that you two are my extended family members. I will be forever thankful for what you two have done to me and my husband Wenfeng.

I want to thank all my labmates for friendship and support. Thank you Matthew Molusky for generously contributing your time to our collaborative project. Thank you Crystal Rui for being such a fantastic research assistant. Thank you Zhuoxian Meng for the scientific discussion and solving all problems with broken machines. Thank you Guoxiao (Grace) Wang for making the lab a warm and wonderful place to stay. Thank you Lin Wang and Qi Yu for your technical support. Thank you Xuyun Zhao and Yuanyuan Xiao for sharing your expertise of research. Thank you Xiao-wei Chen (extended lab member) for the scientific discussion and generous contribution of enormous reagents. I would also like to thank the past lab members Carlos Hernandez, Fang Fang, Lei (Layla) Yu, Chang Liu, Fernanda Jiminez-Otero, Amanda A. Baker, Yaqiang Li, and Shengjuan Gu. I am very

thankful for your support.

I would like to thank my committee members for giving me guidance, suggestions, and sharing reagents over the years that make my projects move forward.

I also want to thank my collaborators Jun-Lin Guan, Fei Liu, Lin Chang, Yuqing (Eugene) Chen, Satchidananda Panda, Elizabeth K. Lucas, Rita M. Cowell. I could not finish my thesis without any of you. In addition, I want to thank Danming Tang, Yanzhuang Wang, Dotty Sorenson, Nathan Qi, Michelle Puchowicz, and Dana Lee for technical support, Jessica Schwartz, Marco Sandri, David Sabatini, Joseph Takahashi, Noboru Mizushima, and Gökhan S. Hotamisligil for reagents and animals, Elizabeth Speliotes, Geoffrey Murphy for scientific discussion. I would like to thank Shawn Xu and Daniel Goldman for taking me as rotation student, and Scott Barolo for taking me as teaching assistant.

Thank you to my friends in Neuroscience2007, CDB, and Chinese BioClub. Thanks to Ting Han, Ke Wang, and Jingya Wang for your support and suggestions. Thanks to my college friends Qiyan Mao, Wulan Deng, Bin He, He Bian, Xiaolei Su, Bo Zhou, Xu Zhou, Xiaodong Zhang, Xuan Geng, Qi Xiao, and Ji Zhang for your continuous support during my PhD life. May our friendship last forever.

TABLE OF CONTENTS

LIST OF TABLES

LIST OF FIGURES

CHAPTER 1 INTRODUCTION

1.1 Introduction

Metabolic syndrome is emerging as a global healthcare challenge. It is defined as a combination of multiple metabolic disorders, including obesity, fatty liver, type-2 diabetes, and dyslipidemia (Flier, 2004; Zimmet et al, 2001). According to data from Centers for Disease Control and Prevention (CDC) in 2009-2010, 35.9% of US adults aged 20 and over are obese. Similarly, data from World Health Organization indicates more than 1.4 billion (approximately 1/3) adults aged 20 and over in the world, were overweight in 2008. Besides, 10.7% of US adults 20 years and older was estimated to have diabetes during 2003-2006. The pessimistic estimation by International Diabetes Federation predicted that the total number of people worldwide with diabetes is expected to rise to 552 million with diabetes and an additional 398 million people at high risk by 2030. Metabolic syndrome significantly increases the risk for cardiovascular disease, stroke, cancer, liver cirrhosis, and kidney failure. It was estimated that over 20% adults aged 20 and over has uncontrolled high LDL cholesterol, which poses significant risks for cardiovascular disease and stroke. These facts underscore the importance of understanding the mechanisms of metabolic syndrome and developing novel therapeutic approaches.

One active area of metabolic research is to investigate the role of circadian clock disruption in the pathogenesis of metabolic disorders. Circadian clock is an intrinsic mechanism in the body to drive daily rhythms of biological processes. A variety of organisms evolve daily cycles of behaviors and physiological processes to adapt to the light-dark cycle on the earth. Maintaining normal circadian rhythm is essential for health. As such, individuals with chronic circadian disruption, e.g. night-shift workers, have a higher risk to develop cancer and metabolic diseases, such as obesity and diabetes (Antunes et al, 2010; Haus & Smolensky, 2012; Scheer et al, 2009; Spiegel et al, 1999).

Why is the circadian rhythm required to maintain metabolic homeostasis? One explanation is that the disruption of circadian rhythm in the brain leads to sleep disorders, which have been shown to associate with respiratory, cardiovascular, and metabolic dysfunctions (Taheri, 2004). However, emerging data in the past decades suggest that the biological clock can directly regulate metabolic pathways in peripheral tissues. It can control the expression of a large number of genes in a variety of pathways (Panda et al, 2002). Genetic perturbations of peripheral clocks in the liver, adipose tissues, or pancreas have been shown to cause hyperglycemia, obesity, and diabetes (Bass & Takahashi, 2010), characteristics of metabolic syndrome. However, it remains unclear how major metabolic processes are integrated with the peripheral clocks.

One such critical process is autophagy. Autophagy is a cellular process that delivers cargo to lysosomes for degradation and is critical for degradations of long lived proteins, pathogens, protein aggregates, organelles, and other cellular components. Several studies in the 1970s showed that autophagosome number varies throughout the day (Pfeifer, 1972; Pfeifer & Scheller, 1975; Pfeifer & Strauss, 1981; Reme & Sulser, 1977; Sachdeva & Thompson, 2008). Although the methodology for assessing autophagy activity has been improved during the past four decades, the circadian autophagy phenomenon has not been conclusively established. In addition, the underlying mechanisms remain largely unexplored. This thesis focuses on defining the biological regulation of circadian autophagy rhythms (Chapter 2). Moreover, I explored the role of autophagy in the regulation of hepatic lipid metabolism and the pathogenesis of non-alcoholic fatty liver disease (Chapter 3).

1.2 Mechanisms of metabolic regulation by circadian clock

1.2.1 The core components of mammalian clock

The circadian pacemaker consists of transcriptional activators and repressors assembled into auto-regulatory loops that generate cyclic transcriptional activation of target genes with a period of approximately 24 hours (Reppert & Weaver, 2001). Several core components of the clockwork have been identified, including transcriptional activators Bmal1 and Clock, and repressors Period (Per1, Per2, and Per3) and Cryptochrome (Cry1 and Cry2) (Fig. 1.1). Heterodimer of Bmal1 and Clock promotes the transcription of Period

and Cryptochrome, which instead form a complex to inhibit Bmal1/Clock's transcriptional activity (Etchegaray et al, 2003; Gekakis et al, 1998; Jin et al, 1999; Kume et al, 1999). In addition, the expression of Bmal1 is induced by the ROR/PGC-1α transcriptional activator complex while repressed by the Rev-erbα repressor complex (Cho et al, 2012; Liu et al, 2007; Preitner et al, 2002; Sato et al, 2004; Ueda et al, 2002). As the transcription of Rev-erbα is controlled by Bmal1/Clock, the inhibition of Rev-erbα on Bmal1 mRNA forms a second inhibitory feedback loop. The components of the clock regulatory network are further modulated by post-translational mechanisms such as phosphorylation, acetylation, deacetylation, and ubiquitination, which modulate the stability and/or activities of clock proteins (Lee et al, 2001; Mehra et al, 2009).

1.2.2 Reciprocal signaling between the clock and metabolic regulatory networks

Nutrient and energy metabolism is temporally organized in mammalian tissues to synchronize the storage and utilization of energy with light/dark cycles (Asher & Schibler, 2011; Green et al, 2008; Rutter et al, 2002). Circulating metabolites and hormones ebb and flow according to distinct diurnal patterns. In addition, rhythmic metabolic gene expression is prevalent in major metabolic tissues, such as the liver, adipose tissue, and skeletal muscle (Baggs & Hogenesch, 2010; Lowrey & Takahashi, 2004). As a consequence, the activities of many metabolic pathways are restricted not only to specific tissues in the body, but also to unique periods during the day. For example, hepatic gluconeogenesis, *de novo* lipogenesis, VLDL secretion, cholesterol biosynthesis, and xenobiotic detoxification are

precisely timed and reach their respective peaks at different time (Edwards et al, 1972; Gachon et al, 2006; Hems et al, 1975; Pan et al, 2010; Phillips & Berry, 1970). These observations form the basis for the emerging concept that nutrient and energy metabolism is tightly coupled to the timing cues in mammalian tissues. The temporal restriction of metabolic functions may provide advantages for organisms as they anticipate and synchronize their feeding and activity cycles to the environment.

The integration of clock and metabolism is mediated through reciprocal crosstalk between these two pathways (Fig. 1.2). Transcriptional profiling revealed that a large number of genes involved in different metabolic pathways are temporally controlled. For example, diurnal regulation of xenobiotic detoxification is mediated through the DBP/TEF/HLF family of transcription factors, all of which are clock targets (Gachon et al, 2006). Hepatic lipogenesis is rhythmically controlled by histone deacetylase 3 (HDAC3), which interacts with core clock component Rev-erbα (Feng et al, 2011). Recent chromatin-immunoprecipitation sequencing studies support the notion that many of rhythmically expressed genes are direct transcriptional targets of clock genes, such as Bmal1 and Rev-erbα (Feng et al, 2011; Koike et al, 2012; Rey et al, 2011).

Nuclear hormone receptors (NHR) are a family of transcriptional regulators that respond to diverse classes of metabolites and play important roles in metabolic regulation. The expression of many NHRs exhibits circadian regulation (Yang et al, 2006), some of which

also directly interact with clock proteins (Lamia et al, 2011; Schmutz et al, 2011), potentially synchronizing the expression of clock and metabolic genes. NHRs control the expression of target genes through recruiting coactivator and corepressor proteins that participate in chromatin remodeling. PGC-1α is a transcriptional coactivator initially found to stimulate mitochondrial biogenesis, fatty acid β-oxidation, and hepatic gluconeogenesis (Finck & Kelly, 2006; Lin et al, 2005). Recent work demonstrated that PGC-1α also directly regulates the expression of core clock genes and is indispensable for circadian pacemaker function (Liu et al, 2007). The expression of PGC-1α is diurnally regulated and it is modulated by casein kinase 1δ (CK1δ) (Li et al, 2011), an important regulator of the clock oscillator. Similarly, HDAC3 is recruited to Rev-erbα and regulates a program of metabolic and clock gene expression in the liver (Duez & Staels, 2009; Feng et al, 2011; Yin & Lazar, 2005). As such, the regulatory networks that govern clock and metabolism are highly intertwined and integrated.

Nutrient signaling also directly exerts its effects on the clock network. Sirtuin 1 (SIRT1) is an NAD^+-dependent histone deacetylase that deacetylates several clock proteins (Asher et al, 2008; Nakahata et al, 2008). Poly (ADP-ribose) polymerase 1 (PARP-1), an NAD^+-dependent ADP-ribosyltransferase, poly(ADP-ribosyl)ates Clock and alters the affinity of the Bmal1/Clock transcriptional complex to its target DNA (Asher et al, 2010). PARP-1 also regulates SIRT1 activity indirectly through its modulation of NAD^+ levels in the cell (Bai et al, 2011). In parallel, AMP-activated protein kinase (AMPK), a sensor for

cellular AMP/ATP and ADP/ATP ratios, phosphorylates clock proteins such as Cry and casein kinase 1ε (CK1ε) (Lamia et al, 2009; Um et al, 2007). Because intracellular NAD^+ levels and energy charge are regulated by nutrient status, these studies highlight a direct role for metabolic signaling in fine-tuning pacemaker function. The reciprocal crosstalk between the clock and metabolic regulatory networks potentially provides a real-time mechanism for synchronizing cellular metabolism with other biological processes.

1.2.3 Circadian clock and health

Clock perturbations have been associated with disease pathogenesis in humans, including sleep disorder, metabolic syndrome, cardiovascular disease, rheumatoid arthritis, and cancer (Copinschi et al, 2000; Green et al, 2008). Acute disruption of sleep rhythm in healthy individuals results in decreased insulin sensitivity while chronic circadian misalignment increases the risk for metabolic disorders in shift workers (Antunes et al, 2010; Scheer et al, 2009; Spiegel et al, 1999). Various clock-deficient animal models have been generated and characterized in recent years. Clock mutant mice develop symptoms reminiscent of metabolic syndrome, whereas pancreatic islets lacking clock have impaired glucose-stimulated insulin secretion (Marcheva et al, 2010; Turek et al, 2005). Disruption of liver clock perturbs hepatic gluconeogenesis, lipid metabolism, and bile acid homeostasis (Lamia et al, 2008; Le Martelot et al, 2009). Exposure of mice to inverted circadian environment has also been shown to cause excessive weight gain (Fonken et al, 2010). These studies underscore a potentially important role for circadian misalignment in

the pathogenesis of metabolic disorders in humans.

1.3 Role of autophagy in metabolic disease

1.3.1 Introduction on autophagy process

Autophagy literally means ‘self-eating’ and refers to a lysosome-dependent degradation process in the cell (Yang & Klionsky, 2010). Autophagy includes macroautophagy, microautophagy, and chaperone-mediated autophagy. This introduction focuses on macroautophagy and refers it as autophagy hereafter. Autophagy is initiated when double-membraned phagophore elongates, encloses cytosolic components, and fuses into autophagosome (Fig. 1.3). The autophagosome subsequently fuses with lysosome to form autolysosome, where degradation occurs. The identification of factors that carry out autophagy has led to discoveries of molecular framework for autophagic degradation and its physiological significance (He & Klionsky, 2009). These studies have led to the conclusion that autophagy is critical for cellular homeostasis and nutrient metabolism. Autophagy is induced in neonatal tissues and in adult tissues in response to starvation (Kuma et al, 2004; Mizushima et al, 2004). Defects in autophagy induction result in lower plasma glucose and amino acid levels and compromise survival during the early postnatal period. In parallel, autophagy is required for removing protein aggregates, damaged organelles, and certain pathogens (Mizushima & Komatsu, 2011). Autophagy deficiency has been implicated in the pathogenesis of various disease conditions, such as cancer,

diabetes, hepatic steatosis, skeletal myopathy and neurodegeneration (Ebato et al, 2008; Grumati et al, 2010; Jung et al, 2008; Komatsu et al, 2006; Liang et al, 1999; Singh et al, 2009).

1.3.2 Molecular control of autophagy

Genetic screens for yeast mutants that are defective in nonselective autophagy, pexophagy, and the cytoplasm to vacuole targeting pathway led to the discovery of more than 30 genes involved in autophagy (Harding et al, 1995; Titorenko et al, 1995; Tsukada & Ohsumi, 1993). Recent work has identified additional factors responsible for mitophagy (Kanki et al, 2009; Okamoto et al, 2009). In addition, genome-wide RNAi screens and proteomic studies in mammalian cells or genetic screens in multicellular organisms have further extended the list of autophagy related genes (Behrends et al, 2010; Lipinski et al, 2010; Orvedahl et al, 2011; Tian et al, 2010).

The core autophagy machinery includes five complexes: Ulk1-FIP200-Atg13 complex, Beclin 1-PI3-kinase-Atg14 complex, Atg9, Atg5-Atg12-Atg16L1 complex, and LC3-phosphatidylethanolamine (PE) conjugation complex (He & Klionsky, 2009; Kroemer et al, 2010). The Ulk1-FIP200-Atg13 complex regulates the initiation of autophagy. Under nutrition rich condition, the mammalian target of rapamycin (mTOR) kinase interacts with Ulk1-FIP200-Atg13 complex and phosphorylates Ulk1 and Atg13, thereby inhibiting Ulk1 kinase activity and autophagy induction (Alers et al, 2012; He &

Klionsky, 2009). AMPK is a sensor for cellular energy status and is able to phosphorylate Ulk1 in response to energy stress. In contrast to mTOR, AMPK phosphorylation increases the kinase activity of Ulk1 and promotes autophagy (Egan et al, 2011). Other factors in the autophagy pathway may serve as targets for nutritional regulation. For example, ATG7 can be degraded by calcium-dependent protease in the liver, resulting in impaired autophagy in obesity (Yang et al, 2010).

Transcriptional regulation of autophagy genes is emerging as an important mechanism in the control of cellular autophagy activity. Forkhead transcription factor O3 (FoxO3) induces the expression of several autophagy genes in skeletal myocytes, including LC3B, Gabarapl1, Bnip3, and Bnip3l (Mammucari et al, 2007; Zhao et al, 2007). The regulation of autophagic protein degradation by FoxO3 contributes to muscle atrophy induced by starvation. In addition to FoxO3, FoxO1 has also been reported to regulate autophagy in cardiomyocytes (Sengupta et al, 2009). An elegant recent study demonstrated that transcription factor TFEB controls a large number of genes involved in autophagy and lysosome dynamics in HeLa cells and is sufficient to promote lysosome biogenesis, autophagy, and lysosomal exocytosis (Medina et al, 2011; Sardiello et al, 2009; Settembre et al, 2011). Interestingly, TFEB is localized in cytosolic compartment under normal growth conditions and translocates into the nuclear in response to lysosomal stress or nutrient limitation. In addition, Seo et al. reported that SREBP-2, a key cholesterol metabolism regulator, can promote the expression of several autophagy genes (Seo et al,

2011).

1.3.3 Regulation of hepatic lipid metabolism

The liver regulates several major aspects of lipid metabolism, including lipogenesis, lipoprotein uptake and secretion, and fatty acid β-oxidation. These pathways are under the control of nutritional and hormonal signals.

In the lipogenesis process, the liver either undergoes *de novo* lipogenesis or synthesizes triglycerides using non-esterified fatty acids (NEFAs), which derives from absorption of intestine or lipolysis of white adipose tissue (WAT) (Lavoie & Gauthier, 2006). Under fasting condition, hormone-sensitive lipase (HSL) in WAT is activated and enhances the hydrolysis and release of fatty acids from adipocytes. These fatty acids are subsequently taken up by the liver for fatty acid β-oxidation or serve as a source for triglyceride synthesis. Hepatic lipogenic pathway is regulated by several transcriptional factors, including SREBP-1c, LXR, ChREBP, and PPARγ (Lavoie & Gauthier, 2006).

The synthesized triglyceride in the liver is either assembled as very low-density lipoprotein (VLDL) particles and secreted into circulation or stored as lipid droplets (LDs) in hepatocytes. VLDL assembly and secretion requires coordinated regulation of lipid synthesis, lipid transfer by microsomal triacylglycerol transfer protein (MTP), APOB assembly and trafficking through the secretory pathway. Currently, the mechanism for LD

formation is still elusive, except that LDs primarily arise from the ER (Walther & Farese, 2012). It is also unclear what determines the fate of triglycerides in the liver.

Fatty acid oxidation occurs in the liver and is strongly augmented during the fasting condition as a result of increased fatty acid influx and altered hormonal signals. The gene program of fat oxidation is regulated by several transcription factors and cofactors, including PPARα, AMPK, PGC-1α, and BAF60a (Lavoie & Gauthier, 2006; Li et al, 2008). The mobilization and oxidation of triglycerides in the lipid droplet was previously proposed to be catalyzed by cytosolic lipases, including adipose triglyceride lipase (ATGL), hormone-sensitive lipase (HSL), and monoacylglycerol lipase (MGLL) (Walther & Farese, 2012). Recent research pointed out that triglyceride in lipid droplet can also be mobilized through autophagy process (Singh et al, 2009). Singh et al. showed that lipid droplets co-localize with autophagic components, and inhibition of autophagy increases triglyceride content in the hepatocytes. This study raised a novel mechanism of lipolysis, which prompted further investigation.

1.3.4 The involvement of autophagy deficiency in diseases

Autophagy is a fundamental cellular process that has been implicated in various disease conditions (Mizushima & Komatsu, 2011). Beclin 1 deletion was found in patients with breast cancer, providing the first link between autophagy and tumorigenesis (Liang et al, 1999). Genetic deletion of Atg5 or Atg7 in the liver leads to the development of benign

liver adenomas, likely as a result of mitochondrial dysfunction, oxidative stress, and impaired DNA damage response (Takamura et al, 2011). The relationship between autophagy and cancer is likely complex as autophagy deficiency caused by FIP200 deletion suppresses mammary tumorigenesis (Wei et al, 2011). Because autophagy is critical for the removal of protein aggregates, defects in autophagy have also been linked to the pathogenesis of neurodegenerative disease, muscular dystrophy as well as liver damage caused by mutant α1-antitrypsin Z (Grumati et al, 2010; Hidvegi et al, 2010; Komatsu et al, 2006). Genetic and pharmacological activation of autophagy alleviates disease progression and severity in these animal models.

Potential involvements of autophagy in the pathogenesis of metabolic disease are drawing increasing attention. Autophagy activity appears to be reduced in the liver in diet-induced and genetic obese mice (Liu et al, 2009; Yang et al, 2010). Importantly, rescue of autophagy function in the liver restores hepatic insulin signaling and glucose homeostasis. Autophagy also plays a direct role in the hydrolysis of triglycerides stored in lipid droplets (Singh et al, 2009). In this case, lysosomal hydrolysis of triglycerides provides a previously unappreciated mechanism for lipid hydrolysis and fatty acid β-oxidation. As hepatic steatosis is a common feature in insulin resistant state, it is possible that defects in autophagy may contribute to excess triglyceride accumulation in the liver. The extent to which autophagy contributes to hepatic steatosis and potentially non-alcoholic steatohepatitis remains to be established. A second pathway that links autophagy to hepatic

lipid metabolism is through autophagy-mediated ApoB degradation. Under physiological conditions, a significant proportion of nascent ApoB-containing VLDL particles is diverted from the secretory pathway for autophagic degradation (Ohsaki et al, 2006). It is possible that defective clearance of these lipid-containing particles may further aggravate hepatic steatosis. Finally, autophagy is also required for adipogenesis, insulin secretion by β-cells as well as muscle metabolism and function (Ebato et al, 2008; Grumati et al, 2010; Jung et al, 2008; Zhang et al, 2009). The coupling of autophagy and metabolism is emerging as a novel factor underlying metabolic homeostasis and disease.

Fig. 1.1. The core clock machinery. The center of core clock machinery is Bmal1/Clock heterodimer, which is regulated by two arms of inhibition feedback loop. One arm of inhibition is from Per/Cry complex, which regulates the transcriptional activity of Bmal1/Clock complex. The second inhibitory arm centers on the Rev-erbα repressor complex, which negatively regulates Bmal1 expression. In contrast, Bmal1 expression is positively regulated by ROR/PGC-1α complex. RORE, Rev-erb/ROR responsive element.

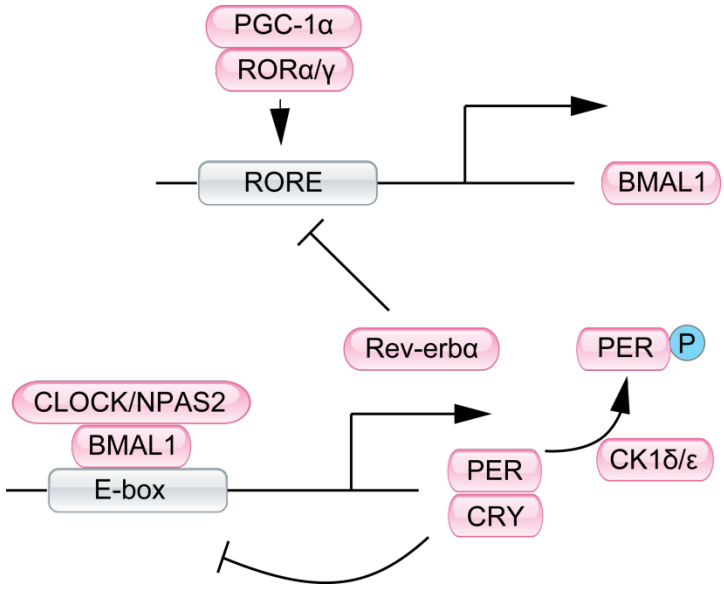

Fig. 1.2. Integration of clock and metabolism. Core components of the clock oscillator (pink) are gated by factors that relay nutrient and hormonal signals (green). In parallel, the timing cues are integrated with the metabolic regulatory network to drive rhythmic metabolic gene expression and output. GR, glucocorticoid receptor; RORE, Rev-erb/ROR responsive element.

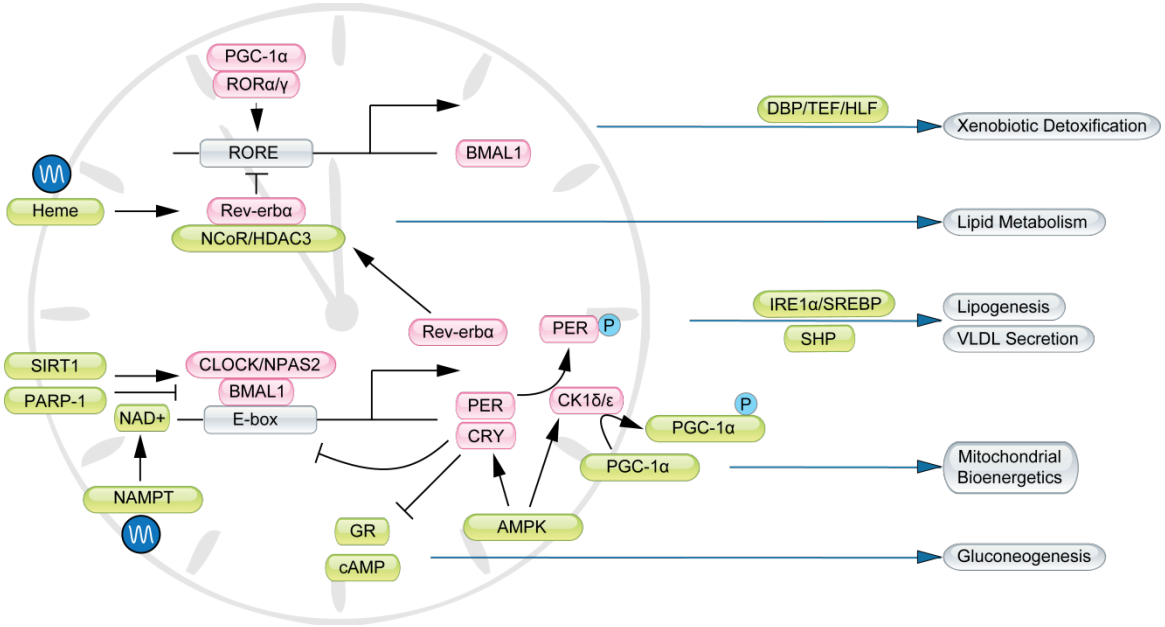

Fig. 1.3. Transcriptional and post-translational regulation of autophagy. Nutrient regulation of autophagy is mediated by mTOR and AMPK, which phosphorylate components of the ULK1-FIP200-ATG13 complex. The autophagy and lysosome gene program is controlled by several transcription factors, including FOXO, SREBP2 and TFEB. Autophagy is involved in the degradation of certain cellular components, such as protein aggregates, damaged or polarized mitochondria, peroxisomes, lipid droplets, and certain pathogens.

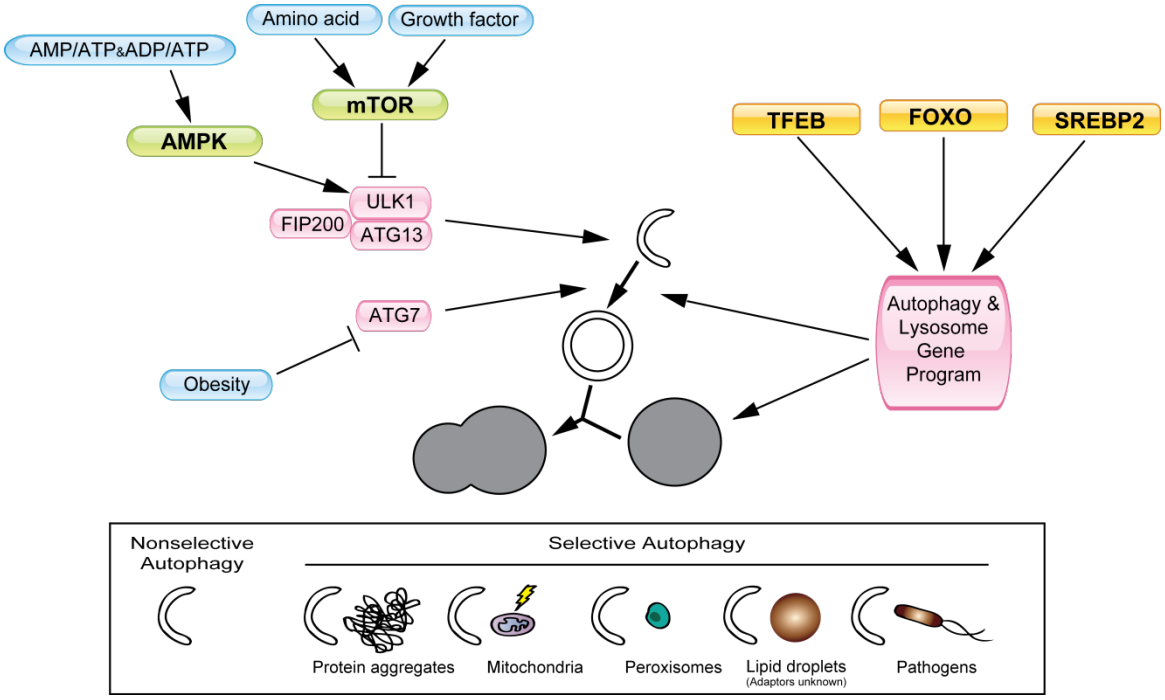

1.4 References

Alers S, Loffler AS, Wesselborg S, Stork B (2012) Role of AMPK-mTOR-Ulk1/2 in the Regulation of Autophagy: Cross Talk, Shortcuts, and Feedbacks. *Mol Cell Biol* **32:** 2-11

Antunes LC, Levandovski R, Dantas G, Caumo W, Hidalgo MP (2010) Obesity and shift work: chronobiological aspects. *Nutr Res Rev* **23:** 155-168

Asher G, Gatfield D, Stratmann M, Reinke H, Dibner C, Kreppel F, Mostoslavsky R, Alt FW, Schibler U (2008) SIRT1 regulates circadian clock gene expression through PER2 deacetylation. *Cell* **134:** 317-328

Asher G, Reinke H, Altmeyer M, Gutierrez-Arcelus M, Hottiger MO, Schibler U (2010) Poly(ADP-ribose) polymerase 1 participates in the phase entrainment of circadian clocks to feeding. *Cell* **142:** 943-953

Asher G, Schibler U (2011) Crosstalk between components of circadian and metabolic cycles in mammals. *Cell Metab* **13:** 125-137

Baggs JE, Hogenesch JB (2010) Genomics and systems approaches in the mammalian circadian clock. *Curr Opin Genet Dev* **20:** 581-587

Bai P, Canto C, Oudart H, Brunyanszki A, Cen Y, Thomas C, Yamamoto H, Huber A, Kiss B, Houtkooper RH, Schoonjans K, Schreiber V, Sauve AA, Menissier-de Murcia J, Auwerx J (2011) PARP-1 inhibition increases mitochondrial metabolism through SIRT1 activation. *Cell Metab* **13:** 461-468

Bass J, Takahashi J (2010) Circadian integration of metabolism and energetics. *Science* **330:** 1349-1354

Behrends C, Sowa ME, Gygi SP, Harper JW (2010) Network organization of the human autophagy system. *Nature* **466:** 68-76

Cho H, Zhao X, Hatori M, Yu RT, Barish GD, Lam MT, Chong LW, DiTacchio L, Atkins AR, Glass CK, Liddle C, Auwerx J, Downes M, Panda S, Evans RM (2012) Regulation of circadian behaviour and metabolism by REV-ERB-alpha and REV-ERB-beta. *Nature* **485:** 123-127

Copinschi G, Spiegel K, Leproult R, Van Cauter E (2000) Pathophysiology of human circadian rhythms. *Novartis Found Symp* **227:** 143-157; discussion 157-162

Duez H, Staels B (2009) Rev-erb-alpha: an integrator of circadian rhythms and metabolism.

J Appl Physiol **107:** 1972-1980

Ebato C, Uchida T, Arakawa M, Komatsu M, Ueno T, Komiya K, Azuma K, Hirose T, Tanaka K, Kominami E, Kawamori R, Fujitani Y, Watada H (2008) Autophagy is important in islet homeostasis and compensatory increase of beta cell mass in response to high-fat diet. *Cell Metab* **8:** 325-332

Edwards PA, Muroya H, Gould RG (1972) In vivo demonstration of the circadian thythm of cholesterol biosynthesis in the liver and intestine of the rat. *J Lipid Res* **13:** 396-401

Egan DF, Shackelford DB, Mihaylova MM, Gelino S, Kohnz RA, Mair W, Vasquez DS, Joshi A, Gwinn DM, Taylor R, Asara JM, Fitzpatrick J, Dillin A, Viollet B, Kundu M, Hansen M, Shaw RJ (2011) Phosphorylation of ULK1 (hATG1) by AMP-activated protein kinase connects energy sensing to mitophagy. *Science* **331:** 456-461

Etchegaray JP, Lee C, Wade PA, Reppert SM (2003) Rhythmic histone acetylation underlies transcription in the mammalian circadian clock. *Nature* **421:** 177-182

Feng D, Liu T, Sun Z, Bugge A, Mullican SE, Alenghat T, Liu XS, Lazar MA (2011) A circadian rhythm orchestrated by histone deacetylase 3 controls hepatic lipid metabolism. *Science* **331:** 1315-1319

Finck BN, Kelly DP (2006) PGC-1 coactivators: inducible regulators of energy metabolism in health and disease. *J Clin Invest* **116:** 615-622

Flier J (2004) Obesity wars: molecular progress confronts an expanding epidemic. *Cell* **116:** 337-350

Fonken LK, Workman JL, Walton JC, Weil ZM, Morris JS, Haim A, Nelson RJ (2010) Light at night increases body mass by shifting the time of food intake. *Proc Natl Acad Sci U S A* **107:** 18664-18669

Gachon F, Olela FF, Schaad O, Descombes P, Schibler U (2006) The circadian PAR-domain basic leucine zipper transcription factors DBP, TEF, and HLF modulate basal and inducible xenobiotic detoxification. *Cell Metab* **4:** 25-36

Gekakis N, Staknis D, Nguyen HB, Davis FC, Wilsbacher LD, King DP, Takahashi JS, Weitz CJ (1998) Role of the CLOCK protein in the mammalian circadian mechanism. *Science* **280:** 1564-1569

Green CB, Takahashi JS, Bass J (2008) The meter of metabolism. *Cell* **134:** 728-742

Grumati P, Coletto L, Sabatelli P, Cescon M, Angelin A, Bertaggia E, Blaauw B, Urciuolo A, Tiepolo T, Merlini L, Maraldi NM, Bernardi P, Sandri M, Bonaldo P (2010) Autophagy is defective in collagen VI muscular dystrophies, and its reactivation rescues myofiber degeneration. *Nat Med* **16:** 1313-1320

Harding TM, Morano KA, Scott SV, Klionsky DJ (1995) Isolation and characterization of yeast mutants in the cytoplasm to vacuole protein targeting pathway. *J Cell Biol* **131:** 591-602

Haus E, Smolensky M (2012) Shift work and cancer risk: Potential mechanistic roles of circadian disruption, light at night, and sleep deprivation. *Sleep medicine reviews*

He C, Klionsky DJ (2009) Regulation mechanisms and signaling pathways of autophagy. *Annu Rev Genet* **43:** 67-93

Hems DA, Rath EA, Verrinder TR (1975) Fatty acid synthesis in liver and adipose tissue of normal and genetically obese (ob/ob) mice during the 24-hour cycle. *Biochem J* **150:** 167-173

Hidvegi T, Ewing M, Hale P, Dippold C, Beckett C, Kemp C, Maurice N, Mukherjee A, Goldbach C, Watkins S, Michalopoulos G, Perlmutter D (2010) An autophagy-enhancing drug promotes degradation of mutant alpha1-antitrypsin Z and reduces hepatic fibrosis. *Science* **329:** 229-232

Jin X, Shearman LP, Weaver DR, Zylka MJ, de Vries GJ, Reppert SM (1999) A molecular mechanism regulating rhythmic output from the suprachiasmatic circadian clock. *Cell* **96:** 57-68

Jung HS, Chung KW, Won Kim J, Kim J, Komatsu M, Tanaka K, Nguyen YH, Kang TM, Yoon KH, Kim JW, Jeong YT, Han MS, Lee MK, Kim KW, Shin J, Lee MS (2008) Loss of autophagy diminishes pancreatic beta cell mass and function with resultant hyperglycemia. *Cell Metab* **8:** 318-324

Kanki T, Wang K, Baba M, Bartholomew CR, Lynch-Day MA, Du Z, Geng J, Mao K, Yang Z, Yen WL, Klionsky DJ (2009) A genomic screen for yeast mutants defective in selective mitochondria autophagy. *Mol Biol Cell* **20:** 4730-4738

Koike N, Yoo SH, Huang HC, Kumar V, Lee C, Kim TK, Takahashi JS (2012) Transcriptional architecture and chromatin landscape of the core circadian clock in mammals. *Science* **338:** 349-354

Komatsu M, Waguri S, Chiba T, Murata S, Iwata J, Tanida I, Ueno T, Koike M, Uchiyama

Y, Kominami E, Tanaka K (2006) Loss of autophagy in the central nervous system causes neurodegeneration in mice. *Nature* **441:** 880-884

Kroemer G, Marino G, Levine B (2010) Autophagy and the integrated stress response. *Mol Cell* **40:** 280-293

Kuma A, Hatano M, Matsui M, Yamamoto A, Nakaya H, Yoshimori T, Ohsumi Y, Tokuhisa T, Mizushima N (2004) The role of autophagy during the early neonatal starvation period. *Nature* **432:** 1032-1036

Kume K, Zylka MJ, Sriram S, Shearman LP, Weaver DR, Jin X, Maywood ES, Hastings MH, Reppert SM (1999) mCRY1 and mCRY2 are essential components of the negative limb of the circadian clock feedback loop. *Cell* **98:** 193-205

Lamia KA, Papp SJ, Yu RT, Barish GD, Uhlenhaut NH, Jonker JW, Downes M, Evans RM (2011) Cryptochromes mediate rhythmic repression of the glucocorticoid receptor. *Nature*

Lamia KA, Sachdeva UM, DiTacchio L, Williams EC, Alvarez JG, Egan DF, Vasquez DS, Juguilon H, Panda S, Shaw RJ, Thompson CB, Evans RM (2009) AMPK regulates the circadian clock by cryptochrome phosphorylation and degradation. *Science* **326:** 437-440

Lamia KA, Storch KF, Weitz CJ (2008) Physiological significance of a peripheral tissue circadian clock. *Proc Natl Acad Sci U S A* **105:** 15172-15177

Lavoie JM, Gauthier MS (2006) Regulation of fat metabolism in the liver: link to non-alcoholic hepatic steatosis and impact of physical exercise. *Cellular and molecular life sciences* **63:** 1393-1409

Le Martelot G, Claudel T, Gatfield D, Schaad O, Kornmann B, Sasso GL, Moschetta A, Schibler U (2009) REV-ERBalpha participates in circadian SREBP signaling and bile acid homeostasis. *PLoS Biol* **7:** e1000181

Lee C, Etchegaray JP, Cagampang FR, Loudon AS, Reppert SM (2001) Posttranslational mechanisms regulate the mammalian circadian clock. *Cell* **107:** 855-867

Li S, Chen XW, Yu L, Saltiel AR, Lin JD (2011) Circadian Metabolic Regulation through Crosstalk between Casein Kinase 1delta and Transcriptional Coactivator PGC-1alpha. *Mol Endocrinol* **25:** 2084-2093

Li S, Liu C, Li N, Hao T, Han T, Hill DE, Vidal M, Lin JD (2008) Genome-wide coactivation analysis of PGC-1alpha identifies BAF60a as a regulator of hepatic lipid metabolism. *Cell Metab* **8:** 105-117

Liang XH, Jackson S, Seaman M, Brown K, Kempkes B, Hibshoosh H, Levine B (1999) Induction of autophagy and inhibition of tumorigenesis by beclin 1. *Nature* **402:** 672-676

Lin J, Handschin C, Spiegelman BM (2005) Metabolic control through the PGC-1 family of transcription coactivators. *Cell Metab* **1:** 361-370

Lipinski MM, Hoffman G, Ng A, Zhou W, Py BF, Hsu E, Liu X, Eisenberg J, Liu J, Blenis J, Xavier RJ, Yuan J (2010) A genome-wide siRNA screen reveals multiple mTORC1 independent signaling pathways regulating autophagy under normal nutritional conditions. *Dev Cell* **18:** 1041-1052

Liu C, Li S, Liu T, Borjigin J, Lin JD (2007) Transcriptional coactivator PGC-1alpha integrates the mammalian clock and energy metabolism. *Nature* **447:** 477-481

Liu HY, Han J, Cao SY, Hong T, Zhuo D, Shi J, Liu Z, Cao W (2009) Hepatic autophagy is suppressed in the presence of insulin resistance and hyperinsulinemia: inhibition of FoxO1-dependent expression of key autophagy genes by insulin. *J Biol Chem* **284:** 31484-31492

Lowrey PL, Takahashi JS (2004) Mammalian circadian biology: elucidating genome-wide levels of temporal organization. *Annu Rev Genomics Hum Genet* **5:** 407-441

Mammucari C, Milan G, Romanello V, Masiero E, Rudolf R, Del PP, Burden SJ, Di LR, Sandri C, Zhao J, Goldberg AL, Schiaffino S, Sandri M (2007) FoxO3 controls autophagy in skeletal muscle in vivo. *Cell Metab* **6:** 458-471

Marcheva B, Ramsey KM, Buhr ED, Kobayashi Y, Su H, Ko CH, Ivanova G, Omura C, Mo S, Vitaterna MH, Lopez JP, Philipson LH, Bradfield CA, Crosby SD, JeBailey L, Wang X, Takahashi JS, Bass J (2010) Disruption of the clock components CLOCK and BMAL1 leads to hypoinsulinaemia and diabetes. *Nature* **466:** 627-631

Medina DL, Fraldi A, Bouche V, Annunziata F, Mansueto G, Spampanato C, Puri C, Pignata A, Martina JA, Sardiello M, Palmieri M, Polishchuk R, Puertollano R, Ballabio A (2011) Transcriptional activation of lysosomal exocytosis promotes cellular clearance. *Dev Cell* **21:** 421-430

Mehra A, Baker CL, Loros JJ, Dunlap JC (2009) Post-translational modifications in circadian rhythms. *Trends Biochem Sci* **34:** 483-490

Mizushima N, Komatsu M (2011) Autophagy: renovation of cells and tissues. *Cell* **147:** 728-741

Mizushima N, Yamamoto A, Matsui M, Yoshimori T, Ohsumi Y (2004) In vivo analysis of autophagy in response to nutrient starvation using transgenic mice expressing a fluorescent autophagosome marker. *Mol Biol Cell* **15:** 1101-1111

Nakahata Y, Kaluzova M, Grimaldi B, Sahar S, Hirayama J, Chen D, Guarente LP, Sassone-Corsi P (2008) The NAD+-dependent deacetylase SIRT1 modulates CLOCK-mediated chromatin remodeling and circadian control. *Cell* **134:** 329-340

Ohsaki Y, Cheng J, Fujita A, Tokumoto T, Fujimoto T (2006) Cytoplasmic lipid droplets are sites of convergence of proteasomal and autophagic degradation of apolipoprotein B. *Mol Biol Cell* **17:** 2674-2683

Okamoto K, Kondo-Okamoto N, Ohsumi Y (2009) Mitochondria-anchored receptor Atg32 mediates degradation of mitochondria via selective autophagy. *Dev Cell* **17:** 87-97

Orvedahl A, Sumpter R, Jr., Xiao G, Ng A, Zou Z, Tang Y, Narimatsu M, Gilpin C, Sun Q, Roth M, Forst CV, Wrana JL, Zhang YE, Luby-Phelps K, Xavier RJ, Xie Y, Levine B (2011) Image-based genome-wide siRNA screen identifies selective autophagy factors. *Nature* **480:** 113-117

Pan X, Zhang Y, Wang L, Hussain MM (2010) Diurnal regulation of MTP and plasma triglyceride by CLOCK is mediated by SHP. *Cell Metab* **12:** 174-186

Panda S, Antoch MP, Miller BH, Su AI, Schook AB, Straume M, Schultz PG, Kay SA, Takahashi JS, Hogenesch JB (2002) Coordinated transcription of key pathways in the mouse by the circadian clock. *Cell* **109:** 307-320

Pfeifer U (1972) Inverted diurnal rhythm of cellular autophagy in liver cells of rats fed a single daily meal. *Virchows Arch B Cell Pathol* **10:** 1-3

Pfeifer U, Scheller H (1975) A morphometric study of cellular autophagy including diurnal variations in kidney tubules of normal rats. *J Cell Biol* **64:** 608-621

Pfeifer U, Strauss P (1981) Autophagic vacuoles in heart muscle and liver. A comparative morphometric study including circadian variations in meal-fed rats. *J Mol Cell Cardiol* **13:** 37-49

Phillips LJ, Berry LJ (1970) Circadian rhythm of mouse liver phosphoenolpyruvate carboxykinase. *Am J Physiol* **218:** 1440-1444

Preitner N, Damiola F, Lopez-Molina L, Zakany J, Duboule D, Albrecht U, Schibler U

(2002) The orphan nuclear receptor REV-ERBalpha controls circadian transcription within the positive limb of the mammalian circadian oscillator. *Cell* **110:** 251-260

Reme CE, Sulser M (1977) Diurnal variation of autophagy in rod visual cells in the rat. *AlbrechtVonGraefes ArchKlinExpOphthalmol* **203:** 261-270

Reppert SM, Weaver DR (2001) Molecular analysis of mammalian circadian rhythms. *Annu Rev Physiol* **63:** 647-676

Rey G, Cesbron F, Rougemont J, Reinke H, Brunner M, Naef F (2011) Genome-wide and phase-specific DNA-binding rhythms of BMAL1 control circadian output functions in mouse liver. *PLoS Biol* **9:** e1000595

Rutter J, Reick M, McKnight SL (2002) Metabolism and the control of circadian rhythms. *Annu Rev Biochem* **71:** 307-331

Sachdeva UM, Thompson CB (2008) Diurnal rhythms of autophagy: implications for cell biology and human disease. *Autophagy* **4:** 581-589

Sardiello M, Palmieri M, di Ronza A, Medina DL, Valenza M, Gennarino VA, Di Malta C, Donaudy F, Embrione V, Polishchuk RS, Banfi S, Parenti G, Cattaneo E, Ballabio A (2009) A gene network regulating lysosomal biogenesis and function. *Science* **325:** 473-477

Sato TK, Panda S, Miraglia LJ, Reyes TM, Rudic RD, McNamara P, Naik KA, FitzGerald GA, Kay SA, Hogenesch JB (2004) A functional genomics strategy reveals Rora as a component of the mammalian circadian clock. *Neuron* **43:** 527-537

Scheer FA, Hilton MF, Mantzoros CS, Shea SA (2009) Adverse metabolic and cardiovascular consequences of circadian misalignment. *Proc Natl Acad Sci U S A* **106:** 4453-4458

Schmutz I, Ripperger JA, Baeriswyl-Aebischer S, Albrecht U (2011) The mammalian clock component PERIOD2 coordinates circadian output by interaction with nuclear receptors. *Genes Dev* **24:** 345-357

Sengupta A, Molkentin JD, Yutzey KE (2009) FoxO transcription factors promote autophagy in cardiomyocytes. *J Biol Chem* **284:** 28319-28331

Seo Y-K, Jeon T-I, Chong H, Biesinger J, Xie X, Osborne T (2011) Genome-wide localization of SREBP-2 in hepatic chromatin predicts a role in autophagy. *Cell Metab* **13:** 367-375

Settembre C, Di Malta C, Polito VA, Garcia Arencibia M, Vetrini F, Erdin S, Erdin SU, Huynh T, Medina D, Colella P, Sardiello M, Rubinsztein DC, Ballabio A (2011) TFEB links autophagy to lysosomal biogenesis. *Science* **332:** 1429-1433

Singh R, Kaushik S, Wang Y, Xiang Y, Novak I, Komatsu M, Tanaka K, Cuervo A, Czaja M (2009) Autophagy regulates lipid metabolism. *Nature* **458:** 1131-1135

Spiegel K, Leproult R, Van Cauter E (1999) Impact of sleep debt on metabolic and endocrine function. *Lancet* **354:** 1435-1439

Taheri S (2004) The genetics of sleep disorders. *Minerva medica* **95:** 203-212

Takamura A, Komatsu M, Hara T, Sakamoto A, Kishi C, Waguri S, Eishi Y, Hino O, Tanaka K, Mizushima N (2011) Autophagy-deficient mice develop multiple liver tumors. *Genes Dev* **25:** 795-800

Tian Y, Li Z, Hu W, Ren H, Tian E, Zhao Y, Lu Q, Huang X, Yang P, Li X, Wang X, Kovacs AL, Yu L, Zhang H (2010) C. elegans screen identifies autophagy genes specific to multicellular organisms. *Cell* **141:** 1042-1055

Titorenko VI, Keizer I, Harder W, Veenhuis M (1995) Isolation and characterization of mutants impaired in the selective degradation of peroxisomes in the yeast Hansenula polymorpha. *J Bacteriol* **177:** 357-363

Tsukada M, Ohsumi Y (1993) Isolation and characterization of autophagy-defective mutants of Saccharomyces cerevisiae. *FEBS Lett* **333:** 169-174

Turek FW, Joshu C, Kohsaka A, Lin E, Ivanova G, McDearmon E, Laposky A, Losee-Olson S, Easton A, Jensen DR, Eckel RH, Takahashi JS, Bass J (2005) Obesity and metabolic syndrome in circadian Clock mutant mice. *Science* **308:** 1043-1045

Ueda HR, Chen W, Adachi A, Wakamatsu H, Hayashi S, Takasugi T, Nagano M, Nakahama K, Suzuki Y, Sugano S, Iino M, Shigeyoshi Y, Hashimoto S (2002) A transcription factor response element for gene expression during circadian night. *Nature* **418:** 534-539

Um JH, Yang S, Yamazaki S, Kang H, Viollet B, Foretz M, Chung JH (2007) Activation of 5'-AMP-activated kinase with diabetes drug metformin induces casein kinase Iepsilon (CKIepsilon)-dependent degradation of clock protein mPer2. *J Biol Chem* **282:** 20794-20798

Walther T, Farese R (2012) Lipid droplets and cellular lipid metabolism. *Annu Rev*

Biochem **81:** 687-714

Wei H, Wei S, Gan B, Peng X, Zou W, Guan JL (2011) Suppression of autophagy by FIP200 deletion inhibits mammary tumorigenesis. *Genes Dev* **25:** 1510-1527

Yang L, Li P, Fu S, Calay E, Hotamisligil G (2010) Defective hepatic autophagy in obesity promotes ER stress and causes insulin resistance. *Cell Metab* **11:** 467-478

Yang X, Downes M, Yu RT, Bookout AL, He W, Straume M, Mangelsdorf DJ, Evans RM (2006) Nuclear receptor expression links the circadian clock to metabolism. *Cell* **126:** 801-810

Yang Z, Klionsky D (2010) Eaten alive: a history of macroautophagy. *Nature cell biology* **12:** 814-822

Yin L, Lazar MA (2005) The orphan nuclear receptor Rev-erbalpha recruits the N-CoR/histone deacetylase 3 corepressor to regulate the circadian Bmal1 gene. *Mol Endocrinol* **19:** 1452-1459

Zhang Y, Goldman S, Baerga R, Zhao Y, Komatsu M, Jin S (2009) Adipose-specific deletion of autophagy-related gene 7 (atg7) in mice reveals a role in adipogenesis. *Proc Natl Acad Sci U S A* **106:** 19860-19865

Zhao J, Brault JJ, Schild A, Cao P, Sandri M, Schiaffino S, Lecker SH, Goldberg AL (2007) FoxO3 coordinately activates protein degradation by the autophagic/lysosomal and proteasomal pathways in atrophying muscle cells. *Cell Metab* **6:** 472-483

Zimmet P, Alberti K, Shaw J (2001) Global and societal implications of the diabetes epidemic. *Nature* **414:** 782-787

CHAPTER 2 TEMPORAL ORCHESTRATION OF CIRCADIAN AUTOPHAGY RHYTHM BY C/EBPB

2.1 Abstract

Temporal organization of tissue metabolism is important for maintaining nutrient and energy homeostasis in mammals. Autophagy is a conserved cellular pathway that is activated in response to nutrient limitation, resulting in the degradation of cytoplasmic components and the release of amino acids and other nutrients. Here we show that autophagy exhibits robust circadian rhythm in mouse liver, which is accompanied by cyclic induction of genes involved in various steps of autophagy. Functional analyses of transcription factors and cofactors identified C/EBPβ as a potent activator of autophagy. C/EBPβ is rhythmically expressed in the liver and is regulated by both circadian and nutritional signals. In cultured primary hepatocytes, C/EBPβ stimulates the program of autophagy gene expression and is sufficient to activate autophagic protein degradation. Adenoviral-mediated RNAi knockdown of C/EBPβ *in vivo* abolishes diurnal autophagy rhythm in the liver. Further, circadian regulation of C/EBPβ and autophagy is disrupted in mice lacking a functional liver clock. We have thus identified C/EBPβ as a key factor that links autophagy to biological clock and maintains nutrient homeostasis throughout light/dark cycles.

2.2 Introduction

Organisms evolve diverse strategies to adapt their nutrient and energy metabolisms to the light/dark cycles on the earth. In mammals, the circadian clocks coordinate diurnal rhythms of behavior and physiology, including major pathways of nutrient and energy metabolism (Green et al, 2008; Rutter et al, 2002; Wijnen & Young, 2006). These pacemakers are self-sustained oscillators in the brain and peripheral tissues, which synchronize their downstream transcriptional output (Panda et al, 2002; Storch et al, 2002; Ueda et al, 2002). Clocks in different tissues can be entrained by distinct external cues, such as light, temperature and nutritional signals. Genetic disruption of components in mammalian clock results in metabolic disorders, including perturbations in lipid and glucose homeostasis (Lamia et al, 2008; Rudic et al, 2004; Turek et al, 2005). In humans, disruption of circadian rhythm has been associated with increased risk for obesity and cardiovascular disease (Leproult & Van Cauter, 2010).

Autophagy is a cellular process that delivers cytosolic components to lysosomes for degradation (Levine & Kroemer, 2008; Mizushima et al, 2008; Yang & Klionsky, 2010). In response to metabolic stress, such as starvation, autophagy is highly induced to degrade glycogen, lipid droplets and cytosolic components to provide a source of nutrients and metabolic fuel (Rabinowitz & White, 2010). The essential role of autophagy is underscored by neonatal lethality in pups lacking ATG5, an essential factor in the autophagy pathway

(Kuma et al, 2004). In addition, autophagy plays an important role in removing protein aggregates and damaged organelles (Ebato et al, 2008; Jung et al, 2008; Komatsu et al, 2006; Komatsu et al, 2007; Komatsu et al, 2005). Genetic disruption of autophagy genes results in the accumulation of ubiquitinated protein aggregates and abnormal organelles in hepatocytes, neurons and pancreatic β-cells. Recent studies have also implicated autophagy in the control of hepatic lipid metabolism and the development of insulin resistance (Singh et al, 2009; Yang et al, 2010).

Electron microscopy studies conducted in 1970s have demonstrated that the abundance of autophagic vacuoles varies according to the time of day in several rat tissues (Pfeifer, 1972; Pfeifer & Scheller, 1975; Pfeifer & Strauss, 1981; Reme & Sulser, 1977; Sachdeva & Thompson, 2008). However, whether autophagy is regulated by clock and the molecular mechanisms underlying circadian autophagy rhythm have not been defined. In this study, we show that autophagy displays robust circadian rhythm in mouse liver, which is accompanied by rhythmic induction of autophagy genes. We further identified C/EBPβ as a key transcription factor that links autophagy to circadian pacemaker and maintain nutrient homeostasis throughout light/dark cycles.

2.3 Results

2.3.1 Autophagy undergoes diurnal rhythm during the day

To determine whether autophagy is rhythmically activated during light/dark cycle, we examined molecular markers of autophagy, performed electron microscopy and expression profiling of autophagy-related genes. Microtubule-associated protein 1 light chain 3 (LC3) is the mammalian homologue of yeast Atg8 that undergoes conjugation with phosphatidylethanolamine (PE) upon autophagy induction (Klionsky et al, 2012; Mizushima, 2004). The unconjugated LC3 (LC3-I) is localized to cytosol whereas lipid-conjugated form (LC3-II) resides on autophagosome membrane. Immunoblotting analyses of mouse liver lysates harvested at different time points indicate that relative amounts of LC3-I and LC3-II exhibit a strong circadian rhythm in the liver (Fig. 2.1A). In general, the ratio of LC3-I/LC3-II is higher in dark phase and lower in light phase. We further examined the expression of sequestosome 1 (p62), a protein that interacts with LC3 and delivers autophagy cargos for lysosomal degradation (Komatsu et al, 2007). We found that p62 protein levels also undergo cyclic regulation through light/dark cycle (Fig. 2.1A). Circadian regulation of LC3-I/II and p62 was also observed in other tissues, including skeletal muscle, heart, and kidney (Fig. 2.S1).

While the relative abundance of LC3-I and LC3-II is a useful marker for autophagy under certain conditions, their steady-state levels do not provide an accurate assessment of autophagy flux. A new method using leupeptin, a lysosomal protease inhibitor, was

recently developed to measure autophagy flux in mouse liver (Haspel et al, 2011). In this method, we used the rate of LC3-II degradation to estimate the autophagy flux. Specifically, we injected a single dose of PBS or leupeptin into mice kept under constant darkness and harvested tissues 3 hrs following injection. The leupeptin induced LC3-II accumulation was quantitated to represent autophagy flux. To evaluate autophagy flux throughout 24 hours, a total of six time points spanning one light/dark cycle was examined. As shown in Fig. 2.1B-C, the leupeptin induced LC3-II accumulation peaks at Circadian Time (CT) 6-9 and reaches a trough in the dark phase. We next performed transmission electron microscopy on liver samples to assess autophagosome formation at different time points. Consistent with the flux studies, we found that autophagosome is most abundant at Zeitgeber Time (ZT)11 in the afternoon, rapidly decreases at night (ZT17), and rise again throughout the light phase (ZT5) (Fig. 2.1D-E). Cyclic appearance of autophagic vacuoles was also observed in previous electron microscopy studies in rat tissues (Pfeifer & Scheller, 1975; Reme & Sulser, 1977; Sachdeva & Thompson, 2008). Together, our results indicate that autophagy activity is highly rhythmic in the liver with the peak in the light phase.

We next examined whether the expression of autophagy genes is regulated by circadian signals. Quantitative PCR (qPCR) analyses indicate that several genes involved in autophagy display robust oscillation throughout the light/dark cycle, including genes involved in the autophagosome formation (Unc-51 like kinase 1 (Ulk1), GABA(A) receptor-associated protein like 1 (Gabarapl1), LC3B), mitophagy (BCL2/adenovirus E1B

interacting protein 3 (Bnip3)), and lysosomal degradation (lysosomal protease Cathepsin L (Ctsl) and lysosomal ATPase subunit (Atp6v1d)) (Fig. 2.2A). Cyclic mRNA expression of these genes was also observed in microarray dataset of high-resolution temporal transcriptional profiling of livers from mice kept under constant darkness (Hughes et al, 2009) (Fig. 2.S2). Similarly, protein levels of Ulk1 and Gabarapl1 are rhythmically regulated (Fig. 2.2B). In contrast, the expression of Atg7 and beclin 1 (Becn1) remains similar at different time points. Pronounced rhythmic autophagy gene expression was also observed in heart, and to a lesser extent, in the skeletal muscle (Fig. 2.S3 and 2.S4). Recent studies demonstrate that only a small fraction of rhythmic genes is truly clock-regulated (Vollmers et al, 2009). We next analyzed temporal regulation of autophagy genes under starvation conditions to assess the relative contribution of circadian and nutritional signals. While the mRNA levels of several autophagy genes (LC3B, Gabarapl1, Ulk1, Bnip3, and Ctsl) remain elevated at all time points in the fasted state, they appear to retain circadian regulation, albeit with altered phase characteristics (Fig. 2.S5).

2.3.2 C/EBPβ induces autophagy gene expression and protein degradation

In the liver, approximately 10% of all transcribed genes are rhythmically expressed (Panda et al, 2002; Storch et al, 2002; Ueda et al, 2002). Cyclic induction of autophagy genes suggests that transcriptional regulation may play an important role in driving the circadian autophagy rhythm. While the molecular components that execute various steps of autophagy have been extensively studied, the regulatory network that governs the program

of autophagy gene transcription remains poorly understood. Forkhead box O3 (Foxo3) has been recently implicated in the nutritional regulation of skeletal muscle autophagy (Mammucari et al, 2007; Zhao et al, 2007). However, we failed to observe robust induction of autophagy genes by Foxo3 in cultured primary hepatocytes, suggesting that tissue-specific regulatory mechanisms are likely involved.

To identify factors that control the program of autophagy gene expression, we examined a set of transcription factors and cofactors known to regulate mammalian clock and/or hepatic starvation response, including Bmal1, RORα, RORγ, Crtc2, C/EBPα, C/EBPβ, BAF60a, BAF60c, and PPARα. We transduced primary hepatocytes with adenovirus expressing individual factors and analyzed autophagy gene expression and activation by qPCR and immunoblotting, respectively. These analyses revealed that C/EBPβ strongly stimulates the expression of autophagy genes and the appearance of LC3-II in transduced hepatocytes. In contrast, other factors have modest effects on this pathway. Microarray profiling of primary hepatocytes transduced with control (GFP) or C/EBPβ adenoviruses indicates that C/EBPβ stimulates the expression of many genes involved in different steps of the autophagy pathway, such as Ulk1, Gabarapl1, LC3B, and Bnip3 (Fig.2.3A-C). Notably, C/EBPβ also induces the expression of a number of lysosomal genes, particularly subunits of the vacuolar-type H^+-ATPase that is responsible for lysosomal acidification. The expression of Atg4c and Atg7 appears largely unaffected by C/EBPβ, suggesting that not all autophagy genes are subjected to transcriptional regulation.

We next examined the effects of C/EBPβ on autophagic protein degradation in cultured hepatocytes. Compared to control, adenoviral-mediated expression of C/EBPβ significantly increased LC3-II levels in transduced hepatocytes (Fig. 2.3D-E). The induction of LC3-II is further augmented in the presence of concanamycin, a vacuolar ATPase inhibitor. The induction of LC3-II by C/EBPβ is abolished by 3-methyladenine (3-MA), an autophagy inhibitor, but not by proteasome inhibitor PS341 (Fig. 2.S6). We do not observe changes in p62 protein levels, likely as a result of concomitant increase in its mRNA expression and turnover when autophagy is stimulated by C/EBPβ. Interestingly, C/EBPβ increases LC3-II levels without affecting mTOR activity (Fig. 2.S7). Further, inhibition of mTOR by Torin1 leads to autophagy induction but has modest effects on C/EBPβ expression, suggesting that mTOR and C/EBPβ may regulate autophagy through distinct mechanisms. To determine whether C/EBPβ is sufficient to stimulate autophagic protein degradation, we transduced hepatocytes with GFP or C/EBPβ adenoviruses, labeled the cells with [^{3}H]-valine for 24 hrs, and measured the release of radiolabeled amino acid in culture medium to estimate protein. Compared to GFP, protein degradation rate is significantly enhanced in primary hepatocytes transduced with C/EBPβ adenovirus. Further, this augmentation of protein degradation is sensitive to 3-MA treatments (Fig. 2.3F). Together, we conclude that C/EBPβ stimulates the program of autophagy gene expression and is sufficient to enhance autophagic protein degradation.

2.3.3 C/EBPβ stimulates the transcription of autophagy genes through direct promoter occupancy

To determine whether C/EBPβ directly regulates autophagy gene transcription, we constructed luciferase reporter constructs for the proximal promoters of Gabarapl1, Bnip3, and Ctsl, most highly induced genes by C/EBPβ, and examined the effects of C/EBPβ on their transcriptional activity. Transient cotransfection of C/EBPβ strongly induces luciferase activity in reporter gene assays (Fig. 2.4A). Motif analyses revealed several putative C/EBPβ binding sites on these promoter sequences. We next performed chromatin immunoprecipitation (ChIP) analyses to assess direct occupancy of C/EBPβ in the native chromatin environment using chromatin extracts prepared from mouse livers. Compared to IgG control, we observed robust enrichment of C/EBPβ in the proximity of predicted binding sites on Bnip3, Ctsl and Gabarapl1 promoters. In addition, we also found that C/EBPβ is recruited to a C/EBPβ binding site residing in the first intron of Bnip3l (Fig. 2.4B).

2.3.4 C/EBPβ is regulated by both circadian and nutritional signals

We next explored whether C/EBPβ itself is under the control of biological clock and nutritional status in mice. qPCR analysis of liver RNA isolated at different time points revealed that C/EBPβ mRNA expression exhibits a robust diurnal rhythm and peaks at ZT13 (Fig. 2.5A). Accordingly, C/EBPβ protein expression is also cyclic and reaches its

highest levels during the dark phase (Fig. 2.5B). We note that the induction of several autophagy genes tends to lag C/EBPβ protein expression, likely reflecting the time needed for the accumulation of these target mRNA. In response to starvation, hepatic C/EBPβ mRNA and protein expression is significantly elevated (Fig. 2.5C-D), accompanied by increased LC3-II and reduced p62 protein levels. In addition, mRNA expressions of autophagy genes, such as Ulk1, Gabarapl1, LC3B, Bnip3, Bnip3l, and Ctsl, are also induced following starvation (Fig. 2.5E).

Unlike the central pacemaker residing in the suprachiasmatic nucleus, peripheral clocks are highly sensitive to feeding (Damiola et al, 2000). Altered meal timing, or restricted feeding, in mice results in phase resetting of peripheral clocks within several days. To examine whether the phase of C/EBPβ expression and autophagy is tightly aligned with the phase of liver clock, we subjected C/57Bl6J male mice to night feeding from ZT13 to ZT1 for a period of ten days and switch half of the group to day feeding from ZT1 to ZT13 for an additional four days (Fig. 2.6A). We harvested the livers at the end of the feeding switch and examined autophagy gene expression and autophagy markers. As shown in Fig. 2.6B, we found that, as expected, feeding switch leads to phase resetting of the expression of Bmal1, a core clock gene that is indispensable for oscillator function. The expression of other clock genes also undergoes phase resetting following restricted feeding (Fig. 2.S8). C/EBPβ expression is higher at ZT13 before food addition in the night-feeding group and this temporal pattern is completely reversed following the switch to day-feeding (Fig.

2.6B-C). Phase resetting of C/EBPβ expression is accompanied by a switch of autophagy genes, such as Gabarapl1 and Bnip3, as well as a phase reversal of p62 protein levels. These results suggest that C/EBPβ is downstream of circadian and nutritional signaling pathways.

To test whether diurnal regulation of C/EBPβ is dependent on a functional tissue clock, we examined hepatic gene expression in liver-specific Bmal1 knockout mice. Hepatic Bmal1 deficiency disrupts clock in the liver without affecting the central pacemaker (Lamia et al, 2008; Storch et al, 2007), allowing us to dissect tissue-autonomous role of the clock oscillator on C/EBPβ and autophagy gene expression. Similar to previous studies, rhythmic expression of core clock genes is defective in liver-specific Bmal1 knockout mice (Fig. 2.7A and 2.S9). Interestingly, the amplitude of C/EBPβ mRNA oscillation is greatly diminished in the Bmal1-deficient mouse livers. In addition, diurnal regulation of Bnip3 and Ulk1 mRNA expression is nearly completely abolished, whereas the amplitude of Gabarapl1 mRNA expression is significantly reduced in the absence of Bmal1. Autophagy marker and flux assays indicate that while the steady-state levels of LC3 isoforms and p62 are modestly affected, peak autophagy flux (ZT6-9) is significantly diminished in clock-deficient mouse livers (Fig. 2.7B-C). These results strongly suggest that cyclic expressions of C/EBPβ and autophagy genes are under the control of biological clock in a tissue-autonomous manner.

2.3.5 C/EBPβ is essential for physiological regulation of autophagy in the liver

To critically assess whether C/EBPβ is required for physiological regulation of autophagy, we performed *in vivo* RNAi knockdown of C/EBPβ in the liver. We transduced mice with adenoviruses that express control shRNA or shRNA directed against C/EBPβ through tail vein injection (Cui et al, 2005). Recombinant adenoviruses efficiently and selectively transduce hepatocytes and have been widely used to knock down endogenous genes in the liver. We first examined whether C/EBPβ is required for the induction of autophagy in response to starvation. Compared to control, C/EBPβ mRNA and protein levels are significantly reduced in livers transduced with siC/EBPβ adenovirus (Fig. 2.8). Basal and starvation-induced expression of autophagy genes, such as Gabarapl1, Bnip3, and Ulk1, is severely diminished when endogenous C/EBPβ is depleted. Further, p62 protein levels are drastically elevated in the knockdown liver, consistent with a blockade of autophagy in the liver of C/EBPβ knockdown mice.

We next examined whether C/EBPβ is responsible for driving the daily cycles of autophagy gene expression and autophagy process in the liver. We harvested liver from mice transduced with control or siC/EBPβ adenoviruses at four time points. As expected, rhythmic expression of C/EBPβ mRNA and protein is significantly diminished in livers transduced with siC/EBPβ adenovirus (Fig. 2.9A-B). Gene expression analysis revealed that C/EBPβ knockdown significantly perturbs circadian regulation of autophagy genes, such as Ulk1 and Gabarapl1 (Fig. 2.9A). Immunoblotting analyses indicate that while p62

protein is cyclic in control livers, its levels are constitutively elevated in the knockdown livers (Fig. 2.9B). In addition, diurnal regulation of LC3-I and LC3-II protein levels are also altered when hepatic C/EBPβ is reduced. To ascertain whether autophagy flux is reduced in response to C/EBPβ knockdown, we examined leupeptin-induced LC3-II accumulation during peak hours of autophagy (ZT6-9) and found that autophagy flux was nearly abolished in mouse livers transduced with siC/EBPβ (Fig. 2.9C). Together, we proposed that C/EBPβ serves as a link between nutritional and circadian signals and the autophagy gene program to coordinate rhythmic activation of autophagy (Fig. 2.9D).

2.4 Discussion

In this study, we characterized the temporal organization of autophagy in mouse tissues and identified C/EBPβ as a key factor that orchestrates circadian autophagy rhythm in the liver. Circadian induction of autophagy was observed in mouse liver, skeletal muscle, heart, and kidney (Fig. 2.1 and 2.S1). In the liver, autophagy flux is highest in the afternoon, rapidly decreases at night, and rises again throughout the light phase. Interestingly, the periods with low autophagy activity appear to correlate with feeding that occurs after the onset of dark phase in rodents. This correlation is consistent with the fact that autophagy activity is highly sensitive to nutritional status. In mice fasted for 24 hours, hepatic expression of several autophagy genes still appears to be cyclic, suggesting that circadian timing cues also impinge on the autophagy gene program. Furthermore, liver-specific Bmal1 deficiency results in altered rhythmic expression of autophagy genes and significantly

reduced autophagy flux at peak hours, indicating that the core molecular clock is required for normal circadian regulation of autophagy.

Interestingly, robust rhythmic autophagy gene expression was only observed in the liver and heart, suggesting that autophagy is likely regulated by distinct mechanisms in peripheral tissues (Fig. 2.S3 and 2.S4). Previous studies have demonstrated that FoxO3 is nutritionally regulated and induces autophagy in skeletal muscle (Mammucari et al, 2007; Zhao et al, 2007). However, it only modestly increases autophagy gene expression in hepatocytes, suggesting that distinct transcriptional networks may be responsible for the regulation of autophagy in different tissues. In support of this notion, we identified bZIP transcription factor C/EBPβ as a potent activator of the autophagy gene program and autophagic protein degradation. C/EBPβ stimulates the expression of a set of core autophagy genes as well as lysosomal genes and is required for the induction of autophagy in response to starvation. Recently, transcription factor EB (TFEB) was found to regulate lysosomal biogenesis and play an important role in autophagy (Sardiello et al, 2009; Settembre et al, 2011). While the significance of TFEB in circadian autophagy remains unknown, together these studies underscore an important role of transcriptional control in physiological regulation of autophagy.

C/EBPβ appears to serve as a target of both nutritional and circadian signals in the liver. Rhythmic expression of C/EBPβ requires a functional tissue clock, suggesting that the

circadian pacemaker may exert direct effects on C/EBPβ expression. Consistently, we found that rhythmic autophagy gene expression persists in constant darkness and during starvation (Fig. 2.S5). As such, nutritional and circadian signals likely provide distinct cues that are integrated by C/EBPβ in physiological regulation of autophagy. The molecular mechanism underlying clock regulation of C/EBPβ remains unknown. The significance of C/EBPβ in autophagy is supported by the observations that starvation-induced autophagy gene expression and autophagy flux are impaired in response to RNAi knockdown. In addition, knockdown of C/EBPβ severely impairs autophagy gene expression and disrupts physiological regulation of autophagy throughout light/dark cycles. These studies strongly implicate C/EBPβ as a key integrator of nutritional and circadian signals that orchestrates cyclic autophagy activation in the liver.

Rhythmic activation of autophagy in mammalian tissues likely provides a steady supply of nutrients throughout the light/dark cycles. The bulk degradation of cellular components provides amino acids and lipids that serve as a critical source of fuel and substrates for biosynthetic pathways in the tissue. In addition, these nutrients also enter systemic circulation and supply metabolites for organismal energy homeostasis, such as blood glucose control. Recent studies have implicated autophagy in the regulation of hepatic lipid metabolism, adipocyte function, and the pathogenesis of insulin resistance (Singh et al, 2009; Yang et al, 2010). Impaired autophagy reduces triglyceride hydrolysis in lipid droplets and may participate in the pathogenesis of hepatic steatosis. Whether C/EBPβ is

involved in this context remains presently unknown. Given that disruption of circadian clock increases the risk for metabolic disorders (Copinschi et al, 2000), it is possible that aberrant temporal regulation of autophagy may contribute to altered hepatic lipid metabolism in obesity.

2.5 Materials and methods

Animals – All animal experiments were performed according to procedures approved by the University Committee on Use and Care of Animals. C57BL/6J male mice were fed *ad lib* and maintained in 12/12 h light/dark cycles. For circadian studies, four mice were dissected every 3 hrs for a period of 24 hrs. Tissues were immediately frozen for the preparation of protein lysates and total RNA. Bmal1 flox/flox mice were purchased from Jackson Laboratory (Stock #007668) and crossed with Albumin-Cre transgenic mice (Stock #003574) to obtain the liver-specific Bmal1 knockout mouse. In restricted feeding experiment, C57BL/6J male mice were fed exclusively at night (night feeding from ZT13 to ZT1, NF) for a total of 10 days. On day 11, the animals were divided into two groups that were kept on NF or switched to day feeding (DF) from ZT1 to ZT13. Animals were sacrificed at two time points (ZT1 and 13) four days following the feeding switch. For *in vivo* autophagy flux measurements, mice were injected intraperitoneally a single dose of PBS or leupeptin (40 mg/kg). Tissues were harvested 3 hrs following the injection during which food was restricted. All the procedures were performed in a red dim light for

constant darkness condition. Pooled liver lysates from 3-5 mice were used for LC3 immunoblotting. Quantitation of LC3-II protein was performed using ImageJ (http://rsbweb.nih.gov/ij/). The autophagy flux rate was determined by leupeptin-induced LC3-II accumulation normalized to β-actin.

In vitro and in vivo adenoviral transduction - Primary hepatocytes were transduced with recombinant adenoviruses expressing GFP or C/EBPβ with moiety of infection from approximately 2 to 10. For *in vivo* adenoviral transduction, C57BL/6J male mice (3-5 per group) were transduced with purified adenoviruses through tail vein injection (0.2 OD per mouse), as previously described (Li et al, 2008). The titers of all adenoviruses were determined based on the expression of GFP and adenoviral gene AdE4 before use to ensure similar doses were administered in the studies.

Protein and RNA analysis - Immunoblotting studies were performed using specific antibodies for LC3 (LC3-5F10, Nanotools), p62 (PW9860, Enzo Life Sciences), Gabarapl1 (11010-1-AP, ProteinTech Group, Inc), Ulk1 (A7481, Sigma), Atg4c (AP1810c, Abgent), Atg7 (AP1813b, Abgent), C/EBPβ (sc-150, Santa Cruz), and β-actin (A4700, Sigma). For inhibitor treatments, transduced hepatocytes were incubated in the presence of vehicle, 100nM concanamycin A, 10mM 3-MA, or 500nM PS341 for 60 or 90 min before harvest. Hepatic gene expression was analyzed by qPCR using specific primers as previously described (Liu et al, 2007) or in Table. 2.S1. Data represent mean ± SD. Microarray was

carried out using total RNA from primary hepatocytes transduced with GFP or C/EBPβ adenoviruses for 48 hrs using Affymetrix mouse 430 2.0 chips and analyzed using dChip software.

ChIP Assay - Chromatin immunoprecipitation assay was performed essentially as described (Li et al, 2008). To obtain chromatin lysates from mouse livers, liver nuclei were isolated and then crosslinked in 1% formaldehyde for 15 min followed by sonication. After being precleared with protein G agarose beads, chromatin lysates were immunoprecipitated using antibodies against C/EBPβ (sc-150X, Santa Cruz) or control mouse IgG in the presence of BSA and salmon sperm DNA. Beads were extensively washed before reverse cross-linking. DNA was purified using a purification kit (QIAGEN) and subsequently analyzed by qPCR using primers flanking the predicted binding sites on promoter or intron regions (Table. 2.S1).

Reporter gene assays - AD293 cells were transiently transfected with indicated plasmids using polyethylenimine (Polysciences, Inc) in triplicates. Equal amounts of DNA were used for all transfection combinations by adding appropriate vector DNA. Relative luciferase activities were determined 24 hrs following transfection.

Transmission electron microscopy - Mice were first perfused with Sorensen's buffer (0.1M, pH7.4) and then Karnovsky's fixative buffer. The liver is post-fixed in Karnovsky's fixative

buffer for 24-48 hrs before embedding. The sample preparation for EM was performed by Microscopy & Image Analysis Laboratory at University of Michigan. The images were taken by Philips CM-100 transmission electron microscope. The quantitation of autophagosome density was carried out on 10-16 hepatocytes per time point. The autophagosome number was counted manually, and the cytoplasmic area is measured using software ImageJ.

Protein degradation assay - Primary hepatocytes transduced with GFP or C/EBPβ adenovirus were first labeled in valine-free DMEM containing 0.1% BSA plus 1.16 μM [^{3}H] L-valine (863.0 mCi/mmol, Moravek Biochemicals, Inc) for 24 hrs, washed, and then chased in DMEM containing additional 10 mM unlabeled valine for 4 hrs. Following chase, the hepatocytes were washed and incubated in the same chase media in the presence of DMSO or 10mM 3-MA. The culture media was collected 12 hr after the treatments. Radioactive amino acid content in culture media and total radioactivity in hepatocytes lysates were determined (Mizushima, 2004). Protein degradation rate is calculated by normalization of released [^{3}H] L-valine to total radioactivity in the cell.

2.6 Acknowledgements

We are grateful to Shengjuan Gu, Fernanda Jiminez-Otero and Layla Yu for technical assistance and lab members for discussions. We thank Drs. Daniel Klionsky for comments on the manuscript, Jessica Schwartz and Marco Sandri for plasmids, David Sabatini for

sharing Torin1, and Satchidananda Panda for sharing tissue samples. We thank Danming Tang, Dr. Yanzhuang Wang, Dotty Sorenson and the Microscopy & Image Analysis Laboratory of University of Michigan for technical support on EM study. This work was supported by the National Institutes of Health (HL097738 and DK077086, J.D.L.). D.M. is supported by Predoctoral Fellowship from the American Heart Association.

Table. 2.S1. qPCR primer list.

	Forward primer	Reverse primer
Gabarapl1	GCCGGTCATCGTGGAGAA	TGGATCCTCTTCCGGATTAAGA
Bnip3	TTCCACTAGCACCTTCTGATGA	GAACACCGCATTTACAGAACAA
Bnip3l	CGTTCCTTCCTCGTCTTCCA	TGTGGTGAAGGGCTGTCACA
Ctsl	TCTCACGCTCAAGGCAATCA	TCCGTCCTTCGCTTCATAGG
Atp6v1d	ATTGAACGCACCCTTGCCTAT	TCTCCGCCGCTCCAAGT
Ulk1	AGCCCAGTTTCCAGGTGATCT	GTACGGCCGTGGCTCTCTAG
p62	CTCATCTTTCCCAACCCCTTT	AGGACGTGGGCTCCAGTTC
Becn1	GTGCGCTACGCCCAGATC	CAAGCGACCCAGTCTGAAATTA
LC3A	CGACCAGCACCCCAGTAAGA	TGACCAACTCGCTCATGTTAACA
LC3B	AGTGGAAGATGTCCGGCTCAT	TCAGGCACCAGGAACTTGGT
Atg4c	GTGGCCGTCTTTGGCTTACA	CCGGATGCCTTGCTTCTTC
Atg7	TTCTGGTCTCCTTGCTCAAACA	AATTCCTCAAAGGCCATCCA
Gabarapl1_ChIP	GGCACTTTTCCAACTCCAGA	TCCCTCCCCTTCAAGTTTCT
Bnip3l_ChIP	TGGAAGCCATCCCTCTTATG	GTCACAGGGCCAGATGAAGT
Bnip3_ChIP	TGACCCATAGTTCCCCAATC	CGTGCATAGAGACAGCGAGA
Ctsl_ChIP	AAAATGTGCAGGGTGGAGAG	TGTCCTCCGCTCTGTCTTCT

Fig. 2.1. Rhythmic induction of autophagy in the liver. (A) Immunoblotting of liver lysates using indicated antibodies. Pooled samples from 4 mice were used for each time point. ZT0 and 12 represent the onset of light and dark cycles, respectively. The figure represents one of three independent sets of circadian samples. (B) Immunoblots showing LC3-II levels in the livers from mice injected with PBS (-) or leupeptin (+) 3 hrs before tissue harvest. Pooled samples from three mice were used for each lane. (C) Quantitation of *in vivo* autophagy flux. Following normalization to β-actin in B, relative leupeptin-induced LC3-II accumulation was calculated by subtracting LC3-II levels in PBS-treated from leupeptin-treated mice for each time point. Data represent mean ± SD of one representative experiment. (D) Transmission electron micrograph of liver sections at ZT5, 11, 17, and 23. The scale bar in the upper right corner of ZT5 figure represents 2 microns. The right lower corner shows the higher magnification highlighting a cytosolic region. Note the presence of double-membraned autophagosomes (arrow head). (E) Quantitation of autophagosome abundance in D. Data represent mean ± SE. * $p<0.000001$ (ZT11 vs. 17, n=10-16 cells). Student's t-test was applied.

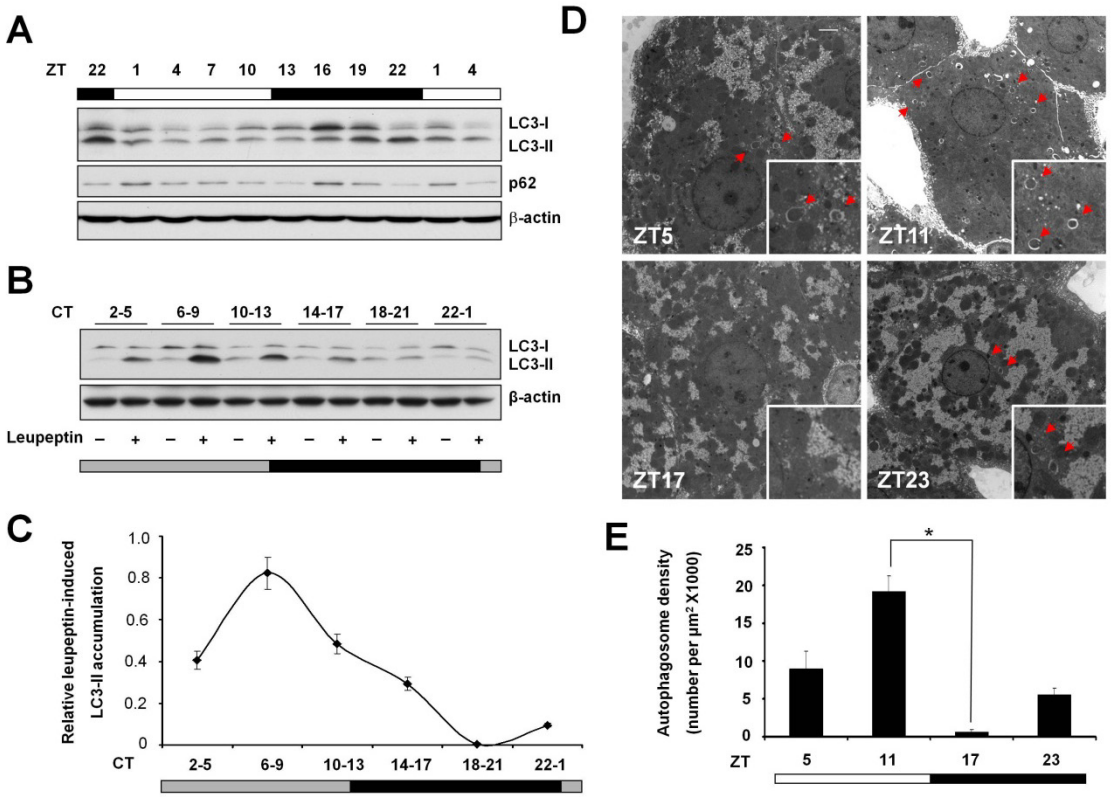

Fig. 2.2. Rhythmic induction of autophagy gene expression in the liver. (A) qPCR analysis of autophagy genes at different time points of mouse livers. Pooled samples from 4 mice were used for each time point. Data represent mean ± SD of one of three independent studies. Becn1 serves as an example gene with modest diurnal oscillation at mRNA level. (B) Immunoblots of autophagy proteins in mouse livers at indicated time points. Pooled samples from four mice were used for each time point.

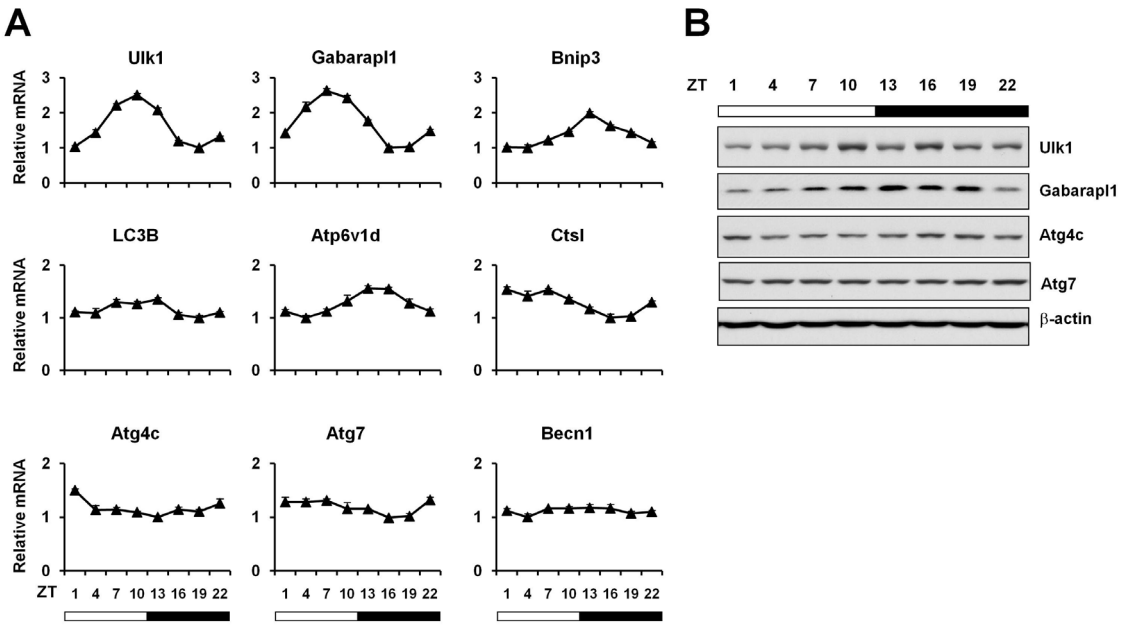

Fig. 2.3. Induction of autophagy gene expression and autophagy process by C/EBPβ. (A) Clustering analysis of autophagy-related genes in primary hepatocytes transduced with GFP or C/EBPβ adenoviruses for 48 hrs. Blue and yellow represent low and high mRNA expression, respectively. (B) qPCR analysis of autophagy gene expression. Shown is fold-induction by C/EBPβ in primary hepatocytes 24 hrs (blue) or 48 hrs (red) following adenoviral transduction. Data represent mean ± SD of one representative experiment. (C) Protein expression of autophagy genes in hepatocytes transduced with GFP or C/EBPβ adenoviruses. Arrowheads point to two C/EBPβ isoforms generated from alternative translation start sites. (D) Immunoblots of total lysates from transduced primary hepatocytes treated with vehicle or concanamycin in triplicates. Blots with different exposure time were shown to illustrate LC3-I and LC3-II signals. (E) Quantitation of LC3-II protein levels following normalization to β-actin. Data represent mean ± SE. Student's t-test was applied. * $p<0.01$. ** $p<0.001$. (F) Protein degradation assay in transduced hepatocytes in the absence (open) or presence of 3-MA (filled). Note that C/EBPβ-inducible proteolysis is sensitive to 3-MA treatment. Student's t-test was applied. * $p<0.05$.

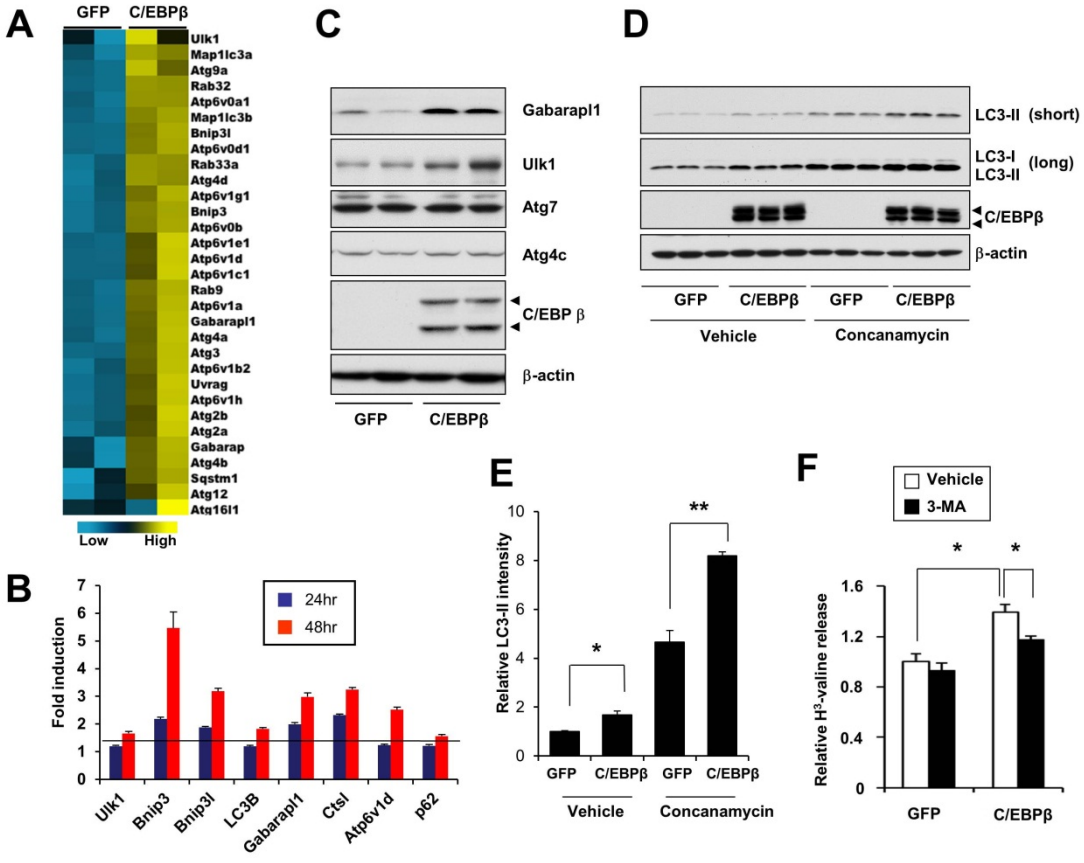

Fig. 2.4. C/EBPβ stimulates the transcription of autophagy genes through direct promoter occupancy. (A) Transcriptional assays using indicated promoter luciferase constructs in the presence of vector (open), 25 ng (grey), or 100 ng (filled) of C/EBPβ expression plasmid. Predicted C/EBPβ binding sites are indicated with solid bars. Data represent mean ± SE. Student's t-test was applied. * $p<0.01$ (vector vs. 25ng C/EBPβ), ** $p<0.001$ (vector vs. 100ng C/EBPβ). (B) ChIP assay using control IgG (open) or C/EBPβ (filled) antibodies. Relative enrichment was determined by qPCR.

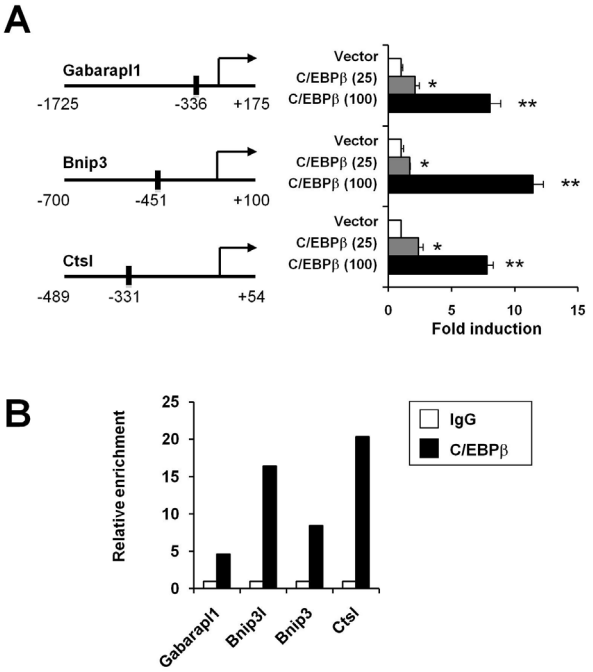

Fig.2.5. C/EBPβ expression is regulated by circadian and nutritional signals. (A and B) Hepatic C/EBPβ mRNA and protein expression at different time points. (C) Immunoblotting of liver lysates from fed, 24h-fasted or 24h-refed mice (after 24h-fast). Samples were collected at ZT4. (D and E) qPCR analysis of hepatic gene expression from fed, 24h-fasted or 24h-refed mice, the same group as in C. Pooled samples from 3-5 mice were used for each data point. Data in A, D, and E represent mean ± SD.

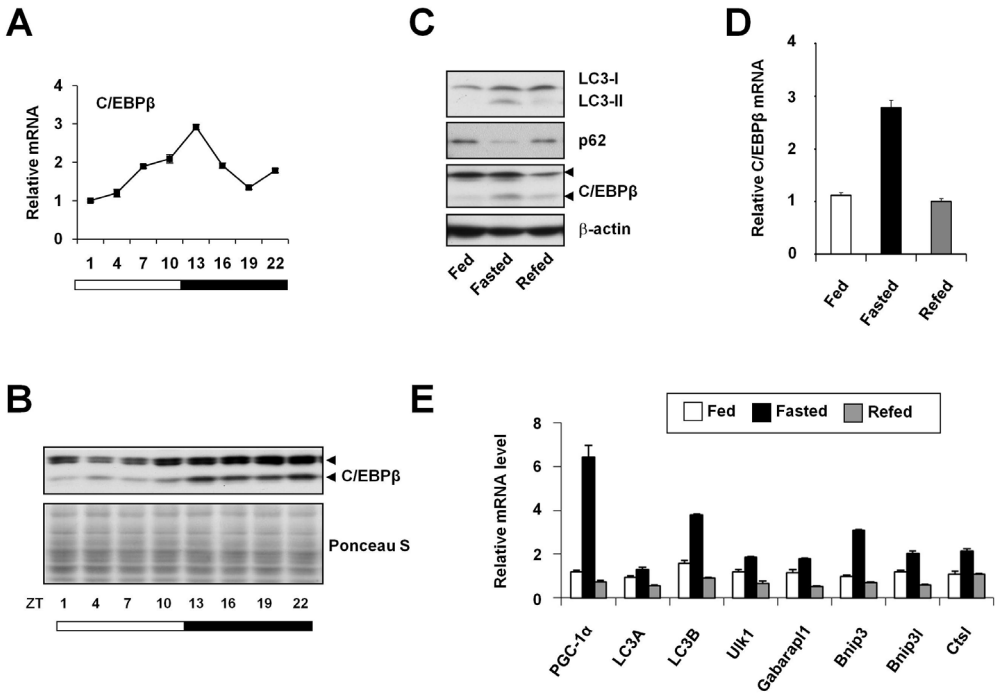

Fig. 2.6. Regulation of C/EBPβ and autophagy by restricted feeding. (A) The diagram indicates restricted feeding schedule and food availability (grey box, arrows indicate tissue harvest times). (B) qPCR analysis of hepatic gene expression in mice fed during dark (NF) or light (DF) phase. (C) Immunoblotting of liver lysates from mice undergoing restricted feeding. Pooled samples from 3-5 mice were used for each data point. Data in B represent mean ± SD.

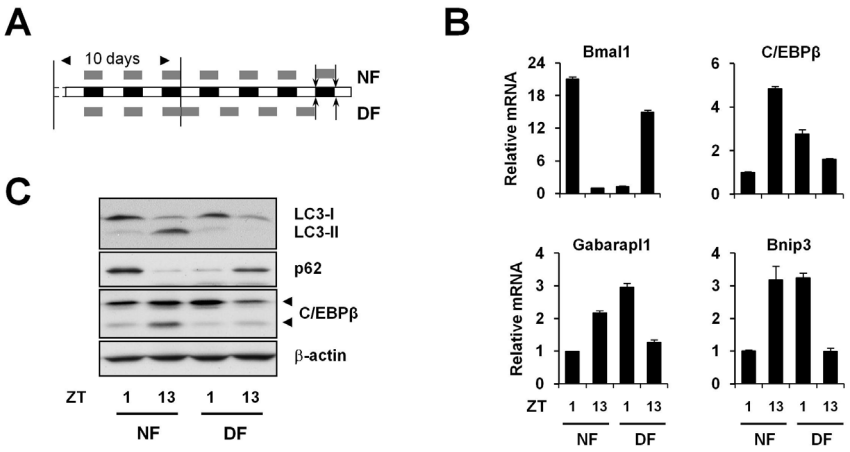

Fig. 2.7. Liver autonomous clock is required for normal autophagy rhythm. (A) qPCR analysis of hepatic genes in control (filled diamond) and liver-specific Bmal1 knockout mice (open square, Bmal1 LKO). (B) Immunoblots of total liver lysates in control and Bmal1 LKO mice using indicated antibodies. (C) *In vivo* autophagy flux assay was performed at ZT6-9. Pooled samples from 3-4 mice were used for each group. Data in A represent mean ± SD.

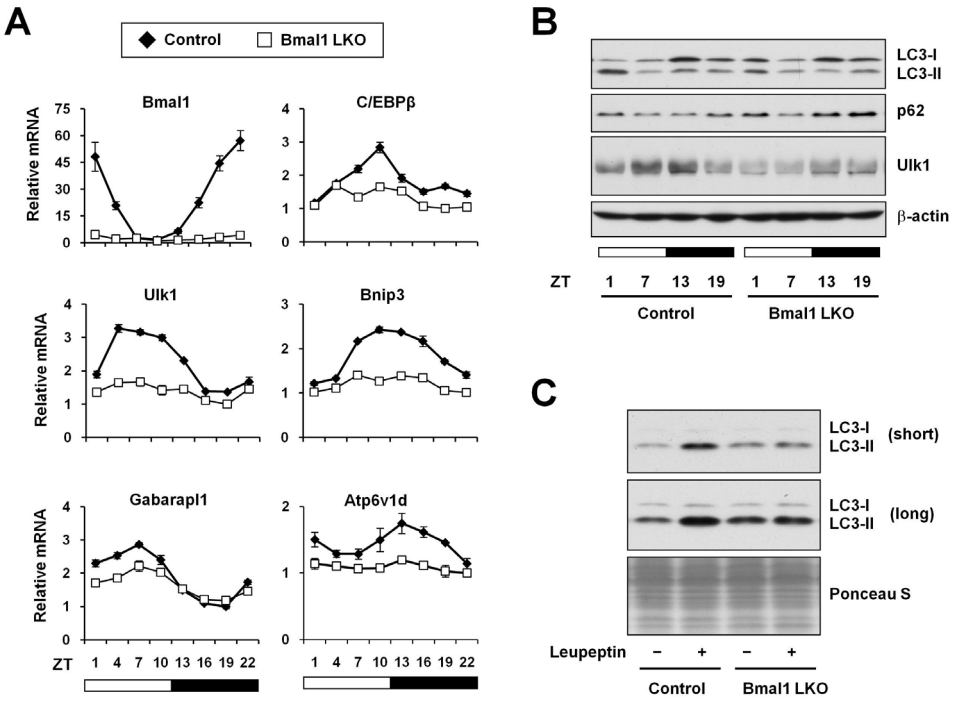

Fig. 2.8. C/EBPβ is essential for physiological regulation of autophagy in the liver. (A) qPCR analysis of hepatic genes in mice transduced with control (Scrb) or siC/EBPβ (siC) adenoviruses under fed (open) and 16 hr-fasted (filled) conditions. Samples were harvested at ZT19. (B) Immunoblots of liver lysates in mice from A under fed and fasted conditions. Pooled samples from 3-5 mice were used for each data point. Data in A represent mean ± SD.

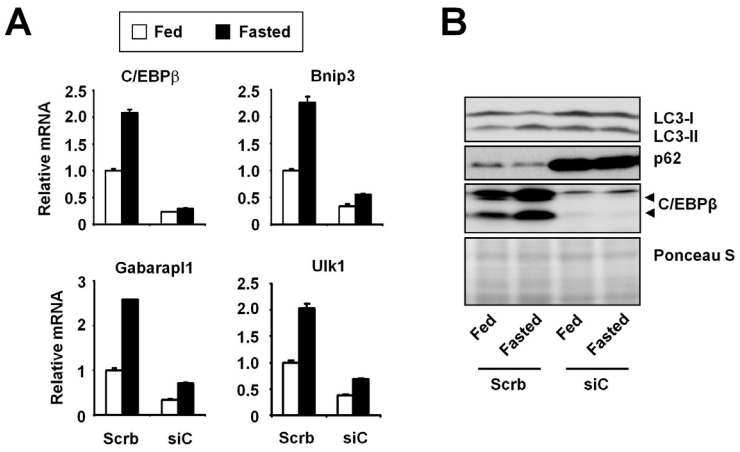

Fig. 2.9. C/EBPβ is essential for circadian autophagy regulation in the liver. (A) qPCR analysis of hepatic genes in mice transduced with control (Scrb, filled diamond) or siC/EBPβ (siC, open square) adenoviruses harvested at indicated time points. Data represent mean ± SD. (B) Immunoblots of liver lysates in mice from A at indicated time points. (C) *In vivo* autophagy flux assay was performed in mice transduced with control (Scrb) or siC/EBPβ (siC) adenoviruses at ZT6-9. Pooled samples from 3-5 mice per group were analyzed. (D) Model depicting circadian autophagy regulation through C/EBPβ. Note that C/EBPβ receives both circadian and nutritional input and coordinately regulates the program of autophagy gene expression.

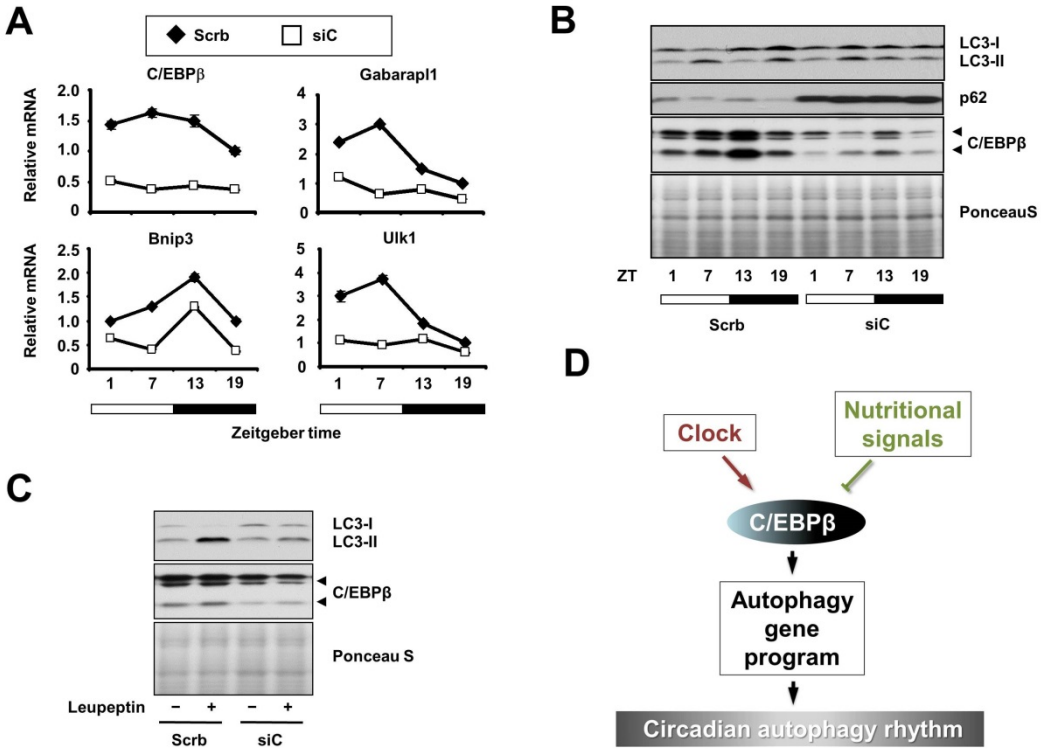

Fig. 2.S1. Rhythmic induction of autophagy in the heart, skeletal muscle and kidney. Immunoblots of total tissue lysates using indicated antibodies. Ponceau S staining serves as loading control.

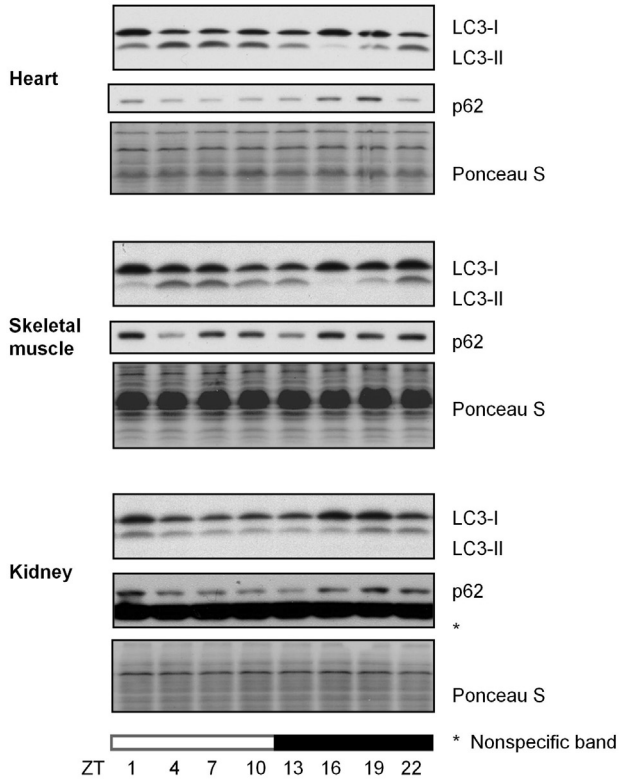

Fig. 2.S2. Oscillation of autophagy genes according to online database Circa. Graphs of autophagy gene expression generated using dataset provided at: http://wasabi.itmat.upenn.edu/circa (Hughes et al. 2009). Note that transcriptional profiling was performed every hour for a total of 48 hrs in livers from mice kept under constant darkness.

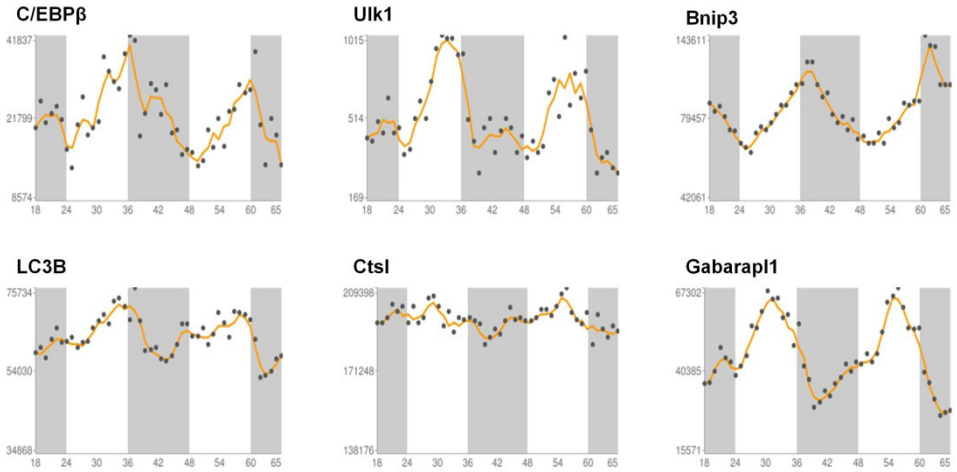

Fig.2.S3. Rhythmic expression of autophagy genes in the heart. Shown is qPCR analysis of Per1 and autophagy genes at different time points. Data represent mean ± SD. ZT0 and 12 represent the onset of light and dark cycles, respectively.

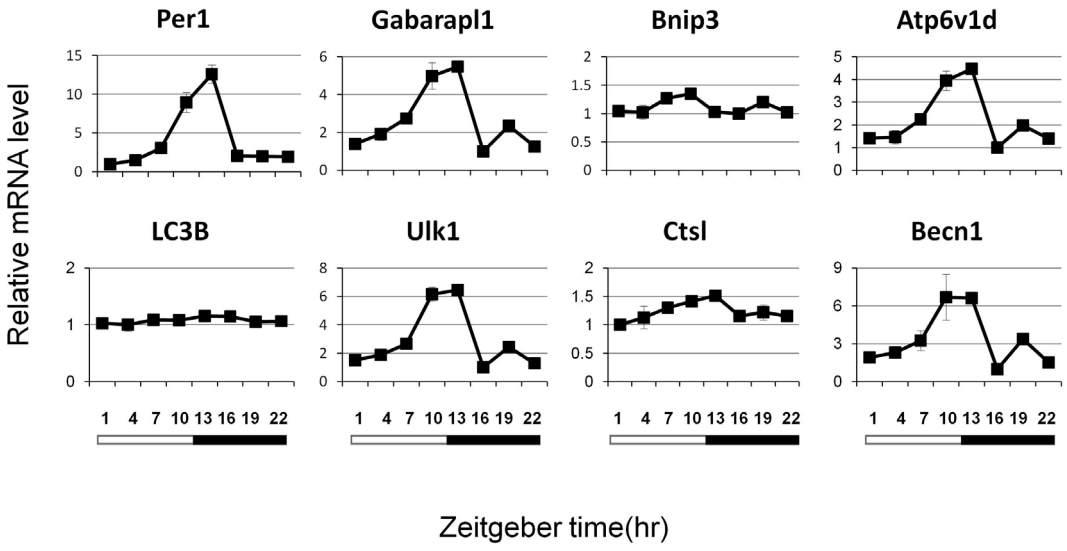

Fig. 2.S4. Daily expression of autophagy genes in skeletal muscle. Shown is qPCR analysis of Per1 and autophagy genes at different time points. Data represent mean ± SD. ZT0 and 12 represent the onset of light and dark cycles, respectively.

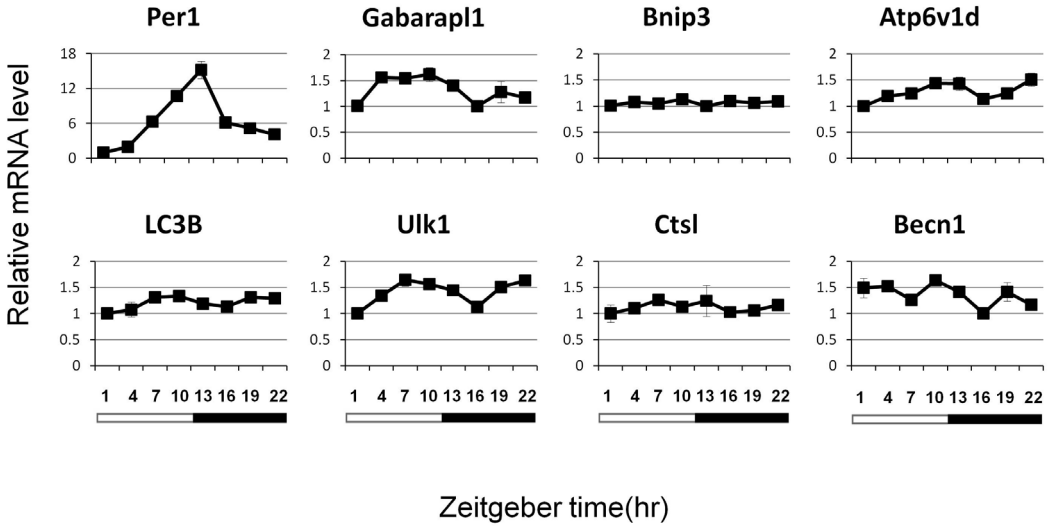

Fig. 2.S5. qPCR analysis of hepatic autophagy and core clock gene expression under starvation. The expression level in fed (filled diamond) or 24-hour fasted mice (open square) was plotted against Zeitgeber time. For fasted group, food had been withdrawn for exactly 24 hours before harvest. Pooled samples from 3-4 mice were used per data point. Data represent mean ± SD.

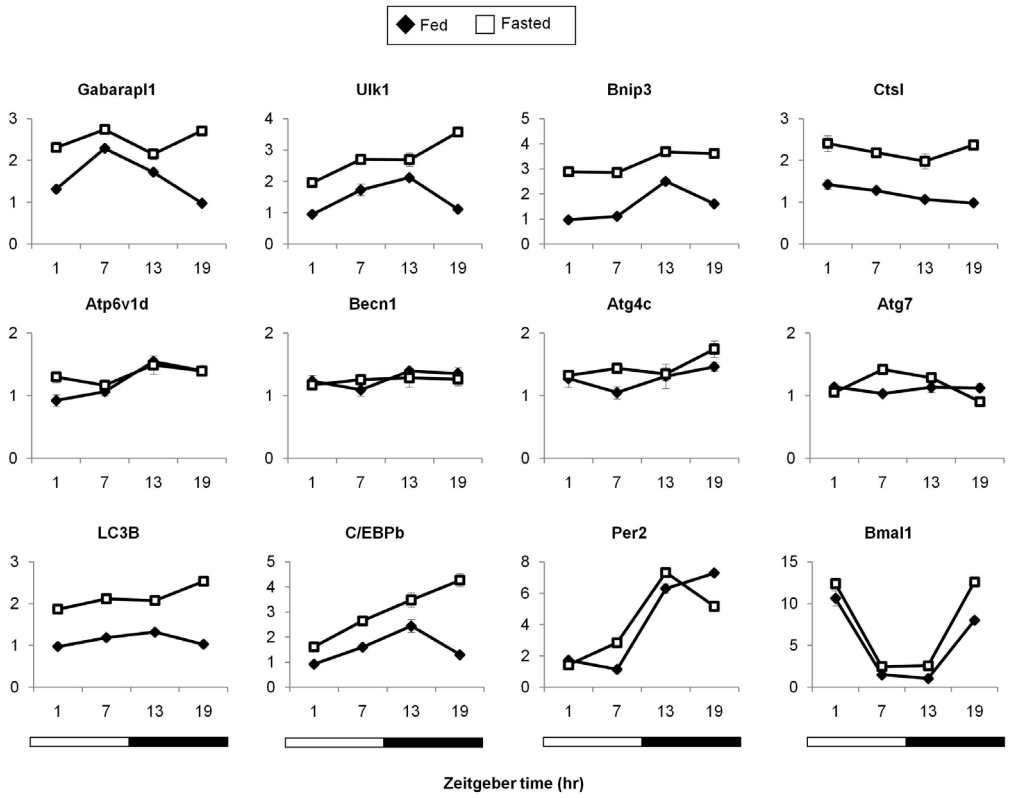

Fig. 2.S6. Immunoblotting analyses of total lysates from primary hepatocytes transduced with GFP or C/EBPβ adenoviruses in the presence of vehicle, 3-MA, or PS341. Immunoblots with different exposure time were shown to illustrate LC3-I and LC3-II in cells. Pooled samples from triplicates were used for each condition.

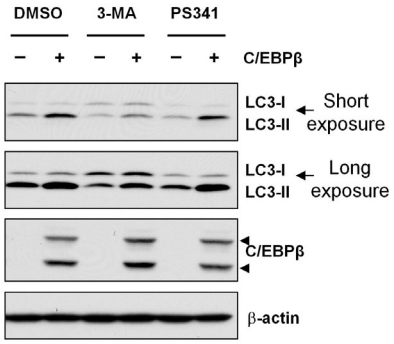

Fig. 2.S7. Interaction between C/EBPβ and mTOR pathways. (A) C/EBPβ overexpression does not alter nutrient regulation of mTOR, as indicated by S6 phosphorylation. The amino acid was deprived for 1 hour. The lanes shown were from same original immunoblots. (B) Inhibition of mTOR activity by Torin1 for 4 hours does not alter C/EBPβ expression in primary hepatocytes.

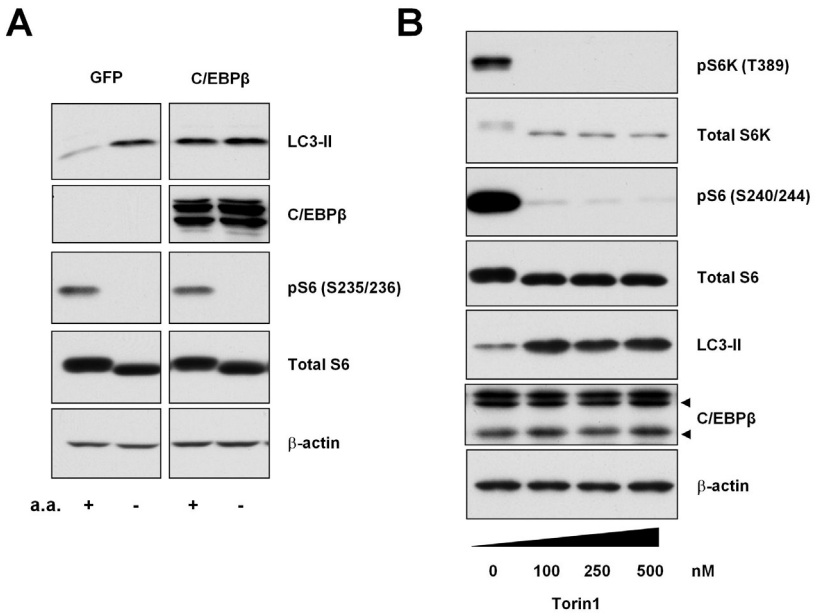

Fig. 2.S8. qPCR analysis of hepatic autophagy and core clock gene expression under restricted feeding. The expression levels at ZT1 and ZT13 in mouse fed during dark (NF) or light (DF) phase were displayed. Pooled samples from 3-5 mice were used for each data point. Data represent mean ± SD.

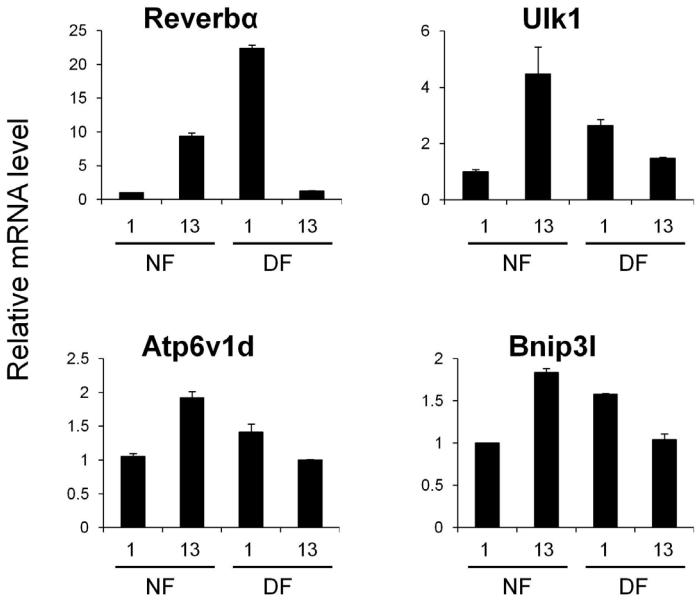

Fig. 2.S9. Bmal1 LKO abolishes the rhythmic expression of hepatic clock genes. qPCR analysis of hepatic clock genes in control (filled diamond) and liver-specific Bmal1 knockout (open square) mice was performed. Pooled samples from 3-5 mice were used for each data point. Data represent mean ± SD.

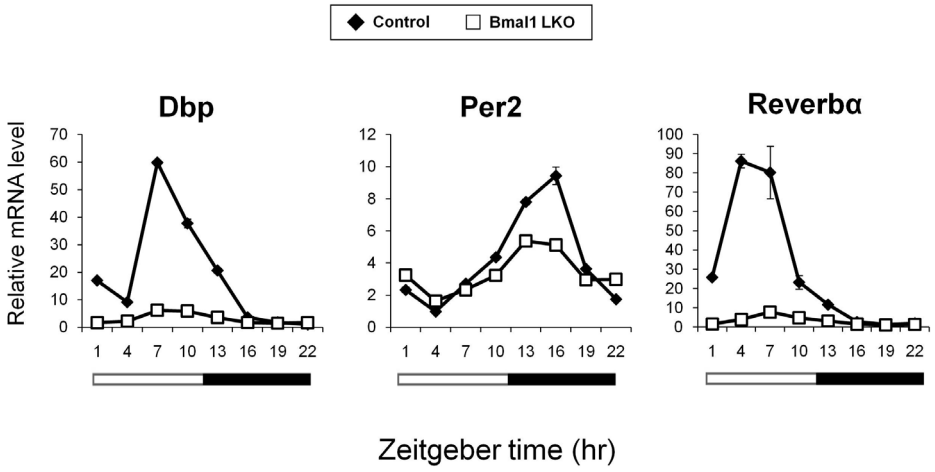

2.7 References

Copinschi G, Spiegel K, Leproult R, Van Cauter E (2000) Pathophysiology of human circadian rhythms. *Novartis Found Symp* **227:** 143-157; discussion 157-162

Cui TX, Piwien-Pilipuk G, Huo JS, Kaplani J, Kwok R, Schwartz J (2005) Endogenous CCAAT/enhancer binding protein beta and p300 are both regulated by growth hormone to mediate transcriptional activation. *Mol Endocrinol* **19:** 2175-2186

Damiola F, Le Minh N, Preitner N, Kornmann B, Fleury-Olela F, Schibler U (2000) Restricted feeding uncouples circadian oscillators in peripheral tissues from the central pacemaker in the suprachiasmatic nucleus. *Genes Dev* **14:** 2950-2961

Ebato C, Uchida T, Arakawa M, Komatsu M, Ueno T, Komiya K, Azuma K, Hirose T, Tanaka K, Kominami E, Kawamori R, Fujitani Y, Watada H (2008) Autophagy is important in islet homeostasis and compensatory increase of beta cell mass in response to high-fat diet. *Cell Metab* **8:** 325-332

Green CB, Takahashi JS, Bass J (2008) The meter of metabolism. *Cell* **134:** 728-742

Haspel J, Shaik RS, Ifedigbo E, Nakahira K, Dolinay T, Englert JA, Choi AM (2011) Characterization of macroautophagic flux in vivo using a leupeptin-based assay. *Autophagy* **7:** 629-642

Hughes ME, DiTacchio L, Hayes KR, Vollmers C, Pulivarthy S, Baggs JE, Panda S, Hogenesch JB (2009) Harmonics of circadian gene transcription in mammals. *PLoS Genet* **5:** e1000442

Jung HS, Chung KW, Won Kim J, Kim J, Komatsu M, Tanaka K, Nguyen YH, Kang TM, Yoon KH, Kim JW, Jeong YT, Han MS, Lee MK, Kim KW, Shin J, Lee MS (2008) Loss of autophagy diminishes pancreatic beta cell mass and function with resultant hyperglycemia. *Cell Metab* **8:** 318-324

Klionsky DJ, Abdalla FC, Abeliovich H, Abraham RT, Acevedo-Arozena A, Adeli K, Agholme L, Agnello M, Agostinis P, Aguirre-Ghiso JA, Ahn HJ, Ait-Mohamed O, Ait-Si-Ali S, Akematsu T, Akira S, Al-Younes HM, Al-Zeer MA, Albert ML, Albin RL, Alegre-Abarrategui J et al (2012) Guidelines for the use and interpretation of assays for monitoring autophagy. *Autophagy* **8:** 445-544

Komatsu M, Waguri S, Chiba T, Murata S, Iwata J, Tanida I, Ueno T, Koike M, Uchiyama Y, Kominami E, Tanaka K (2006) Loss of autophagy in the central nervous system causes

neurodegeneration in mice. *Nature* **441:** 880-884

Komatsu M, Waguri S, Koike M, Sou Y-S, Ueno T, Hara T, Mizushima N, Iwata J-I, Ezaki J, Murata S, Hamazaki J, Nishito Y, Iemura S-I, Natsume T, Yanagawa T, Uwayama J, Warabi E, Yoshida H, Ishii T, Kobayashi A et al (2007) Homeostatic levels of p62 control cytoplasmic inclusion body formation in autophagy-deficient mice. *Cell* **131:** 1149-1163

Komatsu M, Waguri S, Ueno T, Iwata J, Murata S, Tanida I, Ezaki J, Mizushima N, Ohsumi Y, Uchiyama Y, Kominami E, Tanaka K, Chiba T (2005) Impairment of starvation-induced and constitutive autophagy in Atg7-deficient mice. *J Cell Biol* **169:** 425-434

Kuma A, Hatano M, Matsui M, Yamamoto A, Nakaya H, Yoshimori T, Ohsumi Y, Tokuhisa T, Mizushima N (2004) The role of autophagy during the early neonatal starvation period. *Nature* **432:** 1032-1036

Lamia KA, Storch KF, Weitz CJ (2008) Physiological significance of a peripheral tissue circadian clock. *Proc Natl Acad Sci U S A* **105:** 15172-15177

Leproult R, Van Cauter E (2010) Role of sleep and sleep loss in hormonal release and metabolism. *Endocr Dev* **17:** 11-21

Levine B, Kroemer G (2008) Autophagy in the pathogenesis of disease. *Cell* **132:** 27-42

Li S, Liu C, Li N, Hao T, Han T, Hill DE, Vidal M, Lin JD (2008) Genome-wide coactivation analysis of PGC-1alpha identifies BAF60a as a regulator of hepatic lipid metabolism. *Cell Metab* **8:** 105-117

Liu C, Li S, Liu T, Borjigin J, Lin JD (2007) Transcriptional coactivator PGC-1alpha integrates the mammalian clock and energy metabolism. *Nature* **447:** 477-481

Mammucari C, Milan G, Romanello V, Masiero E, Rudolf R, Del PP, Burden SJ, Di LR, Sandri C, Zhao J, Goldberg AL, Schiaffino S, Sandri M (2007) FoxO3 controls autophagy in skeletal muscle in vivo. *Cell Metab* **6:** 458-471

Mizushima N (2004) Methods for monitoring autophagy. *Int J Biochem Cell Biol* **36:** 2491-2502

Mizushima N, Levine B, Cuervo AM, Klionsky DJ (2008) Autophagy fights disease through cellular self-digestion. *Nature* **451:** 1069-1075

Panda S, Antoch MP, Miller BH, Su AI, Schook AB, Straume M, Schultz PG, Kay SA, Takahashi JS, Hogenesch JB (2002) Coordinated transcription of key pathways in the

mouse by the circadian clock. *Cell* **109:** 307-320

Pfeifer U (1972) Inverted diurnal rhythm of cellular autophagy in liver cells of rats fed a single daily meal. *Virchows Arch B Cell Pathol* **10:** 1-3

Pfeifer U, Scheller H (1975) A morphometric study of cellular autophagy including diurnal variations in kidney tubules of normal rats. *J Cell Biol* **64:** 608-621

Pfeifer U, Strauss P (1981) Autophagic vacuoles in heart muscle and liver. A comparative morphometric study including circadian variations in meal-fed rats. *J Mol Cell Cardiol* **13:** 37-49

Rabinowitz JD, White E (2010) Autophagy and metabolism. *Science* **330:** 1344-1348

Reme CE, Sulser M (1977) Diurnal variation of autophagy in rod visual cells in the rat. *AlbrechtVonGraefes ArchKlinExpOphthalmol* **203:** 261-270

Rudic RD, McNamara P, Curtis AM, Boston RC, Panda S, Hogenesch JB, Fitzgerald GA (2004) BMAL1 and CLOCK, two essential components of the circadian clock, are involved in glucose homeostasis. *PLoS Biol* **2:** e377

Rutter J, Reick M, McKnight SL (2002) Metabolism and the control of circadian rhythms. *Annu Rev Biochem* **71:** 307-331

Sachdeva UM, Thompson CB (2008) Diurnal rhythms of autophagy: implications for cell biology and human disease. *Autophagy* **4:** 581-589

Sardiello M, Palmieri M, di Ronza A, Medina DL, Valenza M, Gennarino VA, Di Malta C, Donaudy F, Embrione V, Polishchuk RS, Banfi S, Parenti G, Cattaneo E, Ballabio A (2009) A gene network regulating lysosomal biogenesis and function. *Science* **325:** 473-477

Settembre C, Di Malta C, Polito VA, Garcia Arencibia M, Vetrini F, Erdin S, Erdin SU, Huynh T, Medina D, Colella P, Sardiello M, Rubinsztein DC, Ballabio A (2011) TFEB links autophagy to lysosomal biogenesis. *Science* **332:** 1429-1433

Singh R, Kaushik S, Wang Y, Xiang Y, Novak I, Komatsu M, Tanaka K, Cuervo A, Czaja M (2009) Autophagy regulates lipid metabolism. *Nature* **458:** 1131-1135

Storch KF, Lipan O, Leykin I, Viswanathan N, Davis FC, Wong WH, Weitz CJ (2002) Extensive and divergent circadian gene expression in liver and heart. *Nature* **417:** 78-83

Storch KF, Paz C, Signorovitch J, Raviola E, Pawlyk B, Li T, Weitz CJ (2007) Intrinsic

circadian clock of the mammalian retina: importance for retinal processing of visual information. *Cell* **130:** 730-741

Turek FW, Joshu C, Kohsaka A, Lin E, Ivanova G, McDearmon E, Laposky A, Losee-Olson S, Easton A, Jensen DR, Eckel RH, Takahashi JS, Bass J (2005) Obesity and metabolic syndrome in circadian Clock mutant mice. *Science* **308:** 1043-1045

Ueda HR, Chen W, Adachi A, Wakamatsu H, Hayashi S, Takasugi T, Nagano M, Nakahama K, Suzuki Y, Sugano S, Iino M, Shigeyoshi Y, Hashimoto S (2002) A transcription factor response element for gene expression during circadian night. *Nature* **418:** 534-539

Vollmers C, Gill S, DiTacchio L, Pulivarthy SR, Le HD, Panda S (2009) Time of feeding and the intrinsic circadian clock drive rhythms in hepatic gene expression. *Proc Natl Acad Sci U S A* **106:** 21453-21458

Wijnen H, Young MW (2006) Interplay of circadian clocks and metabolic rhythms. *Annu Rev Genet* **40:** 409-448

Yang L, Li P, Fu S, Calay E, Hotamisligil G (2010) Defective hepatic autophagy in obesity promotes ER stress and causes insulin resistance. *Cell Metab* **11:** 467-478

Yang Z, Klionsky D (2010) Eaten alive: a history of macroautophagy. *Nature cell biology* **12:** 814-822

Zhao J, Brault JJ, Schild A, Cao P, Sandri M, Schiaffino S, Lecker SH, Goldberg AL (2007) FoxO3 coordinately activates protein degradation by the autophagic/lysosomal and proteasomal pathways in atrophying muscle cells. *Cell Metab* **6:** 472-483

CHAPTER 3 THE ROLE OF AUTOPHAGY IN NON-ALCOHOLIC FATTY LIVER DISEASE

3.1 Abstract

Previous literatures indicate that autophagy plays a direct role in the mobilization of triglycerides stored in lipid droplets, and thus autophagy deficiency leads to massive accumulation of lipids in liver. These findings raised a very interesting possibility that autophagy may serve an important function in the physiological regulation of lipid metabolism in the liver and may contribute to the development of hepatic steatosis. However, by analyzing livers with FIP200 deletion in short-term or long-term, as well as those with Atg7 knockdown, we found that defective autophagy per se is not sufficient to cause fatty liver. After further examining the liver injury in autophagy deficient mice, we found that chronic suppression of autophagy leads to liver fibrosis. Our findings suggest that instead of causing steatosis, autophagy deficiency may serve as the long-sought second hit that drives the progression from relatively benign fatty liver to steatohepatitis (NASH).

3.2 Introduction

Non-alcoholic fatty liver disease (NAFLD) emerged as a significant public health

challenge worldwide. In the US, it was estimated to occur in 10%-46% of the general population (Polyzos et al, 2012). NAFLD encompassed a disease spectrum developed in the absence of excessive alcohol intake, ranging from simple steatosis (NAFL) to steatohepatitis (NASH). The histological hallmark for NAFL is the accumulation of lipid droplet as triglycerides within the hepatocytes, and the hallmarks for NASH include inflammatory cell infiltration, liver injury, and fibrosis (Hebbard & George, 2011). While the health of NAFL patients are largely unaffected, 10%-15% of NASH patients evolve to cirrhosis and even hepatocellular carcinoma (HCC) in ten years (Polyzos et al, 2012). Recent genome wide association studies (GWAS) have identified several genes involved in non-alcoholic fatty liver disease (NAFLD) (Chalasani et al, 2010; Speliotes et al, 2011; Stefano et al, 2008). Patatin-like phospholipase domain containing family member A3 (PNPLA3) was identified as the most robust hit, associated with both hepatic fat level and hepatic inflammation (Stefano et al, 2008).

It is known that 15%-30% NAFL patients will progress to NASH (Polyzos et al, 2012). However, the factors that determine this progression are still under investigation. Several models were proposed, including a traditional 'two-hit' model, a current 'multiple-hit' model, and an 'integrated response' model emphasizing the crosstalk between tissues (Hebbard & George, 2011; Polyzos et al, 2012). Nonetheless, who pulls the trigger in the progression is still under debate. Thus far, possible triggers include gut-derived bacterial toxins, cytokine imbalance, mitochondrial dysfunction, oxidative stress, ER stress, and so

on (Hebbard & George, 2011; Pagliassotti, 2012; Polyzos et al, 2012). Would there be a unified mechanism that could potentially explain all these trigger factors?

Emerging evidence from recent reports points to a possible candidate, autophagy. Autophagy is a lysosome-dependent degradation process. Upon activation, autophagosomes are formed, enclose cytosolic components, and fuse to lysosome for degradation. It is important for removing damaged organelles, protein aggregates, and pathogens (Mizushima & Komatsu, 2011; Yang & Klionsky, 2010). It is activated in a circadian rhythmic manner in liver and several other tissues (Ma et al, 2011). Currently, four lines of evidences suggest that autophagy may play an important role in maintaining lipid homeostasis and preventing liver injury. First, autophagosome machinery proteins are found to co-localize with lipid droplets (Shibata et al, 2009; Singh et al, 2009), and autophagy is directly involved in removing lipid droplet (Singh et al, 2009). Second, autophagy activity is compromised by excessive lipid intake (Koga et al, 2010; Yang et al, 2010). Third, autophagy deficiency in liver leads to liver tumors in the long run (Inami et al, 2011; Takamura et al, 2011). Last, Mallory-Denk bodies, cytoplasmic hyaline inclusions in hepatocytes of patients with hepatitis, contain p62, an adaptor for autophagosome cargo (Zatloukal et al, 2007).

Based on these data, we hypothesized that autophagy deficiency plays a key role in entering the vicious cycle of lipid accumulation, and mediating the deterioration of

steatosis. To our surprise, we did not observe a lipid accumulation in the livers with long term or short term autophagy deficiency, by using FIP200 liver specific knockout and Atg7 knockdown models. Nonetheless, we observed a striking liver injury in the autophagy deficient mouse livers with hallmarks of NASH, including inflammatory cell infiltration, hepatocellular ballooning and fibrosis. Our data indicate autophagy could play a crucial role in preventing liver injury and progression from NAFL to NASH. However, this role is unlikely to attribute to its function in removing lipid droplets. Moreover, considering the complex phenotypes of autophagy deficiency in lipid metabolism, our study prompted further investigation in other roles that autophagy may play in maintaining lipid homeostasis.

3.3 Results

3.3.1 Liver-specific FIP200 knockout mice have defective autophagic degradation

To examine the influence of autophagy deficiency on hepatic lipid metabolism, we generated liver-specific FIP200 knockout mice (FIP200 LKO) by breeding FIP200 flox/flox mice with transgenic mice expressing Cre under liver specific albumin promoter (Gan et al, 2006). In FIP200 LKO, protein level of FIP200 is significantly decreased (Fig. 3.1A, Fig. 3.S1). The residual FIP200 protein in liver is likely due to the FIP200 expressed by the infiltrated inflammatory cells (Fig. 3.4E). Consistent with other autophagy deficiency mouse models, autophagic degradation process in FIP200 LKO liver is severely

blocked, causing decreased autophagy flux, accumulation of insoluble protein aggregates comprising ubiquitinated protein, p62, mitochondria and autophagosome marker such as LC3 (Fig. 3.1A-D). The formation of these aggregates has been reported to be due to impaired turnover of p62 (Komatsu et al, 2010; Komatsu et al, 2007). Interestingly, the Mallory-Denk body, one hallmark for hepatitis, comprises abundant amount of p62 (Strnad et al, 2008). Under electron microscope, we observed clusters of abnormal vacuoles containing a large number of small vesicles and structures similar to multilamellar bodies (MLBs) only present in FIP200 LKO (Fig. 3.1E). Besides, Ulk1, which requires FIP200 for appropriate phosphorylation, increases in protein level when FIP200 is deleted (Fig. 3.1A) (Hara et al, 2008). Atg7, another essential autophagy gene, is decreased dramatically in FIP200 LKO (Fig. 3.1A).

3.3.2 Lipid content does not increase under chronic or acute deletion of FIP200 regardless of dietary conditions

To test whether hepatic lipid metabolism is affected by autophagy deficiency, we first examined the liver triglyceride (TG) content in chow fed FIP200 LKO and control mice under random fed and 16-h fasted conditions. Under fed condition, lipid droplet deposition in the liver is very low in both FIP200 LKO and control mice (Fig. 3.2A, B). Under fasted condition, the surging influx of free fatty acid from adipose tissue boosts triglyceride synthesis in the liver. While a significant increase in lipid accumulation occurs in control mice, the lipid content in FIP200 LKO liver only mildly increases by fasting (Fig. 3.2B).

This dramatic difference can be also visualized as lipid droplet amount in the liver section using Oil Red O staining (Fig. 3.2A). Consistent with the idea that TG secretion is proportional to the lipid in the liver, plasma TG are also lower in knockout mice (Fig. 3.2C).

To examine whether autophagy deficiency can cause further lipid accumulation under obese condition, we measured liver TG in control and FIP200 LKO mice under fed condition and 16-fasted condition after feeding high-fat diet for 5 weeks. As shown in Fig. 3.2E, liver TG content in FIP200 LKO is similar to control in fed condition and is significantly lower under fasted condition. This can also be observed in Oil Red O staining (Fig. 3.2D). The decrease of liver TG content in FIP200 LKO does not appear to be caused by increased VLDL secretion, as the plasma TG does not differ among groups (Fig. 3.2F).

To exclude the possibility that chronic absence of FIP200 affects food absorption, we tested our hypothesis in mice that are deleted with FIP200 after 1-month high-fat feeding. As FIP200 flox/flox mice were equally fed with high-fat diet before the injection, the fat loads should be comparable in the two groups. After feeding high-fat diet for a month, we injected these mice with either GFP or Cre adenovirus, which specifically infects liver. As expected, autophagic degradation is blocked in the mouse livers infected with Cre virus (Fig. 3.3A). In this acute FIP200 deficiency model, we also observed a decrease of TG contents in Cre infected mouse livers (Fig. 3.3B, C). This finding suggests the decrease in

liver TG is a specific effect of autophagy deficiency.

3.3.3 Autophagy is essential for preventing liver injury, inflammation and progression to fibrosis

Although autophagy deficiency in FIP200 mouse model is not sufficient to cause hepatic steatosis, it could still be crucial in determining the progression to NASH. So we first examined liver injury by measuring serum aminotransferase activity, Aspartate Aminotransferase (AST) and Alanine Aminotransferase (ALT). We observed a 22-fold and 6-fold induction in FIP200 LKO's ALT and AST respectively (Fig. 3.4A, B). We then performed real-time PCR analysis to examine the mRNA expression of genes involved in inflammation and liver fibrosis. The expression of Acta2, Ccl5, Ccl2, Tgfb1, Col1a1, and Mmp13 are all significantly elevated in FIP200 LKO livers (Fig. 3.4C). In addition, we examined the phosphorylation of JNK at T183 and Y185 sites, an indicator for cell stress. We found a dramatic increase in phosphorylated JNK in FIP200 LKO liver lysates, while the total JNK amount remains the same (Fig. 3.4D). The results of all three analyses point to a more severe liver injury, inflammation, and higher chance of developing liver fibrosis.

To provide histological evidences to support this notion, we performed hematoxylin and eosin stain (H&E stain) to stain the nucleus and cellular structures. We found a strikingly large number of inflammatory cells in FIP200 LKO livers, which is absence in control, even though all of them were fed with high-fat diet (Fig. 3.4E). Furthermore, we performed

Sirius Red Collagen Staining, counterstained proteins with Fast Green (Fig. 3.4F). In the FIP200 LKO liver sections, we observed chicken-wire pattern with collagen surrounding hepatocytes indicating pericellular fibrosis as well as portal-portal bridging fibrosis (Fig. 3.4G). We conclude that hepatic autophagy activity is essential to prevent liver injury and fibrosis.

3.3.4 Short-term knockdown of Atg7 or acute inhibition of lysosomal degradation increases liver injury

To further demonstrate that autophagy deficiency is insufficient to lead to lipid accumulation, we obtained the shAtg7 adenovirus from the Hotamisligil lab (Yang et al, 2010). We first confirmed the knock-down efficiency of shAtg7 adenovirus *in vivo*. As expected, LC3 and p62 trends higher in shAtg7 treated mouse livers (data not shown). Then we compared the liver TG in shAtg7 treated mice with scrambled shRNA treated mice. Under both chow and high-fat diet fed conditions, liver TG does not increase in shAtg7 treated mice (Fig. 3.S2A, Fig. 3.5A). This observation indicates that at least short-term suppression of autophagy through Atg7 knockdown is not sufficient to cause lipid accumulation. This is somewhat consistent with previous report showing liver TG is decreased under fasted condition in Atg7 knockout mice at P22 and 8-week-old (Shibata et al, 2009).

We then examined whether short-term Atg7 knock-down can cause liver injury. We

measured plasma ALT and AST in both chow and high-fat diet fed mice. Under both situations, Atg7 knock-down mice show significantly more severe liver injury (Fig. 3.S2C, D, and Fig. 3.5C, D).

To further study whether autophagy deficiency can serve as a 'hit' in promoting the progression to NASH, we examined the effect of autophagy inhibition in High-fat/LPS model, a 'two-hit' NASH model mimicking the challenge from excessive lipid and leaking gut (Hebbard & George, 2011). When we inhibited autophagy flux by leupeptin, a chemical inhibitor of lysosomal H+ pump, we observed a robust accumulation of LC3-II, indicating that the autophagy flux is dramatically suppressed (Fig. 3.5E). Interestingly, when we injected the high-fat diet fed mice with LPS, the autophagy flux increases (Fig. 3.5E). This may suggest a need for activating autophagy flux to respond to bacteria invasion. We then evaluated the liver injury by measuring ALT and AST level in the plasma. In contrast to the mild induction of ALT and AST value by LPS treatment alone or leupeptin treatment alone, the combination of leupeptin and LPS treatment leads to a synergetic boost in liver injury (Fig. 3.5F, G). This result indicates that autophagy may be required to guard liver from not only intracellular stress but also intestinal bacteria insult. This finding suggests that autophagy deficiency can be an important trigger for the progression to NASH.

3.4 Discussion

In this study, we examined the role of autophagy in formation and progression of NAFLD.

We found that autophagy deficiency is not sufficient to lead to hepatic steatosis. Nonetheless, autophagy deficiency could be an important trigger that determines the progression from NAFL to NASH.

A number of reports have proposed a tight relationship between autophagy and lipid metabolism. The dominant working hypothesis is that autophagosomes directly sequester entire or a portion of lipid droplet and deliver it for degradation in lysosome. Before the discovery of this novel lipolysis model, lipid droplets were degraded through cytosolic lipases, including adipose triglyceride lipase (ATGL), hormone-sensitive lipase (HSL), and monoacylglycerol lipase (MGLL) (Walther & Farese, 2012). After the first report on removal of lipid droplet by autophagy, several publications mentioned the findings of hepatic lipid accumulation in different autophagy deficiency mouse models (Jaber et al, 2012; Takamura et al, 2011; Xiong et al, 2012).

However, the field requires further scrutiny for the following three reasons. First, it is unclear whether the age of mice plays a role in lipid accumulation phenotype in autophagy deficiency mouse model. For example, Atg7 knockout mice do not have increased liver triglyceride content at all ages. Kominami and Uchiyama lab has reported decreased liver triglyceride content in Atg7 knockout mice under fasting condition at P22 and 8-week-old (Shibata et al, 2009). Second, it remains uncharacterized whether chronic liver damage or other pathology could alter hepatic lipid metabolism in the mouse models. For example,

increased lipid accumulation in Atg5 mosaic knockout mice was observed at 19 month old, whereas multiple tumors have already formed in the liver since 12 month old (Takamura et al, 2011). In another example of Vps34 liver specific knockout mice, although increased lipid accumulation was observed in these mice, the significantly smaller size of knockout mice indicates a systematic defect, putting the comparison under question (Jaber et al, 2012). Third, our results using long term as well as short term liver specific FIP200 knockout mice under various dietary conditions indicate autophagy deficiency is not sufficient to lead to excess lipid accumulation. We strengthened our conclusion by performing experiments in liver specific Atg7 knockdown mice. Based on these three reasons, it will be very helpful for the field to examine lipid phenotype in different autophagy deficiency models side by side under the same age, health condition, and nutritional condition.

Although the relationship between autophagy and lipid metabolism seems to be complicated, abundant evidences indicate autophagy is essential for liver health and autophagy deficiency could be a trigger for progression to NASH. Hepatic deletion of Atg5 or Atg7 leads to the accumulation of p62-dependent protein aggregates (Komatsu et al, 2007; Komatsu et al, 2005; Ni et al, 2012). In addition, Atg5 mosaic knockout mice and Atg7 liver specific knockout mice have been found to develop liver tumors at about 1 year old (Inami et al, 2011; Takamura et al, 2011). In our study, we observed the development of NASH in FIP200 liver specific knockout mice, which could be the early stage before liver

tumors. We proposed that during the progression from NAFL to NASH, the deficiency of autophagy derived from genetic, nutritional, or chemical causes, could synchronize with other 'hits' to boost the transition. Further examination on autophagy activity in human NAFLD patients, deeper GWAS analysis in patients with liver diseases, and the identification of autophagy-suppressing nutritional or chemical stimuli are needed to fully strengthen this model. In addition, given several drugs can promote autophagy activity, this model may point to a new direction of therapy to prevent progression to NASH.

3.5 Materials and methods

Animals - All animal experiments were performed according to procedures approved by the University Committee on Use and Care of Animals. The strain of FIP200 flox/flox mice was a gift from Jun-lin Guan Lab (Gan et al, 2006). Albumin-Cre mice were purchased from Jackson Laboratory. High-fat diet used for experiment is purchased from Research Diets (D12492). Genotyping of FIP200 LKO using primer P1, P2, and P3 follows previous protocol (Gan et al, 2006). For High fat/LPS model, wild type male mice were fed with high fat diet for 1 month. On the day of harvest, the mice were injected intraperitoneally a single dose of LPS or saline (0.8mg/kg) at 11am and a single dose of leupeptin (40mg/kg) or phosphate-buffered saline (PBS) at 2pm. Tissues were harvested at 5pm and food was restricted during 2-5pm.

In vivo adenoviral transduction and metabolic analyses - 3-month-old FIP200 flox/flox

male mice (3–5 per group) fed with high-fat diet for 1 month were transduced with purified GFP or Cre adenoviruses through tail vein injection (0.2 OD per mouse), as previously described (Li et al, 2008). The mice were harvested 7 days post infection under 16h-fasted condition. For Atg7 knock-down experiments, siAtg7 adenovirus was generated by Hotamisligil Lab (Yang et al, 2010). Wild type male mice fed with either chow or high-fat diet were transduced with purified scrambled (0.18OD per mouse) or siAtg7 (0.1OD per mouse) adenovirus through tail vein. The mice were harvested 6 days post infection under 16h-fasted condition. The titres of all adenoviruses were determined based on the expression of GFP and adenoviral gene AdE4 before use to ensure similar doses were administered in the studies. Triglyceride, AST, ALT concentrations were measured using commercial assay kits (Sigma, Stanbio Laboratory).

Protein and RNA analysis - Immunoblotting studies were performed using specific antibodies for FIP200 (10043-2-AP, Proteintech Group), LC3 (LC3-5F10, Nanotools), p62 (PW9860, Enzo Life Sciences), Ulk1 (A7481, Sigma), and Atg7 (AP1813b, Abgent). The fractionation of liver lysates to separate soluble and insoluble proteins was performed following published protocol (Waguri & Komatsu, 2009). Hepatic gene expression was analyzed by qPCR using specific primers in Table 3.S1. Data represent mean±SE.

Transmission electron microscopy - 2-month-old control and FIP200 LKO male mice were first perfused with Sorensen's buffer (0.1 M, pH 7.4) and then Karnovsky's fixative

buffer. The liver is post-fixed in Karnovsky's fixative buffer for 24–48 h before embedding. The sample preparation for EM was performed by Microscopy and Image Analysis Laboratory at University of Michigan. The images were taken by Philips CM-100 transmission electron microscope.

Immunohistochemistry, H&E, Oil Red O staining, and Sirius Red staining -

Paraffin-embedded tissue sections were deparaffinized in xylene, then rehydrated through a graded ethanol series (100, 95, 80, and 70%). Immunohistochemistry using antibodies against p62 (PW9860, Enzo Life Sciences), Tom20 (sc-11415, Santa Cruz BioTech), or Ubiquitin (P4D1, sc-8017, Santa Cruz BioTech) were performed after microwave antigen retrieval (20 min) in 10 mM sodium citrate. A 5% solution of bovine serum albumin in PBS with 0.5% Tween 20 was used as blocking buffer. Sections were incubated with the primary antibodies overnight at 4 degree. Immunoperoxidase staining was detected using the Vectastain Elite ABC and the diaminobenzidine substrate kits according to manufacturer's instructions (Vector Laboratories, Burlingame, CA). Nuclei were counterstained with Gill's hematoxylin. For Sirius Red staining, paraffin sections were de-waxed and hydrated. Then stain nuclei with haematoxylin for 8 minutes, and wash the slides for 10 minutes in running tap water. Stain in picro-sirius red for one hour. After that, wash in two changes of acidified water and dehydrate in three changes of 100% ethanol. Clear in xylene and mount in a resinous medium. H&E staining and Oil Red O staining were performed as previously

described (Ma et al, 2010).

3.6 Acknowledgements

We would like to thank Dr. Jun-lin Guan for their generous gift of FIP200 flox/flox mice and Dr. Gökhan S. Hotamisligil for shAtg7 adenovirus. We are grateful to Drs. Alan Saltiel, Daniel Klionsky, Diane Fingar, Ken Inoki, Elizabeth Speliotes and lab members for discussions. We thank Dotty Sorenson and the Microscopy & Image Analysis Laboratory of University of Michigan for technical support on EM study. The Atg7 knockdown experiments, HFD/LPS experiments and several plasma measurements were performed by Matthew Molusky. This work was supported by the National Institutes of Health.

Table. 3.S1. qPCR primer list.

	Forward primer	Reverse primer
Acta2	CTGACAGAGGCACCACTGAA	CATCTCCAGAGTCCAGCACA
Ccl5	TGCCCACGTCAAGGAGTATTT	TTCTCTGGGTTGGCACACACT
Ccl2	AGGTCCCTGTCATGCTTCTG	TCTGGACCCATTCCTTCTTG
Il1b	AGTTGCCTTCTTGGGACTGA	TCCACGATTTCCCAGAGAAC
Tgfb1	ACCATGCCAACTTCTGTCTGGGAC	ACAACTGCTCCACCTTGGGCTTG
Col1a1	AAGAGGCGAGAGAGGTTTCC	AGAACCATCAGCACCTTTGG
Mmp13	TGCTTCCTGATGATGACGTTCAAGG	TGGGATGCTTAGGGTTGGGGTC

Fig. 3.1. FIP200 LKO mice have defective autophagic degradation in the liver. (A) Protein expression of autophagy genes in the liver and heart of control and FIP200 LKO. Ponceau S stain serves as an internal control. (B) *In vivo* liver autophagy flux assay of control and FIP200 LKO. The amount of increase of LC3-II by leupeptin injection represents the autophagy flux. * refers to a non-specific band. (C) Immuno-staining of p62 or ubiquitin in liver sections of control and FIP200 LKO mice. The slides were counter-stained with H&E (for p62) or Hematoxylin (for ubiquitin). Scale bar represents 40μm. (D) Protein expression of ubiquitin, p62, and LC3 in soluble and insoluble fractions of liver lysates from control and FIP200 LKO mice. Ponceau S stain serves as an internal control. (E) Electron microscopy image showing abnormal intracellular structures only present in FIP200 LKO mouse liver. Red arrows point to abnormal vacuoles containing a large number of small vesicles and structures similar to multilamellar bodies (MLBs). Scale bar under the left image represents 0.5μm.

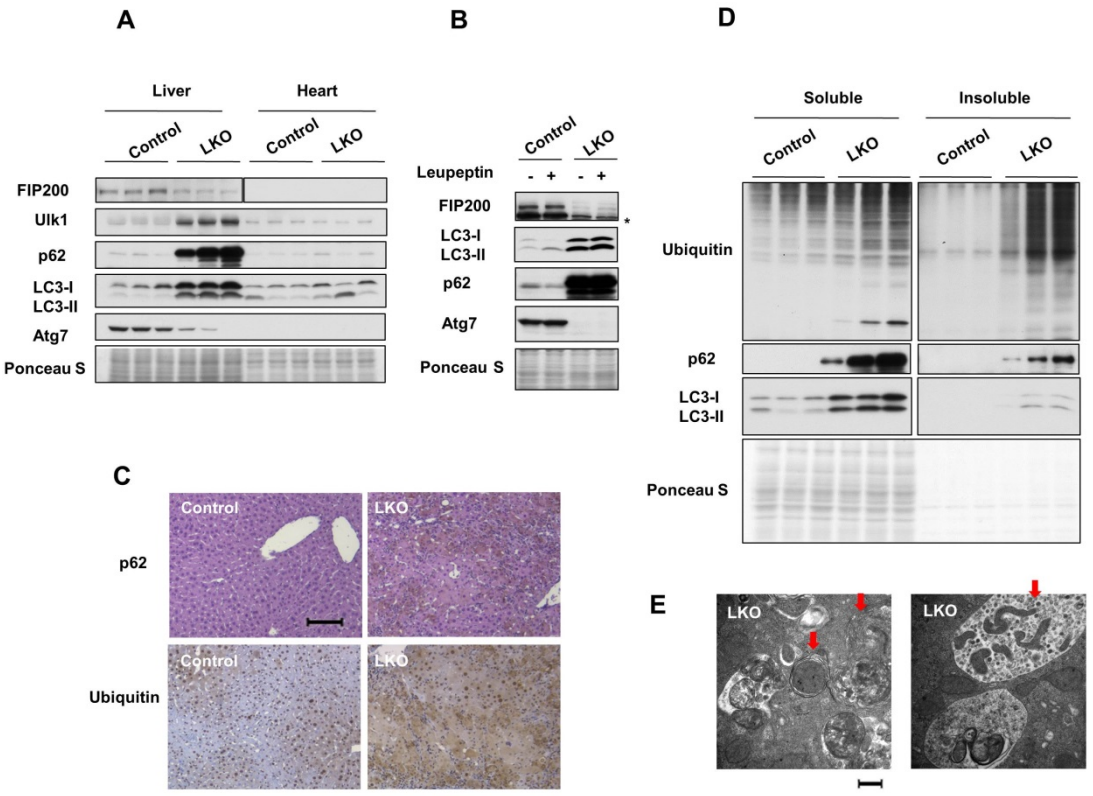

Fig. 3.2. Lipid content does not increase under chronic deletion of FIP200 regardless of dietary conditions. (A) Oil Red O staining of liver sections from control and FIP200 LKO mice under fed or fasted condition. Scale bar represents 100μm. The third row shows the enlarged images from insets of the images in second row. Scale bar represents 20μm. (B) and (C) Liver triglyceride content (B) and plasma triglyceride level (C) of control and FIP200 LKO mice under fed or fasted condition. Data represent mean ± SE. Student's t-test was applied. * $p<0.05$, ** $p<0.01$, *** $p<0.001$. (D) Oil Red O staining of liver sections from control and FIP200 LKO mice fasted overnight after 7-week high fat diet feeding. Scale bar represents 40μm. (E) and (F) Liver triglyceride content (E) and plasma triglyceride level (F) of control and FIP200 LKO mice under fed or fasted condition after 4-week high fat diet. Data represent mean ± SE. Student's t-test was applied. ** $p<0.01$.

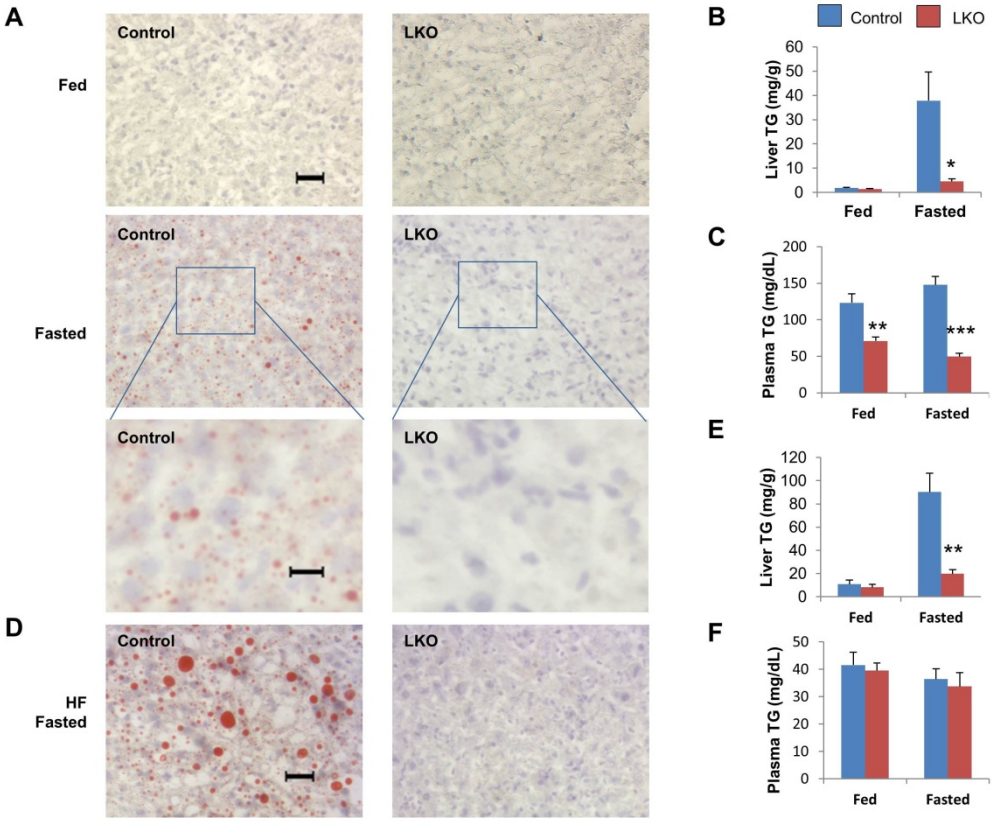

Fig. 3.3. Lipid content does not increase under acute deletion of FIP200 after 1-month high fat diet. (A) Protein expression in liver lysates of GFP or Cre infected FIP200 flox/flox mice. Ponceau S stain serves as an internal control.(B) Liver triglyceride content of GFP or Cre infected FIP200 flox/flox mice. Data represent mean ± SE. Student's t-test was applied. * $p<0.05$. (C) Oil red O staining of liver sections from GFP or Cre infected FIP200 flox/flox mice. Scale bar represents 40μm.

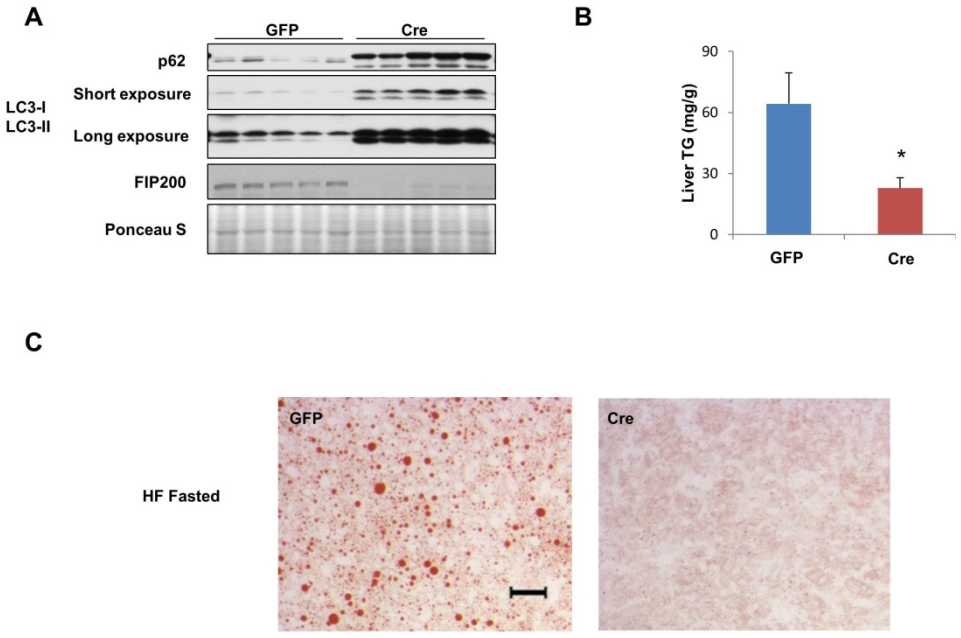

Fig. 3.4. Autophagy deficiency in FIP200 liver specific knockout mice causes increased inflammation and liver injury leading to hepatic fibrosis. (A) and (B) Serum ALT level (A) and AST level (B) in control and FIP200 LKO mice. Data represent mean ± SE. Student's t-test was applied. * $p<0.05$. ** $p<0.01$. (C) qPCR analysis on mRNA expression of genes involved in inflammation and fibrosis. Data represent mean ± SE. Student's t-test was applied. * $p<0.05$, ** $p<0.01$. (D) Phosphorylation of JNK on T183/Y185 sites in liver lysates of control and FIP200 LKO mice. Total JNK and ponceau S stain serve as positive controls. (E) H&E stain of liver sections from control and FIP200 LKO mice after high fat diet feeding for 4 weeks. Red arrow points to clusters of inflammatory cells. Scale bar represents 100μm. (F) Sirius Red/Fast Green staining of liver sections from control and FIP200 LKO mice after high fat diet feeding for 4 weeks. Red arrow points to collagen deposits. Scale bar represents 500μm.

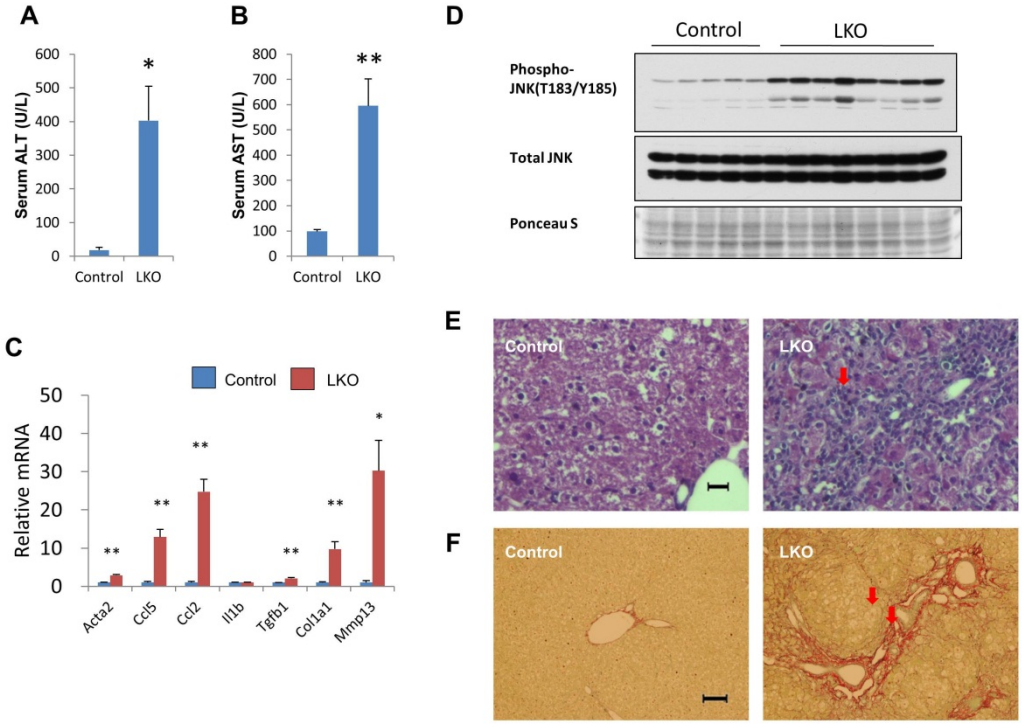

Fig. 3.5. Short-term knockdown of Atg7 or acute inhibition of lysosomal degradation causes liver injury. (A)-(D) Liver triglyceride content (A), plasma triglyceride level (B), plasma ALT level (C), and plasma AST level (D) of fasted high fat diet fed mice infected with shRNA against Atg7 or scrambled (Scrb) RNA. Data represent mean ± SE. Student's t-test was applied. * $p<0.05$. (E) Protein expression of LC3 in liver lysates of high fat diet fed mice injected with saline/PBS, saline/leupeptin, LPS/PBS, and LPS/leupeptin. Ponceau S serves as an internal control. (F)-(G) Plasma AST level (F) and plasma ALT level (G) of mice examined in E. Data represent mean ± SE. Student's t-test was applied. * $p<0.05$, ** $p<0.01$, *** $p<0.001$. (H) Model depicting the potential role of autophagy in the progression of NASH.

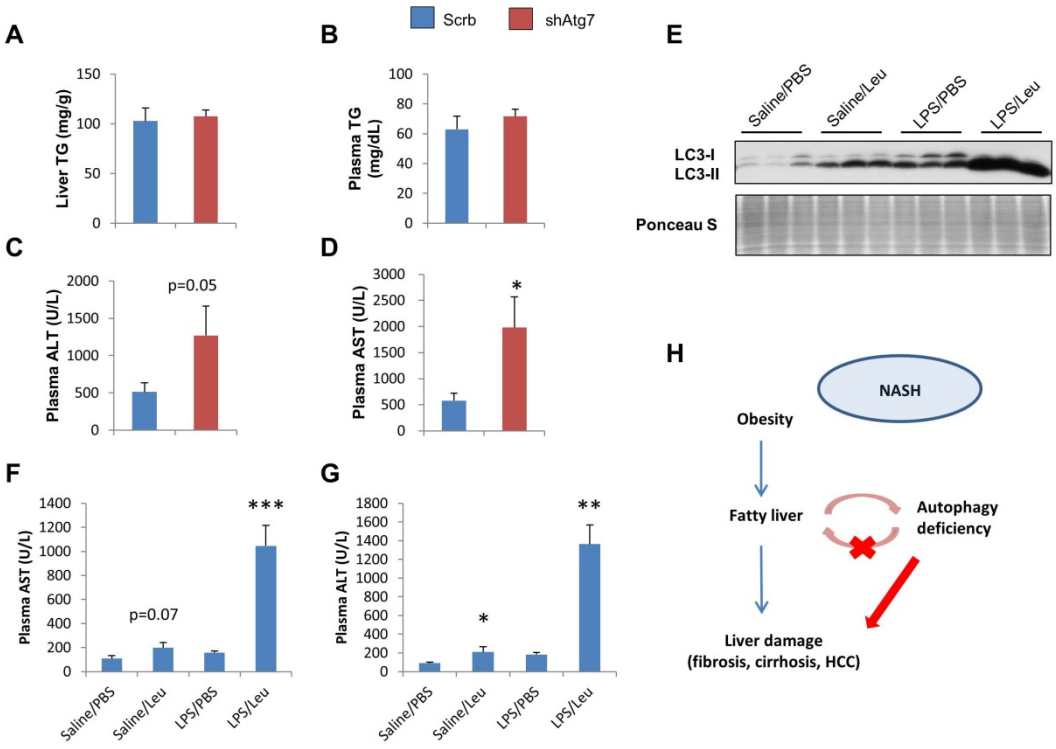

Fig. 3.S1. FIP200 is deleted in the liver of Albumin-Cre;FIP200 flox/flox mice. (A) genotyping of Albumin-Cre;FIP200 flox/flox mice. P1, P2, and P3 refer to three primers previously used (Gan et al, 2006). P2 and P3 amplify franking flox region. The weaker flox allele band in FIP200 LKO liver may be derived from non-hepatocytes in the liver. P1 and P3 confirm the deletion of floxed region. (B) FIP200 protein expression in livers of control and FIP200 LKO mice. The size of FIP200 is confirmed by comparing with the overexpressed FIP200 in cell culture lysates. Ponceau S stain serves as an internal control. * refers to a non-specific band.

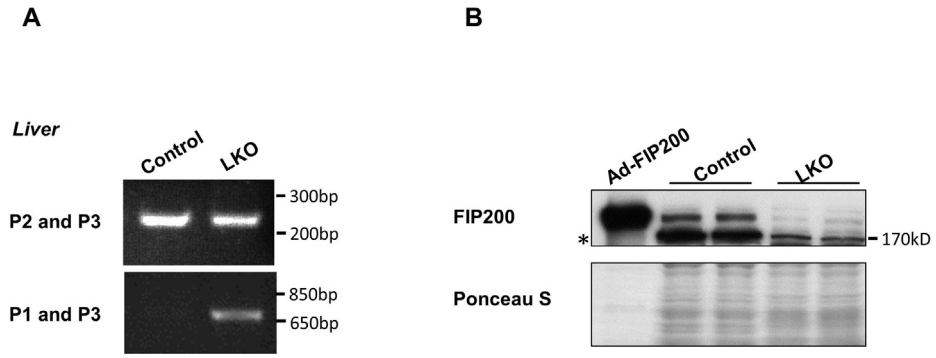

Fig. 3.S2. Atg7 knockdown in chow fed mice is not sufficient to cause lipid accumulation under fasted condition, but it leads to liver injury. (A)-(D) Liver triglyceride content (A), plasma triglyceride level (B), plasma ALT level (C), and plasma AST level (D) of fasted chow fed mice infected with shRNA against Atg7 or scrb RNA. Data represent mean ± SE. Student's t-test was applied. * $p<0.05$, ** $p<0.01$.

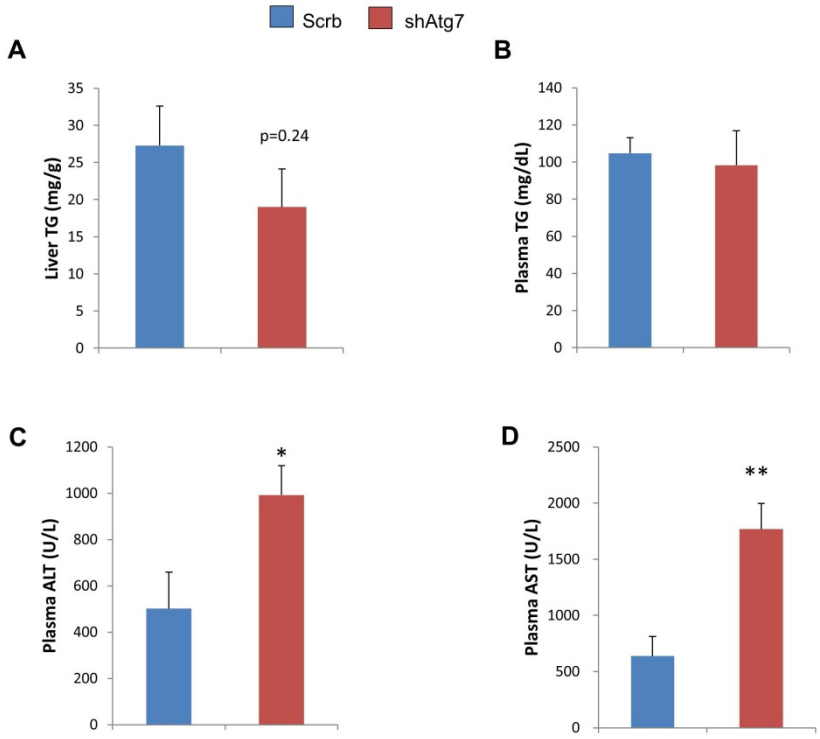

3.7 References

Chalasani N, Guo X, Loomba R, Goodarzi M, Haritunians T, Kwon S, Cui J, Taylor K, Wilson L, Cummings O, Chen Y-DI, Rotter J, Nonalcoholic Steatohepatitis Clinical Research N (2010) Genome-wide association study identifies variants associated with histologic features of nonalcoholic Fatty liver disease. *Gastroenterology* **139:** 1567

Gan B, Peng X, Nagy T, Alcaraz A, Gu H, Guan J-L (2006) Role of FIP200 in cardiac and liver development and its regulation of TNFalpha and TSC-mTOR signaling pathways. *J Cell Biol* **175:** 121-133

Hara T, Takamura A, Kishi C, Iemura S-I, Natsume T, Guan J-L, Mizushima N (2008) FIP200, a ULK-interacting protein, is required for autophagosome formation in mammalian cells. *J Cell Biol* **181:** 497-510

Hebbard L, George J (2011) Animal models of nonalcoholic fatty liver disease. *Nature reviews Gastroenterology & hepatology* **8:** 35-44

Inami Y, Waguri S, Sakamoto A, Kouno T, Nakada K, Hino O, Watanabe S, Ando J, Iwadate M, Yamamoto M, Lee M-S, Tanaka K, Komatsu M (2011) Persistent activation of Nrf2 through p62 in hepatocellular carcinoma cells. *J Cell Biol* **193:** 275-284

Jaber N, Dou Z, Chen J-S, Catanzaro J, Jiang Y-P, Ballou L, Selinger E, Ouyang X, Lin R, Zhang J, Zong W-X (2012) Class III PI3K Vps34 plays an essential role in autophagy and in heart and liver function. *Proc Natl Acad Sci U S A* **109:** 2003-2008

Koga H, Kaushik S, Cuervo A (2010) Altered lipid content inhibits autophagic vesicular fusion. *Faseb J* **24:** 3052-3065

Komatsu M, Kurokawa H, Waguri S, Taguchi K, Kobayashi A, Ichimura Y, Sou Y-S, Ueno I, Sakamoto A, Tong K, Kim M, Nishito Y, Iemura S-i, Natsume T, Ueno T, Kominami E, Motohashi H, Tanaka K, Yamamoto M (2010) The selective autophagy substrate p62 activates the stress responsive transcription factor Nrf2 through inactivation of Keap1. *Nature cell biology* **12:** 213-223

Komatsu M, Waguri S, Koike M, Sou Y-S, Ueno T, Hara T, Mizushima N, Iwata J-I, Ezaki J, Murata S, Hamazaki J, Nishito Y, Iemura S-I, Natsume T, Yanagawa T, Uwayama J, Warabi E, Yoshida H, Ishii T, Kobayashi A et al (2007) Homeostatic levels of p62 control cytoplasmic inclusion body formation in autophagy-deficient mice. *Cell* **131:** 1149-1163

Komatsu M, Waguri S, Ueno T, Iwata J, Murata S, Tanida I, Ezaki J, Mizushima N, Ohsumi Y, Uchiyama Y, Kominami E, Tanaka K, Chiba T (2005) Impairment of starvation-induced

and constitutive autophagy in Atg7-deficient mice. *J Cell Biol* **169:** 425-434

Li S, Liu C, Li N, Hao T, Han T, Hill DE, Vidal M, Lin JD (2008) Genome-wide coactivation analysis of PGC-1alpha identifies BAF60a as a regulator of hepatic lipid metabolism. *Cell Metab* **8:** 105-117

Ma D, Li S, Lucas E, Cowell R, Lin J (2010) Neuronal inactivation of peroxisome proliferator-activated receptor γ coactivator 1α (PGC-1α) protects mice from diet-induced obesity and leads to degenerative lesions. *J Biol Chem* **285:** 39087-39095

Ma D, Panda S, Lin J (2011) Temporal orchestration of circadian autophagy rhythm by C/EBPβ. *EMBO J* **30:** 4642-4651

Mizushima N, Komatsu M (2011) Autophagy: renovation of cells and tissues. *Cell* **147:** 728-741

Ni H-M, Boggess N, McGill M, Lebofsky M, Borude P, Apte U, Jaeschke H, Ding W-X (2012) Liver-specific loss of Atg5 causes persistent activation of Nrf2 and protects against acetaminophen-induced liver injury. *Toxicological sciences : an official journal of the Society of Toxicology* **127:** 438-450

Pagliassotti M (2012) Endoplasmic reticulum stress in nonalcoholic fatty liver disease. *Annu Rev Nutr* **32:** 17-33

Polyzos S, Kountouras J, Zavos C, Deretzi G (2012) Nonalcoholic fatty liver disease: multimodal treatment options for a pathogenetically multiple-hit disease. *Journal of clinical gastroenterology* **46:** 272-284

Shibata M, Yoshimura K, Furuya N, Koike M, Ueno T, Komatsu M, Arai H, Tanaka K, Kominami E, Uchiyama Y (2009) The MAP1-LC3 conjugation system is involved in lipid droplet formation. *Biochem Biophys Res Commun* **382:** 419-423

Singh R, Kaushik S, Wang Y, Xiang Y, Novak I, Komatsu M, Tanaka K, Cuervo A, Czaja M (2009) Autophagy regulates lipid metabolism. *Nature* **458:** 1131-1135

Speliotes E, Yerges-Armstrong L, Wu J, Hernaez R, Kim L, Palmer C, Gudnason V, Eiriksdottir G, Garcia M, Launer L, Nalls M, Clark J, Mitchell B, Shuldiner A, Butler J, Tomas M, Hoffmann U, Hwang S-J, Massaro J, O'Donnell C et al (2011) Genome-wide association analysis identifies variants associated with nonalcoholic fatty liver disease that have distinct effects on metabolic traits. *PLoS Genet* **7**

Stefano R, Julia K, Chao X, Alexander P, David C, Len AP, Eric B, Jonathan CC, Helen HH

(2008) Genetic variation in PNPLA3 confers susceptibility to nonalcoholic fatty liver disease. *Nature Genetics* **40**

Strnad P, Zatloukal K, Stumptner C, Kulaksiz H, Denk H (2008) Mallory-Denk-bodies: lessons from keratin-containing hepatic inclusion bodies. *Biochimica et biophysica acta* **1782:** 764-774

Takamura A, Komatsu M, Hara T, Sakamoto A, Kishi C, Waguri S, Eishi Y, Hino O, Tanaka K, Mizushima N (2011) Autophagy-deficient mice develop multiple liver tumors. *Genes Dev* **25:** 795-800

Waguri S, Komatsu M (2009) Biochemical and morphological detection of inclusion bodies in autophagy-deficient mice. In *Methods in enzymology, Volume 453: Autophagy in disease and clinical applications. Part C*, Klionsky DJ (ed). San Diego, Calif.: Academic Press/Elsevier

Walther T, Farese R (2012) Lipid droplets and cellular lipid metabolism. *Annu Rev Biochem* **81:** 687-714

Xiong X, Tao R, Depinho R, Dong X (2012) The Autophagy-related Gene 14 (Atg14) Is Regulated by Forkhead Box O Transcription Factors and Circadian Rhythms and Plays a Critical Role in Hepatic Autophagy and Lipid Metabolism. *J Biol Chem* **287:** 39107-39114

Yang L, Li P, Fu S, Calay E, Hotamisligil G (2010) Defective hepatic autophagy in obesity promotes ER stress and causes insulin resistance. *Cell Metab* **11:** 467-478

Yang Z, Klionsky D (2010) Eaten alive: a history of macroautophagy. *Nature cell biology* **12:** 814-822

Zatloukal K, French S, Stumptner C, Strnad P, Harada M, Toivola D, Cadrin M, Omary M (2007) From Mallory to Mallory-Denk bodies: what, how and why? *Experimental cell research* **313:** 2033-2049

CHAPTER 4 CONCLUSIONS AND FUTURE DIRECTIONS

4.1 Summary

Autophagy is an essential cellular process responsible for eliminating long half-life proteins, protein aggregates, damaged organelles, and pathogens. However, how autophagy is regulated by physiological signals and its significance in hepatic metabolism remain incompletely understood.

In this thesis, we first explored the temporal regulation of autophagy and its underlying mechanisms. By examining autophagy flux at a series of time points throughout 24 hours, we found that autophagy is most active during the day time. Meanwhile, we discovered that the expression of genes involved in autophagy pathways displays an unexpected oscillatory pattern throughout the light/dark cycles. These observations led us to examine the transcriptional regulation of autophagy circadian rhythm. Functional screening of transcription factors important for clock or nutritional signaling resulted in the identification of C/EBPβ as a potent regulator of autophagy. C/EBPβ overexpression is sufficient to induce autophagy in primary hepatocytes, and it is required for normal autophagy activity. Moreover, its mRNA expression is regulated by both clock and nutritional signals. Our data indicates that C/EBPβ is an essential mediator for clock and

nutritional signals to regulate autophagy circadian rhythm. In the following discussion (Chapter 4.2.1-4.2.3), I will elaborate on our experiments that support key conclusions, and propose three potential functions that autophagy circadian rhythm may play in maintaining hepatic homeostasis.

In addition to studying circadian regulation of autophagy, we examined the role of autophagy in hepatic lipid metabolism and non-alcoholic steatohepatitis (NASH). Previous studies suggest that autophagy deficiency may exacerbate lipid accumulation in fatty liver and chronic autophagy deficiency leads to hepatic adenoma (Inami et al, 2011; Takamura et al, 2011; Yang et al, 2010). Based on these data, we set out to test the hypothesis that autophagy contributes to NAFLD formation and progression. We first examined whether autophagy deficiency leads to excessive lipid accumulation. In contrary to the concept that autophagy is responsible for lipid hydrolysis and fat oxidation, we found that autophagy deficiency is not sufficient to cause hepatic steatosis. We then examined whether autophagy is involved in the progression of NAFLD to NASH. Using multiple autophagy inhibition mouse models, we found that autophagy deficiency accelerates the liver injury in NAFLD mouse model. Our results suggest that autophagy deficiency is not sufficient to cause fatty liver and autophagy plays an important role in the progression of NAFLD to NASH. In the following discussion (Chapter 4.2.4-4.2.6), I will focus on our key studies, explore the potential causes for autophagy deficiency, and describe the new direction of therapy for NAFLD by autophagy-enhancing drugs.

4.2 Key conclusions and future directions

4.2.1 The circadian rhythm of autophagy activity

In the 1970s, a series of electron microscopy studies demonstrated that the number of autophagic vacuoles varies throughout the day in several tissues, including the inner segment of retina rod cells, cardiomyocytes, hepatocytes, pancreatic acinar cells, and proximal tubules of kidney in rats (Pfeifer, 1972; Pfeifer & Scheller, 1975; Pfeifer & Strauss, 1981; Reme & Sulser, 1977). In addition, the activity of certain lysosomal hydrolases exhibits diurnal rhythm in the liver (Bhattacharya & von Mayersbach, 1976). Using more specific molecular markers for autophagy, our study indicates that autophagy activity is temporally restricted in several mouse tissues, including the liver, heart, and skeletal muscle (Ma et al, 2011). We used a recently developed method for measuring autophagy activity *in vivo* and found that autophagy flux peaks during the light phase and decreases to lower levels in the dark phase. The cyclic activation of autophagy flux in the liver is associated with changes in autophagosome abundance and rhythmic expression of autophagy genes.

Interestingly, the expressions of autophagy genes also oscillate in the yeast during continuous growth under nutrient-limited conditions (Tu et al, 2005). In this case, autophagy appears to be restricted to a specific temporal phase associated with reductive

metabolic activities. While the timing cues that drive rhythmic autophagy activation in mammalian tissues and in yeast cells are likely different, the autophagy cycles may reflect a conserved property of cellular metabolism and homeostasis.

4.2.2 The regulation of autophagy circadian rhythm

The nature of timing cues that drive circadian autophagy appears to involve both clock and nutritional signals (Ma et al, 2011). Liver-specific Bmal1 null mice, a liver clock deficient model, have dampened rhythm of autophagy gene expression and autophagy flux, suggesting that clock exerts its effects on circadian autophagy, at least in part, through cell-autonomous mechanisms. Nutritional status provides a strong entrainment signal for peripheral tissues. Restriction feeding resets the phase of peripheral clocks in rodents without affecting the central clock (Damiola et al, 2000). Notably, the phase of autophagy gene expression is also reversed following the feeding switch (Ma et al, 2011; Pfeifer, 1972). While meal timing dominantly resets the phase of autophagy rhythm, it remains unknown whether this is secondary to the realignment of clock with feeding status.

In term of molecular mechanism, C/EBPβ plays a crucial role in coordinating rhythmic expression of autophagy genes in response to circadian and nutritional signals (Ma et al, 2011). C/EBPβ is a basic leucine-zipper transcription factor that regulates diverse biological processes, including immune response, cell differentiation, and metabolism (Akira et al, 1990; Cao et al, 1991; Croniger et al, 2001; Tanaka et al, 1995; Wang et al,

2000). The expression of C/EBPβ is highly responsive to nutritional signals and at the same time regulated by the liver clock in a tissue-autonomous manner. Adenoviral-mediated expression of C/EBPβ stimulates the program of autophagy gene expression and induces autophagic protein degradation in cultured hepatocytes. C/EBPβ directly binds to the promoters of autophagy genes and activates their transcription. Knock-down of C/EBPβ abolishes the diurnal autophagy rhythm. Our data indicates C/EBPβ mediates the nutritional and circadian signals in regulating circadian rhythm of autophagy.

4.2.3 What are the metabolic functions of circadian autophagy rhythm?

While it is clear that autophagy is rhythmically activated in the body, it is far from clear regarding the significance of autophagy cycles in physiology and disease. Conceptually, close coupling of autophagic degradation to biological clock may provide distinct advantages for multicellular organisms to maintain nutrient and energy homeostasis, remodel proteomes and organelles, and achieve temporal compartmentalization of tissue metabolism (Fig. 4.1).

Nutrient and energy homeostasis

A major function of autophagy is to degrade cellular components when nutrients become limited. The concentrations of plasma amino acids and metabolites exhibit robust circadian oscillation that is partially mediated through autophagy (Ezaki et al, 2011; Minami et al, 2009). Thus, the cyclic regulation of amino acid concentrations in plasma, liver, and

skeletal muscle is diminished in liver-specific Atg7 deficient mice. Disruption of circadian autophagy rhythm in liver-specific Bmal1 null mice is also associated with impaired hepatic gluconeogenesis and hypoglycemia during late light phase (Lamia et al, 2008), which coincides with peak autophagy flux.

Proteome and organelle remodeling

Rhythmic autophagic induction may be important for temporal remodeling of proteomes and organelles. A surprising finding with regard to the circadian regulation of hepatic proteome and transcriptome came from comparative analysis of diurnal regulation of protein and mRNA expression (Reddy et al, 2006). While up to 20% of soluble proteins assayed in mouse liver exhibit circadian oscillation, nearly half of them lack corresponding mRNA cycles. Additionally, these oscillated proteins tend to peak in the dark phase when autophagy and lysosomal activity is lower, suggesting that circadian autophagy could play a role in proteome remodeling in the liver. Recently, Gachon group reported the circadianly regulated ribosome biogenesis, which occurs in the opposite phase of autophagy and may coordinate the remodeling of proteome (Jouffe et al, 2013). Moreover, the abundance of mitochondria, peroxisomes, and endoplasmic reticulum varies throughout the day, which is likely mediated through cyclic activation of autophagy (Uchiyama, 1990; Youle & Narendra, 2011). The periodical removal of mitochondria and other organelles may facilitate the modulation of the bioenergetic properties throughout different circadian phases.

Temporal compartmentalization of tissue metabolism

Autophagy-mediated proteome and organelle remodeling may provide an important mechanism for the temporal compartmentalization of tissue metabolism. Biological rhythm is an intrinsic cellular property that is conserved from single-cell eukaryotes to different kingdoms of multicellular eukaryotes. Yeast grown under nutrient-limited condition exhibits robust cycles of oxygen consumption and redox changes in the cell (Tu et al, 2005). In each phase, a subset of oscillating genes peaks, including those involved in ubiquitin/proteasome function and autophagy. It is possible that this rhythmic induction of degradation pathways is necessary for large-scale removal of cellular components that paves the way for metabolic phase transition. As such, the metabolic functions in higher organisms are not only restricted to specific tissues, but also compartmentalized along the temporal axis. The cyclic activation of autophagy may remodel cellular proteomes and organelles, thus defining distinct temporal compartments of metabolic activities.

4.2.4 The role of autophagy in non-alcoholic fatty liver disease

NAFLD is a world-wide public health challenge, as a significant portion of NAFLD patients develop liver fibrosis, cirrhosis, and even hepatocellular carcinoma (Polyzos et al, 2012). The turning point of this disease is the progression from a relatively benign form of fatty liver (NAFLD) to steatohepatitis (NASH). Although a variety of factors, including gut-derived bacterial toxins, cytokine imbalance, mitochondrial dysfunction, oxidative

stress, and ER stress, have been proposed to play important roles in the progression, it is still unclear whether a shared mechanism can reconcile these diverse causal factors (Hebbard & George, 2011; Polyzos et al, 2012; Tuyama & Chang, 2012).

Previous studies suggest that autophagy impairments may influence the progression of NAFLD by promoting excessive accumulation of lipid in liver. Indeed, chronic high fat-diet feeding impairs autophagy activity (Yang et al, 2010). On the other hand, autophagy was reported to be directly involved in lipid droplet hydrolysis and fat oxidation (Singh et al, 2009). This raises an interesting possibility that autophagy deficiency can lead to a virtuous cycle in lipid accumulation, which can accelerate NASH progression through promoting ER stress and lipid toxicity.

By using a new mouse model of liver-specific autophagy deficiency (FIP200 LKO), we found that genetic ablation of autophagy itself is not sufficient to lead to lipid accumulation. These results were further confirmed in Atg7 knockdown studies. Nonetheless, we observed that chronic FIP200 deletion in liver causes liver fibrosis. This indicates that autophagy may play a protective role in preventing the progression from fatty liver to more severe forms of NASH. However, this protective role of autophagy is not related to its potential role in maintaining lipid homeostasis. To further confirm the protective role of autophagy, we transiently deleted FIP200, knocked down Atg7, or suppressed autophagy flux in mouse livers. Our data indicates a strong correlation between autophagy deficiency

and liver damage. These results are consistent with the development of liver adenoma in aged Atg5 mosaic mouse model and Atg7 liver knockout model (Inami et al, 2011; Takamura et al, 2011).

4.2.5 How could autophagy activity be compromised in the liver?

We hypothesized that the autophagy activity plays an important role in determining the progression to liver fibrosis. If this hypothesis is true, then figuring out the factors that compromise autophagy activity may help protect NAFLD patients from progression. Here we propose several possible factors that may influence autophagy activity in the liver.

First, excessive lipid accumulation and hepatic insulin resistance may impair autophagy activity. Long-term high fat diet feeding was reported to decrease autophagy flux in the liver (Yang et al, 2010). Our unpublished data on a variety of obesity mouse models supports this notion. It is under investigation how excessive lipid influences autophagy activity. There are currently two working hypotheses. The first one hypothesizes that the cleavage of Atg7 is enhanced in chronic high fat diet fed mice (Yang et al, 2010). Alternatively, it is possible that excessive lipid intake can change the property of lipid on autophagosome membrane, rendering an impaired fusion ability (Koga et al, 2010).

Besides, other environmental factors such as toxins and pathogens derived from intestinal circulation may inhibit autophagy activity. Interestingly, some bacteria can inhibit or delay

autophagosome maturation to promote its replication (Cemma & Brumell, 2012; Choy et al, 2012). However, hepatitis B virus and hepatitis C virus require normal autophagy process for their replication (Ke & Chen, 2011; Sir et al, 2010). Therefore, further study is needed to identify specific pathogen species that suppress autophagy activity in the liver.

Finally, genetic polymorphism may contribute to the susceptibility of autophagy impairment. Recent genome-wide association study (GWAS) discovered an association between autophagy and diseases such as Crohn's disease and tuberculosis (King et al, 2011; Songane et al, 2012; Stappenbeck et al, 2011). Whether autophagy genes associate with the risks of NASH progression is still to be determined.

4.2.6 The potential for autophagy enhancing drug for treating non-alcoholic fatty liver disease

Our study points to a new direction of developing potential therapies to treat NAFLD patients. Autophagy modulating drugs have been tested as potential therapies for conformation disease (Rubinsztein et al, 2012). For example, carbamazepine, an autophagy-enhancing drug, promotes the degradation of toxic protein aggregates formed by mutant α1-antitrypsin Z in the hepatocytes and alleviates the liver injury in the mouse model (Hidvegi et al, 2010). Rapamycin, which activates autophagy by inhibiting mTOR, has shown therapeutical benefits to mouse models with neurodegenerative diseases, including Parkinson’s disease, Huntington's disease, and Alzheimer's disease (Bové et al,

2011). It is of great interest to test whether compounds specifically activating autophagy can provide beneficial effects in animal models and patients with NAFLD.

Fig. 4.1. Autophagy rhythm and diurnal metabolic homeostasis. Rhythmic activation of autophagy is controlled by biological clock as well as nutritional signals, and may contribute to nutrition and energy homeostasis through light/dark cycles, proteome and organelle remodeling, and the temporal compartmentalization of tissue metabolism.

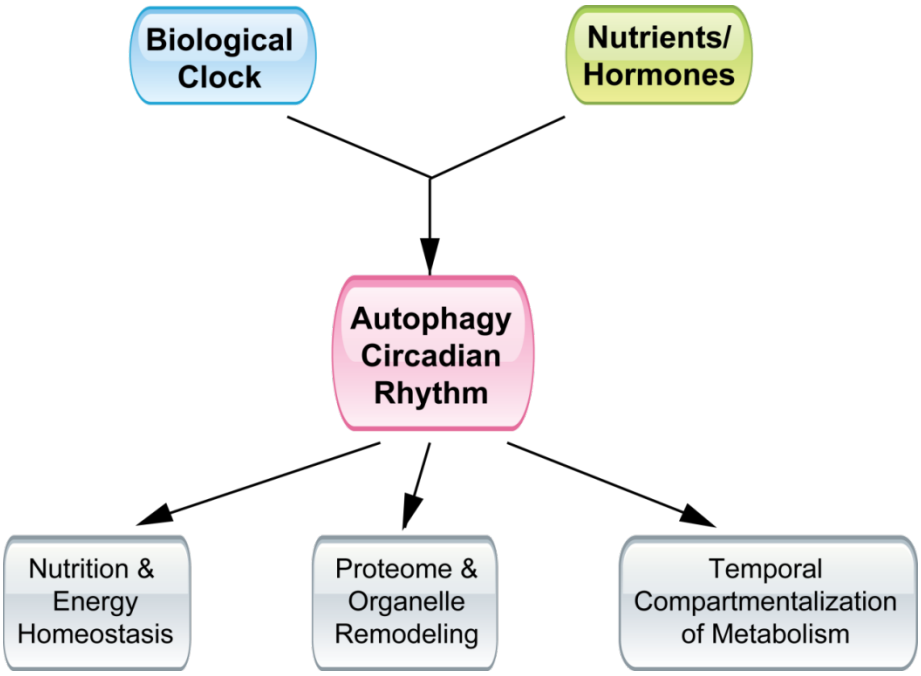

4.3 References

Akira S, Isshiki H, Sugita T, Tanabe O, Kinoshita S, Nishio Y, Nakajima T, Hirano T, Kishimoto T (1990) A nuclear factor for IL-6 expression (NF-IL6) is a member of a C/EBP family. *EMBO J* **9:** 1897-1906

Bhattacharya R, von Mayersbach H (1976) Histochemistry of circadian changes of some lysosomal enzymes in rat liver. *Acta Histochem Suppl* **16:** 109-115

Bové J, Martínez-Vicente M, Vila M (2011) Fighting neurodegeneration with rapamycin: mechanistic insights. *Nature reviews Neuroscience* **12:** 437-452

Cao Z, Umek RM, McKnight SL (1991) Regulated expression of three C/EBP isoforms during adipose conversion of 3T3-L1 cells. *Genes Dev* **5:** 1538-1552

Cemma M, Brumell J (2012) Interactions of pathogenic bacteria with autophagy systems. *Curr Biol* **22:** 5

Choy A, Dancourt J, Mugo B, O'Connor T, Isberg R, Melia T, Roy C (2012) The Legionella effector RavZ inhibits host autophagy through irreversible Atg8 deconjugation. *Science* **338:** 1072-1076

Croniger CM, Millward C, Yang J, Kawai Y, Arinze IJ, Liu S, Harada-Shiba M, Chakravarty K, Friedman JE, Poli V, Hanson RW (2001) Mice with a deletion in the gene for CCAAT/enhancer-binding protein beta have an attenuated response to cAMP and impaired carbohydrate metabolism. *J Biol Chem* **276:** 629-638

Damiola F, Le Minh N, Preitner N, Kornmann B, Fleury-Olela F, Schibler U (2000) Restricted feeding uncouples circadian oscillators in peripheral tissues from the central pacemaker in the suprachiasmatic nucleus. *Genes Dev* **14:** 2950-2961

Ezaki J, Matsumoto N, Takeda-Ezaki M, Komatsu M, Takahashi K, Hiraoka Y, Taka H, Fujimura T, Takehana K, Yoshida M, Iwata J, Tanida I, Furuya N, Zheng DM, Tada N, Tanaka K, Kominami E, Ueno T (2011) Liver autophagy contributes to the maintenance of blood glucose and amino acid levels. *Autophagy* **7:** 727-736

Hebbard L, George J (2011) Animal models of nonalcoholic fatty liver disease. *Nature reviews Gastroenterology & hepatology* **8:** 35-44

Hidvegi T, Ewing M, Hale P, Dippold C, Beckett C, Kemp C, Maurice N, Mukherjee A, Goldbach C, Watkins S, Michalopoulos G, Perlmutter D (2010) An autophagy-enhancing drug promotes degradation of mutant alpha1-antitrypsin Z and reduces hepatic fibrosis.

Science **329:** 229-232

Inami Y, Waguri S, Sakamoto A, Kouno T, Nakada K, Hino O, Watanabe S, Ando J, Iwadate M, Yamamoto M, Lee M-S, Tanaka K, Komatsu M (2011) Persistent activation of Nrf2 through p62 in hepatocellular carcinoma cells. *J Cell Biol* **193:** 275-284

Jouffe C, Cretenet G, Symul L, Martin E, Atger F, Naef F, Gachon F (2013) The circadian clock coordinates ribosome biogenesis. *PLoS biology* **11**

Ke P-Y, Chen S (2011) Activation of the unfolded protein response and autophagy after hepatitis C virus infection suppresses innate antiviral immunity in vitro. *J Clin Invest* **121:** 37-56

King K, Lew J, Ha N, Lin J, Ma X, Graviss E, Goodell M (2011) Polymorphic allele of human IRGM1 is associated with susceptibility to tuberculosis in African Americans. *PloS one* **6**

Koga H, Kaushik S, Cuervo A (2010) Altered lipid content inhibits autophagic vesicular fusion. *Faseb J* **24:** 3052-3065

Lamia KA, Storch KF, Weitz CJ (2008) Physiological significance of a peripheral tissue circadian clock. *Proc Natl Acad Sci U S A* **105:** 15172-15177

Ma D, Panda S, Lin J (2011) Temporal orchestration of circadian autophagy rhythm by C/EBPβ. *EMBO J* **30:** 4642-4651

Minami Y, Kasukawa T, Kakazu Y, Iigo M, Sugimoto M, Ikeda S, Yasui A, van der Horst GT, Soga T, Ueda HR (2009) Measurement of internal body time by blood metabolomics. *Proc Natl Acad Sci U S A* **106:** 9890-9895

Pfeifer U (1972) Inverted diurnal rhythm of cellular autophagy in liver cells of rats fed a single daily meal. *Virchows Arch B Cell Pathol* **10:** 1-3

Pfeifer U, Scheller H (1975) A morphometric study of cellular autophagy including diurnal variations in kidney tubules of normal rats. *J Cell Biol* **64:** 608-621

Pfeifer U, Strauss P (1981) Autophagic vacuoles in heart muscle and liver. A comparative morphometric study including circadian variations in meal-fed rats. *J Mol Cell Cardiol* **13:** 37-49

Polyzos S, Kountouras J, Zavos C, Deretzi G (2012) Nonalcoholic fatty liver disease: multimodal treatment options for a pathogenetically multiple-hit disease. *Journal of*

clinical gastroenterology **46:** 272-284

Reddy AB, Karp NA, Maywood ES, Sage EA, Deery M, O'Neill JS, Wong GK, Chesham J, Odell M, Lilley KS, Kyriacou CP, Hastings MH (2006) Circadian orchestration of the hepatic proteome. *Curr Biol* **16:** 1107-1115

Reme CE, Sulser M (1977) Diurnal variation of autophagy in rod visual cells in the rat. *AlbrechtVonGraefes ArchKlinExpOphthalmol* **203:** 261-270

Rubinsztein D, Codogno P, Levine B (2012) Autophagy modulation as a potential therapeutic target for diverse diseases. *Nature reviews Drug discovery* **11:** 709-730

Singh R, Kaushik S, Wang Y, Xiang Y, Novak I, Komatsu M, Tanaka K, Cuervo A, Czaja M (2009) Autophagy regulates lipid metabolism. *Nature* **458:** 1131-1135

Sir D, Tian Y, Chen W-l, Ann D, Yen T-SB, Ou J-HJ (2010) The early autophagic pathway is activated by hepatitis B virus and required for viral DNA replication. *Proc Natl Acad Sci U S A* **107:** 4383-4388

Songane M, Kleinnijenhuis J, Alisjahbana B, Sahiratmadja E, Parwati I, Oosting M, Plantinga T, Joosten L, Netea M, Ottenhoff T, van de Vosse E, van Crevel R (2012) Polymorphisms in autophagy genes and susceptibility to tuberculosis. *PloS one* **7**

Stappenbeck TS, Rioux JD, Mizoguchi A, Saitoh T, Huett A, Darfeuille-Michaud A, Wileman T, Mizushima N, Carding S, Akira S, Parkes M, Xavier RJ (2011) Crohn disease: a current perspective on genetics, autophagy and immunity. *Autophagy* **7:** 355-374

Takamura A, Komatsu M, Hara T, Sakamoto A, Kishi C, Waguri S, Eishi Y, Hino O, Tanaka K, Mizushima N (2011) Autophagy-deficient mice develop multiple liver tumors. *Genes Dev* **25:** 795-800

Tanaka T, Akira S, Yoshida K, Umemoto M, Yoneda Y, Shirafuji N, Fujiwara H, Suematsu S, Yoshida N, Kishimoto T (1995) Targeted disruption of the NF-IL6 gene discloses its essential role in bacteria killing and tumor cytotoxicity by macrophages. *Cell* **80:** 353-361

Tu BP, Kudlicki A, Rowicka M, McKnight SL (2005) Logic of the yeast metabolic cycle: temporal compartmentalization of cellular processes. *Science* **310:** 1152-1158

Tuyama A, Chang C (2012) Non-alcoholic fatty liver disease. *Journal of diabetes* **4:** 266-280

Uchiyama Y (1990) Rhythms in morphology and function of hepatocytes. *J Gastroenterol*

Hepatol **5:** 321-333

Wang L, Shao J, Muhlenkamp P, Liu S, Klepcyk P, Ren J, Friedman JE (2000) Increased insulin receptor substrate-1 and enhanced skeletal muscle insulin sensitivity in mice lacking CCAAT/enhancer-binding protein beta. *J Biol Chem* **275:** 14173-14181

Yang L, Li P, Fu S, Calay E, Hotamisligil G (2010) Defective hepatic autophagy in obesity promotes ER stress and causes insulin resistance. *Cell Metab* **11:** 467-478

Youle RJ, Narendra DP (2011) Mechanisms of mitophagy. *Nat Rev Mol Cell Biol* **12:** 9-14

APPENDIX A NEURONAL INACTIVATION OF PGC1A PROTECTS MICE FROM DIET-INDUCED OBESITY AND LEADS TO DEGENERATIVE LESIONS

A.1 Abstract

PGC-1α is a transcriptional coactivator that regulates diverse aspects of energy metabolism in peripheral tissues. Mice deficient in PGC-1α have elevated metabolic rate and are resistant to diet-induced obesity. However, it remains unknown whether this alteration in energy balance is due to PGC-1α's action in peripheral tissues or the central nervous system. In this study, we generated neuronal PGC-1α knockout mice (BαKO) using CaMKIIα-Cre to address its role in the regulation of energy balance and neuronal function. Unlike whole body PGC-1α null mice, BαKO mice have normal adaptive metabolic response to starvation and cold exposure in peripheral tissues. In contrast, BαKO mice are hypermetabolic, and similar to whole body PGC-1α null mice, are also resistant to diet-induced obesity, resulting in significantly improved metabolic profiles. Neuronal inactivation of PGC-1α leads to striatal lesions that are reminiscent of neurodegeneration in whole body PGC-1α null brain and impairs nutritional regulation of hypothalamic expression of genes that regulate systemic energy balance. Together, these studies have demonstrated a physiological role for neuronal PGC-1α in the control of energy balance.

Our results also implicate CaMKIIα-positive neurons as an important part of the neural circuitry that governs energy expenditure *in vivo*.

A.2 Introduction

Metabolic syndrome is emerging as a global epidemic in both industrialized and developing countries. Obesity is a central component of this syndrome and arises from a chronic imbalance of energy intake and energy expenditure (Flier, 2004; Spiegelman & Flier, 2001). Excess fat storage in the adipose tissue, and more importantly, ectopic lipid accumulation in skeletal muscle and the liver lead to development of insulin resistance and type 2 diabetes (Erion & Shulman, 2010). While there is no doubt that environmental factors, particularly high-calorie diets and sedentary life style, contribute to the pathogenesis of metabolic syndrome, various genetic and epigenetic factors underlie the predisposition of individuals to metabolic disorders. The homeostatic control of energy intake and expenditure is achieved through a complex network of nutritional, hormonal, and neural cues, which coordinates nutrient storage and fuel oxidation in peripheral tissues. In mammals, nuclear hormone receptors as well as their coactivators and corepressors play an important role in the regulation of diverse aspects of tissue metabolism (Beaven & Tontonoz, 2006; Chawla et al, 2001; Feige & Auwerx, 2007; Lin, 2009).

The PPARγ Coactivator 1 (PGC-1) family of transcriptional coactivators regulates glucose, lipid, and mitochondrial oxidative metabolism through physical interaction with a selective

subset of nuclear hormone receptors and other transcription factors (Finck & Kelly, 2006; Handschin, 2009; Kelly & Scarpulla, 2004; Lin et al, 2005a). PGC-1α and its close homolog PGC-1β are abundantly expressed in tissues with high oxidative capacity, including brown fat, brain, liver as well as cardiac and skeletal muscle (Lin et al, 2002a; Puigserver et al, 1998). Their expression is highly regulated in response to various physiological and environmental signals. For example, PGC-1α is rapidly induced in skeletal muscle following physical exercise (Baar et al, 2002; Goto et al, 2000), whereas its expression is cold-inducible in brown fat (Puigserver et al, 1998). In the skeletal muscle, PGC-1α induces mitochondrial biogenesis and activates a metabolic and contractile program characteristic of slow-twitch myofibers (Lin et al, 2002b; Wu et al, 1999). In the brown fat, it promotes adaptive thermogenesis through stimulating UCP1 expression and mitochondrial respiration (Puigserver et al, 1998). In the liver, PGC-1α regulates hepatic gluconeogenesis and a broader program of metabolic response to starvation (Handschin et al, 2005; Koo et al, 2004; Yoon et al, 2001). The physiological role of this coactivator in adaptive energy metabolism has been demonstrated in multiple tissues in PGC-1α deficient mice (Arany et al, 2008; Arany et al, 2005; Huss et al, 2007; Leone et al, 2005; Lin et al, 2004) . Recent studies demonstrate that reduced PGC-1α expression in skeletal muscle is associated with insulin resistance in humans (Mootha et al, 2003; Patti et al, 2003).

Because PGC-1α stimulates mitochondrial fuel oxidation, a likely outcome of PGC-1α deficiency is increased susceptibility to the development of obesity. Paradoxically, whole

body PGC-1α null mice are resistant to high-fat diet induced obesity (Lin et al, 2004). This alteration in systemic energy balance is associated with elevated metabolic rate and physical activity levels as well as disrupted circadian rhythm (Liu et al, 2007). However, it remains unknown whether PGC-1α influences energy balance and clock function directly through its action in peripheral tissues or via its function in the central nervous system. PGC-1α mRNA and protein expression has been observed in several brain areas and neuronal cell types (Cowell et al, 2007; Tritos et al, 2003). Whole body PGC-1α null mice develop spongioform neurodegeneration, most notably in the striatum and the deep layers of the cerebral cortex. In addition, dysregulation of the PGC-1α pathway was recently implicated in Huntington's disease and Parkinson's disease (Cui et al, 2006; Lin et al, 2004; St-Pierre et al, 2006). These studies strongly suggest PGC-1α plays a critical role in maintaining neuronal health. Whether neuronal PGC-1α is required for systemic metabolic homeostasis has not yet been explored.

To address the role of neuronal PGC-1α in the regulation of energy balance, we generated forebrain-specific PGC-1α null mice by crossing PGC-1α flox/flox mice with CaMKIIα-Cre transgenic mice. We found that inactivation of PGC-1α in CaMKIIα-positive neurons leads to resistance to diet-induced obesity and results in neurodegenerative lesions in the striatum. Our studies reveal an essential role of PGC-1α in CaMKIIα-positive neurons in the regulation of energy balance and neuronal function.

A.3 Results

A.3.1 Generation of brain-specific PGC-1α-deficient mice (BαKO)

PGC-1α deficiency impairs adaptive metabolic responses in multiple tissues, including the liver, brown adipose tissue as well as skeletal and cardiac muscle (Arany et al, 2005; Leone et al, 2005; Lin et al, 2004). Paradoxically, whole body PGC-1α null mice are resistant to diet-induced obesity and have elevated metabolic rate. These findings raise the possibility that PGC-1α may play an important role in the regulation of energy balance through its action in the central nervous system. To test this possibility, we generated brain-specific PGC-1α null mice using the Cre-loxP system. We chose to use CaMKIIα-Cre transgenic mice because PGC-1α is abundantly expressed in forebrain, including cerebral cortex, hippocampus, basal ganglia and hypothalamus (Liu & Jones, 1996). Transgenic expression of Cre recombinase under the control of CaMKIIα promoter has been widely used to inactivate genes in the forebrain (Casanova et al, 2001; Tsien et al, 1996). We generated PGC-1α flox/flox and PGC-1α flox/flox; CaMKIIα-Cre (BαKO) mice for our studies (Fig. A.1A). As shown in Fig. A.1B, BαKO mice have selective deletion of exons 3-5 within the PGC-1α locus in several brain areas, including cerebral cortex, striatum, olfactory bulb, and hypothalamus, but not in any of the peripheral tissues examined.

A.3.2 BαKO mice have normal adaptive metabolic response

We next examined whether adaptive metabolic responses in peripheral tissues are affected in BαKO mice fed chow diet. In contrast to whole body PGC-1α null mice, which are

cold-sensitive due to defects in adaptive thermogenesis, BαKO mice maintain their core body temperature following 3-hr cold exposure at 4℃. We observed a modest but similar decrease in body temperature in both control and BαKO groups (Fig. A.2A). Histological analysis of brown adipose tissues reveals that brown adipocytes appear normal in size with similar accumulation of multilocular lipid droplets (Fig. A.2B). Consistently, cold-inducible expression of genes involved in adaptive thermogenesis, including PGC-1α, deiodinase 2 (Dio2), uncoupling protein 1 (Ucp1), and mitochondrial genes, are similar in control and BαKO brown fat (Fig. A.2C and data not shown). PGC-1α has been demonstrated to regulate multiple aspects of hepatic starvation response. PGC-1α deficient hepatocytes have defective gluconeogenic response and heme biosynthesis (Handschin et al, 2005; Lin et al, 2004). Compared to the control group, BαKO mice have normal induction of gluconeogenic genes following overnight fasting (Fig. A.S1). Plasma glucose levels are also similar in chow-fed control and BαKO mice under both fed and fasted conditions (Fig. A.S1). These results indicate that adaptive energy metabolism in peripheral tissues is largely unperturbed in brain-specific PGC-1α deficient mice.

A.3.3 BαKO mice are resistant to diet-induced obesity

PGC-1α deficient mice have elevated metabolic rate and are resistant to diet-induced obesity. However, whether this can be attributed to neuronal PGC-1α function remains unknown. To determine the significance of central PGC-1α in energy balance, we subjected control and BαKO mice to high-fat diet feeding. While body weight of these two groups of

mice remains similar under chow-fed condition, BαKO mice are significantly resistant to weight gain when fed high-fat diet (Fig. A.3A). The body weight of BαKO mice is approximately 20% lower than control mice following ten weeks of high-fat feeding. Transgenic expression of Cre recombinase alone does not affect body weight upon high-fat feeding (data not shown). Resistance to weight gain following high-fat feeding appears to be more pronounced in whole body PGC-1α null group, which weighs approximately 40% less than the wild type group. Consistently, epididymal white adipose tissue (eWAT) weight and eWAT/body weight ratio are significantly lower in the BαKO and whole body PGC-1α null mice compared to their respective control (Fig. A.3C). In contrast to whole body PGC-1α null mice, which have lower plasma glucose concentrations, plasma glucose remains similar in control and BαKO mice following high-fat feeding (Fig. A.3D). Resting core body temperature is also slightly but significantly higher in the BαKO mice, but not whole body PGC-1α null mice (Fig. A.3E). These results suggest that neuronal PGC-1α participates in the regulation of systemic energy balance and contributes to weight gain resistance in whole body PGC-1α null mice.

A plausible explanation for the resistance to diet-induced obesity in BαKO mice is that they have elevated metabolic rate. We measured metabolic rate and physical movements in control and BαKO mice using the Comprehensive Lab Animal Monitoring System (CLAMS). BαKO mice have increased food intake when normalized to their body weight (Fig. A.4A). On a per mouse basis, food intake is similar between these two groups.

Oxygen consumption rate (VO_2) is approximately 30% higher in BαKO group than control (Fig. A.4B). When normalized to total lean mass, VO_2 remains significantly higher in BαKO mice. Respiratory exchange ratio, a measurement of *in vivo* fuel preference, is slightly lower in BαKO mice (data not shown), suggesting that BαKO mice may prefer fatty acid oxidation for energy production. Surprisingly, total physical activity level and diurnal locomotor profiles appear unaffected in these mice (Fig. A.4C and Fig. A.S2). Analyses of plasma hormones indicate that both insulin and leptin concentrations are significantly lower in BαKO mice, suggesting that they may have improved insulin sensitivity. However, we were unable to observe significant improvement in glucose tolerance in insulin and glucose tolerance tests (data not shown).

To explore whether neuronal deficiency of PGC-1α alters the expression of key regulators of energy balance, we analyzed hypothalamic gene expression using qPCR. The expression of thyrotropin-releasing hormone (TRH), proopiomelanocortin (POMC), Orexin, Melanin-concentrating hormone (MCH), and prohormone convertase 2 (PC2) remains similar in control and BαKO hypothalamus under both fed and fasted conditions (Fig. A.5 and data not shown). In contrast, fasting induction of Agouti-related protein (AgRP) and neuropeptide Y (NPY), two factors known to regulate energy balance, is significantly diminished in hypothalamus from BαKO mice. Similar defects in AgRP and NPY expression were also observed in whole body PGC-1α null hypothalamus. These findings strongly suggest that neuronal PGC-1α may affect diet-induced obesity through its

regulation of hypothalamic neuropeptides that control energy balance.

A.3.4 High-fat diet fed BαKO mice have reduced hepatic steatosis

We further examined the impact of neuronal PGC-1α inactivation on hepatic metabolism following high-fat feeding. Analysis of hepatic triglyceride content indicates that BαKO mice have significantly less lipid accumulation in the liver (Fig. A.6A). In fact, liver triglyceride is reduced by approximately 57% in BαKO mice. Hepatocyte swelling and lipid accumulation is evident in high-fat fed control mice (Fig. A.6B). In contrast, the overall liver appearance and histology are significantly improved in the BαKO group. Analysis of hepatic gene expression indicates that the expression of several lipogenic genes, including fatty acid synthase (FAS) and stearoyl-CoA desaturase (SCD-1) as well as Fsp27, a gene involved in lipid droplet formation, are significantly decreased in BαKO mouse livers (Fig. A.6C). The expression of gluconeogenic genes, such as PEPCK and Glucose-6-phosphatase, and fatty acid β-oxidation genes, remain largely unaltered. These results suggest that neuronal deletion of PGC-1α significantly improves the metabolic profile in the liver following high-fat diet feeding.

A.3.5 Region-specific degenerative lesions in BαKO mouse brains

To determine the effects of PGC-1α inactivation on neuronal health, we performed histological analyses in several brain regions. Consistent with previous findings (Lin et al, 2004), whole body PGC-1α deficiency leads to spongiform neurodegeneration, most

readily observed in striatum and deep layers of cerebral cortex (Fig. A.7). Remarkably, striatum from BαKO mouse brain also contains numerous degenerative lesions that are similar but slightly smaller than those seen in whole body PGC-1α null mice. BαKO mice tend to have fewer lesions in both striatum and deep cortical layers. Immunohistochemical staining using an antibody against neurofilament light chain (NFL), a marker for nerve fibers, indicates that the lesions correlate with apparent degeneration of fibers in the striatum from BαKO mice (Fig. A.8). Our results strongly suggest that PGC-1α is essential for maintaining axon integrity in CaMKIIα-positive neurons in the brain.

A.3.6 PGC-1α deficiency does not perturb autophagy in central nervous system

Autophagy is responsible for bulk degradation of cytoplasmic components in the cell and plays an important role in nutrient homeostasis during starvation (Kuma et al, 2004; Mizushima et al, 2004; Mortimore & Schworer, 1977). Autophagy is also required for the clearance of damaged organelles, such as mitochondria (Sandoval et al, 2008). Inhibition of autophagy leads to accumulation of ubiquitinated protein and results in neuronal death and neurodegeneration (Komatsu et al, 2006; Komatsu et al, 2007b). To determine whether PGC-1α inactivation perturbs autophagy, we performed immunoblotting analyses using antibodies against LC3 and p62, two molecular markers of autophagy activity (Klionsky et al, 2007; Mizushima, 2004; Mizushima et al). LC3 is a cytosolic protein (LC3-I) that, upon autophagy induction, undergoes covalent lipid modification and translocates to the autophagosome membrane (LC3-II) (Kabeya et al, 2000). Relative

abundance of these two LC3 isoforms is indicative of autophagy activity (Komatsu et al, 2007a). As shown in Fig. A.9, LC3-I and LC3-II levels are similar in the posterior cortex and striatum of wild type and whole body PGC-1α null mouse brains. Similarly, we did not observe differences in LC3-I and LC3-II levels in control and BαKO mouse brains. In addition, the protein levels of p62, an LC-3 binding protein that is involved in the formation of ubiquitin-containing inclusions, also remain largely unchanged (Fig. A.9) (Komatsu et al, 2007a). We further examined the expression of genes in the autophagy pathway and found that mRNA levels of autophagy genes are similar between control and PGC-1α null brains (data not shown). Together, these results suggest that impaired neuronal autophagy is not a significant mediator of neurodegeneration in PGC-1α deficient neurons.

A.4 Discussion

The brain is a highly metabolically active tissue and relies on mitochondrial oxidative metabolism for ATP production under normal conditions. Not surprisingly, neurons are exquisitely sensitive to perturbations of mitochondrial function. Impaired mitochondrial energy metabolism has been implicated in numerous heritable neurological disorders as well as neurodegenerative diseases, including Huntington's disease, Parkinson's disease, and Alzheimer's disease (DiMauro & Schon, 2008; Lin & Beal, 2006; Schon & Manfredi, 2003). PGC-1α is abundantly expressed in the brain and its deficiency leads to degenerative lesions in several brain regions. However, whether these lesions arise from cell-autonomous functions of PGC-1α in neurons remains unknown. In addition, the

neuronal cell types that require PGC-1α for their normal function have not been identified. In this study, we demonstrate that PGC-1α in CaMKIIα-positive neurons plays an important role in maintaining systemic energy balance and neuronal health.

We have previously reported that mice lacking PGC-1α are resistant to high-fat diet induced obesity and have significantly improved insulin sensitivity (Lin et al, 2004). This lean phenotype is associated with elevated metabolic rate and activity levels. Because PGC-1α is expressed in several key metabolic tissues, including skeletal muscle, adipose tissues, and liver (Puigserver et al, 1998), it was not immediately clear which tissue(s) underlies altered systemic energy balance in whole body PGC-1α null mice. To complicate the matter further, PGC-1α regulates distinct metabolic programs in different tissues, which influence systemic metabolism through crosstalk and secondary effects. To resolve these issues, we generated brain-specific PGC-1α null mice using CaMKIIα-Cre transgenic line. PGC-1α is abundantly expressed in pyramidal neurons, many of which also express CaMKIIα (Ouimet et al, 1984), as well as GABAergic neurons (Cowell et al, 2007; Tritos et al, 2003). BαKO mice are capable of mounting normal metabolic responses in peripheral tissues. For example, the induction of genes involved in hepatic gluconeogenesis and fatty acid β-oxidation following starvation is similar in control and BαKO mice. In addition, the activation of adaptive thermogenesis in brown fat in response to cold exposure is normal in BαKO mice. Unlike whole body PGC-1α null mice, which are extremely cold-sensitive, BαKO mice are indistinguishable from control mice in maintaining their core body

temperature. These observations allow us to assess the biological function of neuronal PGC-1α in the absence of the confounding metabolic perturbations in peripheral tissues caused by global PGC-1α deficiency.

Perhaps the most remarkable outcome of neuronal PGC-1α deficiency is its influence on systemic energy balance when the mice were fed a high-fat diet. Compared to control mice, BαKO mice gain significantly less body weight and have lower adiposity following ten weeks of high-fat feeding. The resistance to weight gain in BαKO mice appears to be quantitatively less pronounced than whole body PGC-1α null mice, suggesting that PGC-1α in CaMKIIα-negative cells in nervous system and/or peripheral tissues may also contribute to its effects on systemic energy balance. Additionally, in both BαKO and whole body PGC-1α null mice, fasting-induced expression of AgRP and NPY in hypothalamus is impaired in the absence of PGC-1α. These observations are consistent with previous studies that implicate FoxO1, a transcriptional partner for PGC-1α, in the regulation of AgRP gene expression in hypothalamus (Kitamura et al, 2006; Puigserver et al, 2003). A recent report showed that PGC-1α expression is present in NPY expressing neurons of the dorsalmedial hypothalamic nucleus (Draper et al, 2010). Together, these findings illustrate a potential role for FoxO1/PGC-1α pathway in the regulation of hypothalamic transcription and function. The significance of AgRP and NPY in mediating the effects of PGC-1α on energy balance remains unknown at present.

Besides less weight gain under high-fat diet, BαKO mice also have reduced hepatic lipid content and lower plasma insulin levels, suggesting that these mice are more insulin-sensitive. However, BαKO mice are similar to control group in insulin tolerance and glucose tolerance tests. In contrast, whole body PGC-1α null mice have significantly lower blood glucose levels and improved glucose tolerance. A plausible explanation for these differences is that hepatic glucose output is impaired in whole body PGC-1α null mice while it remains normal in BαKO mice. In fact, fasting glucose levels are similar between control and BαKO mice when kept on chow diet (Fig. A.S1). As such, impaired hepatic gluconeogenesis may significantly contribute to improved glucose homeostasis in whole body PGC-1α null mice.

Surprisingly, while BαKO mice have increased oxygen consumption rate in CLAMS studies, these mice appear to have normal activity levels. In addition, diurnal regulation of locomotor activity is apparently unaffected in these mice. These results suggest that distinct neuronal populations might mediate the function of PGC-1α in the regulation of energy balance and circadian pacemaker. In this case, PGC-1α activity in CaMKIIα-positive neurons is essential for the control of metabolic rate and body weight homeostasis, whereas its regulation of biological clock is mediated by a distinct population of PGC-1α expressing neurons. Previous studies have shown that PGC-1α is also expressed in GABAergic neurons (Cowell et al, 2007), which are typically negative for CaMKIIα expression. Whether PGC-1α in GABAergic neurons is required for maintaining normal circadian

metabolic rhythms remains to be addressed. It is also possible that certain CaMKIIα neurons may lack Cre expression. We cannot rule out the possibility that intact PGC-1α expression in a subset of CaMKIIα-positive neurons could mediate its role in circadian regulation.

We observed neurodenegerative lesions in the striatum of BαKO mouse brain. The striking similarity in the appearance of vacuoles in BαKO and whole body PGC-1α null mice strongly suggests that the deficiency of PGC-1α in CaMKIIα-positive neurons is the major neuronal population affected in whole body PGC-1α null mouse brain. Interestingly, we observed fewer lesions in the striatum and deep layers of cerebral cortex in BαKO mice. It remains to be determined whether this is due to partial deletion of PGC-1α in CaMKIIα-positive neurons or other cell types also contribute to neurodegeneration in whole body PGC-1α null mice. Because CaMKIIα is only modestly expressed in the striatum, our data suggest that the degenerative lesions are most likely due to the defects of neurons that reside in other brain areas, such as the cortex. While autophagy is emerging as an important mechanism in neuronal homeostasis, we did not observe significant changes in autophagy activity in whole body PGC-1α null and BαKO mice compared to their respective control. It is likely that disruption of mitochondrial function and reactive oxygen species metabolism may be responsible for the development of neuronal lesions in the absence of PGC-1α.

In summary, we have demonstrated that PGC-1α activity in CaMKIIα neurons plays a key role in the regulation of energy balance and neuronal health. The resistance to diet-induced obesity and brain lesions in BαKO mice are strikingly similar to whole body PGC-1α null mice. These results strongly suggest that neuronal PGC-1α exerts profound effects on the neural circuitry that governs systemic energy balance.

A.5 Materials and methods

Mice - All animal experiments were performed according to procedures approved by the University Committee on Use and Care of Animals. Mice carrying PGC-1α flox alleles were generated as previously described (Lin et al, 2004). These mice were mated with CaMKIIα-Cre transgenic mice to generate flox/flox control and BαKO mice. PCR analysis was performed on genomic DNA isolated from different tissues to assess Cre-mediated deletion. Wild type allele and Cre-mediated deletion allele was detected using primer 1 and 2, 3 and 4, respectively: forward primer1, GTCTAAGATGTCTGCTCTTGAGG; reverse primer2, CCAGTTTCTTCATTGGTGTG; forward primer3, TCCAGTAGGCAGAGATTTATGAC; reverse primer4, CCAACTGTCTATAATTCCAGTTC. Mice were maintained on a standard rodent chow or a high-fat diet containing 60% fat-derived calories (D12492, Research Diets) with 12hr light and dark cycles. For cold exposure, 11-week-old female mice were individually housed in cages prechilled at 4℃ with free access to food and water. Core body temperature was monitored using a rectal thermometer 3 hrs after the initiation of cold

exposure. Brown fat was dissected following cold exposure for gene expression and histological analyses. For hypothalamus analysis, 3-4 months old control, whole body PGC-1α null, and BαKO mice were either fed or fasted for 48 hrs before harvest.

Metabolic analysis - Metabolic rate and activity were measured using a Comprehensive Lab Animal Monitoring System (CLAMS) that simultaneously measures whole-body O_2 consumption and physical movements (Frayn, 1983; Simonson & DeFronzo, 1990). Mice were acclimated in the monitoring chambers for 3 days before the experiment to minimize the effects of housing environment changes on animal behaviors. Data were collected every 10 min for each mouse over a period of three light/dark cycles. CLAMS study was conducted by University of Michigan Animal Phenotyping Core. Plasma concentrations of triglyceride, insulin, and leptin were measured using commercially available assay kits. Liver triglyceride content was extracted and measured using previously described procedures (Lin et al, 2005b).

Histological analysis - Brains were fixed in situ by intracardiac perfusion with 15ml PBS followed by 15ml 4% PFA in PBS, post-fixed in 4% PFA in PBS overnight at 4℃ after dissection, dehydrated in 70% ethanol, and embedded in paraffin. Coronal sections (8μm) were stained using H&E staining method. Immunohistochemistry using antibody against neurofilament light chain (NFL) was performed as previously described (Lin et al, 2004). Other tissues were fixed directly by 4% PFA in PBS overnight at 4℃ after dissection and

underwent the same procedure as the brain for H&E staining. Frozen livers were embedded in O.C.T., sectioned into 12 μm sections, and stained using Oil Red O method.

RNA and protein analysis - Total RNA was isolated from tissues using Trizol reagents (Invitrogen). For quantitative real time PCR (qPCR) analysis, RNA samples were reverse transcribed and used in quantitative PCR reactions in the presence of Sybr Green (Applied Biosystems). Relative abundance of mRNA was normalized to ribosomal protein 36B4 or β-actin. Sequences for qPCR primers used in this study were shown in Supplementary Table A.S1 or previously described (Li et al, 2008; Lin et al, 2004). Immunoblotting studies were performed using specific antibodies for LC3 (LC3-5F10, Nanotools), p62 (PW9860, Enzo Life Sciences) and ubiquitin (sc-8017, Santa Cruz Biotechnology).

A.6 Acknowledgements

We thank Dr. Joseph Takahashi for providing the CaMKIIα-Cre transgenic mice and Dr. Geoffrey Murphy for discussions. We are grateful to Shengjuan Gu, Layla Yu, and Matthew Molusky for technical assistance, and other members of the laboratory for discussions. We thank Dr. Nathan Qi and the University of Michigan Animal Metabolic Phenotyping Core for performing CLAMS study. Immunohistochemical staining experiment was performed by Elizabeth K. Lucas and Rita M. Cowell. Oil Red O staining experiment was performed by Siming Li. This work was supported by National Institutes of Health (DK077086 and HL097738, J.D.L.), Scientist Development Grant and

Predoctoral Fellowship from the American Heart Association.

Table. A.S1. qPCR primer list.

	Forward primer	Reverse primer
Cpt1a	GAGAAATACCCTGACTATGTG	TGTGAGTCTGTCTCAGGGCTAG
FSP27	TCGACCTGTACAAGCTGAACCCT	AGGTGCCAAGCAGCATGTGACC
FAS	GGTTACACTGTGCTAGGTGTTG	TCCAGGCGCATGAGGCTCAGC
SCD1	GCTGGAGTACGTCTGGAGGAA	TCCCGAAGAGGCAGGTGTAG
Dgat1	GCTCTGGCATCATACTCCATC	CGGTAGGTCAGGTTGTCTGG
HMG-CoA Synthase2	GACATCAACTCCCTGTGCCTG	GATGTCAGTGTTGCCTGAATC
Cebpα	AGACATCAGCGCCTACATCGAC	GGGTAGTCAAAGTCACCGCCGC
Cebpβ	CCAAGAAGACGGTGGACAAG	CACCTTCTTCTGCAGCCGCTC
SREBP1c	ATCGGCGCGGAAGCTGTCGGG	GGGAAGTCACTGTCTTGGTTG
Ribosomal 36B4	GAAACTGCTGCCTCACATCCG	GCTGGCACAGTGACCTCACACG
AGRP	GCGGAGGTGCTAGATCCA	AGGACTCGTGCAGCCTTA
TRH	CTCTTCTCTCTGACAGCCC	AGGCGTGGAAGAACCGTC
POMC	ACCTCACCACGGAGAGCA	GCGAGAGGTCGAGTTTGC
Orexin	CTGCCGTCTCTACGAACTGTTG	CGCTTTCCCAGAGTCAGGATA
MCH	ATTCAAAGAACACAGGCTCCAAAC	CGGATCCTTTCAGAGCAAGGTA
NPY	CTCCGCTCTGCGACACTAC	AATCAGTGTCTCAGGGCT
PC2	CTGTGGAGTCGGCGTAGCAT	GTTGAGGCATGTGGCTGATG
β-actin	TCGTACCACGGGCATTGTGATG	CCACGCTCGGTCAGGATCTTC

Fig. A.1. Generation of BαKO mice. (A) Strategy for Cre recombinase-mediated deletion of PGC-1α exons 3-5 in the brain. (B) PCR analysis of genomic DNA isolated from tissues of flox/flox (-) and BαKO (+) mice. Note the deletion of PGC-1α exons is only detected in cortex, striatum, olfactory bulb, and hypothalamus. PCR primers are indicated in A.

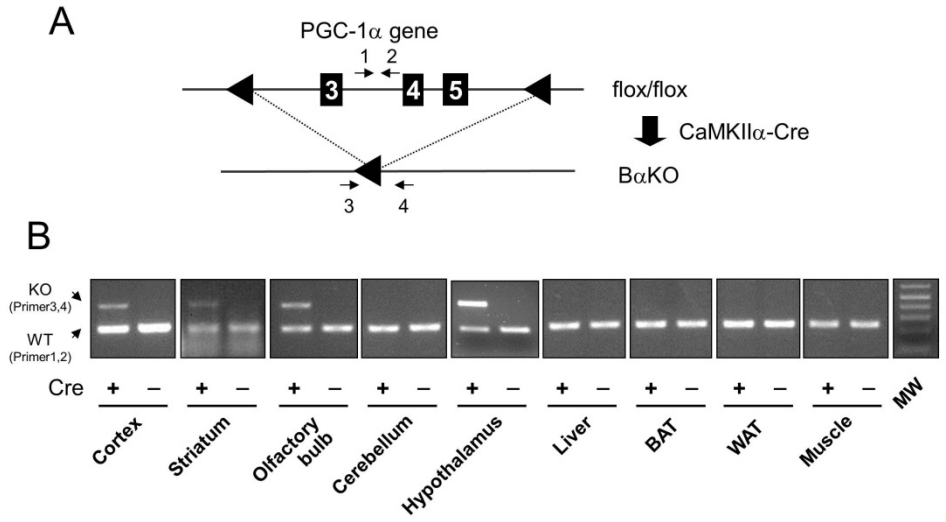

Fig. A.2. Adaptive thermogenesis in response to cold exposure. (A) Rectal temperature of flox/flox (filled box) and BαKO (open box) mice kept at room temperature (RT) or exposed to 4℃ for 3 hrs. * $p<0.05$. (B) H&E staining of paraffin-embedded brown fat sections. (C) qPCR analysis of gene expression in brown fat. Data represent mean±SEM (n=3 per group). * $p<0.004$.

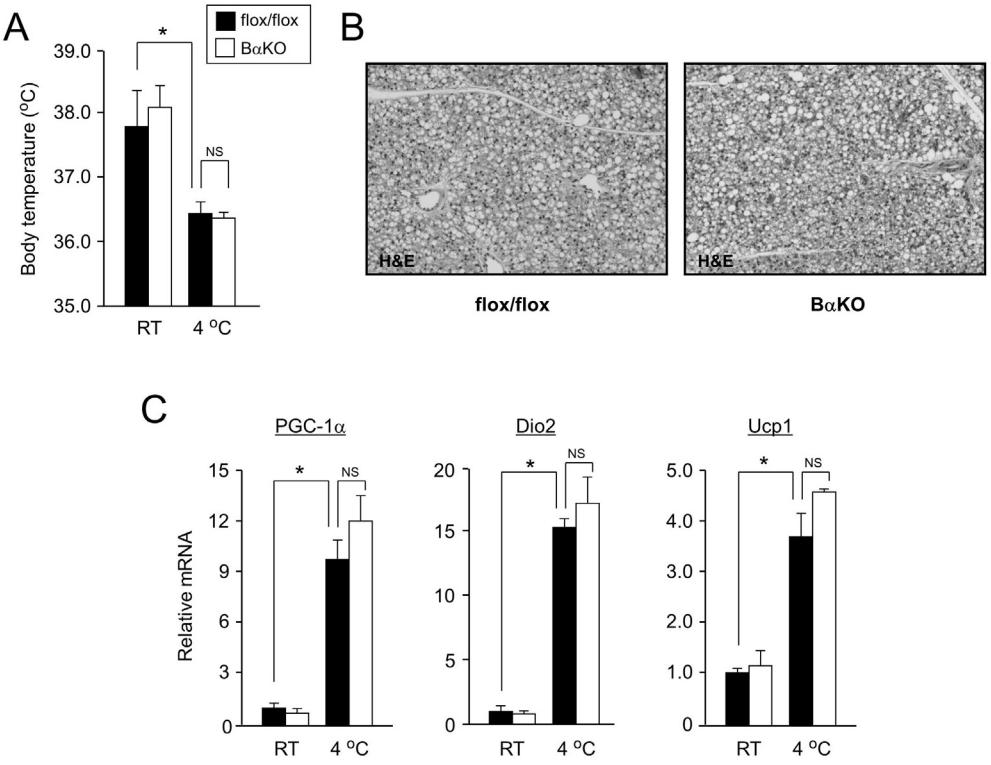

Fig. A.3. High-fat diet induced obesity. (A) Body weight of flox/flox, BαKO, wildtype (WT), and whole body PGC-1α null (KO) mice fed high-fat diet for ten weeks. * $p<0.001$; ** $p<0.01$ BαKO vs. KO group. (B) Appearance of control and BαKO mice following high-fat diet feeding. (C) Epididymal fat (eWAT) weight and eWAT to body weight ratio in flox/flox, BαKO, wildtype (WT) and whole body PGC-1α null (KO) mice. *$p<0.02$. (D)-(E), Plasma glucose (D) concentration and rectal temperature (E) in high-fat fed flox/flox, BαKO, wild type (WT), and whole body PGC-1α null mice (KO). Data represent mean±SEM (n=7-8 per group). * $p<0.02$.

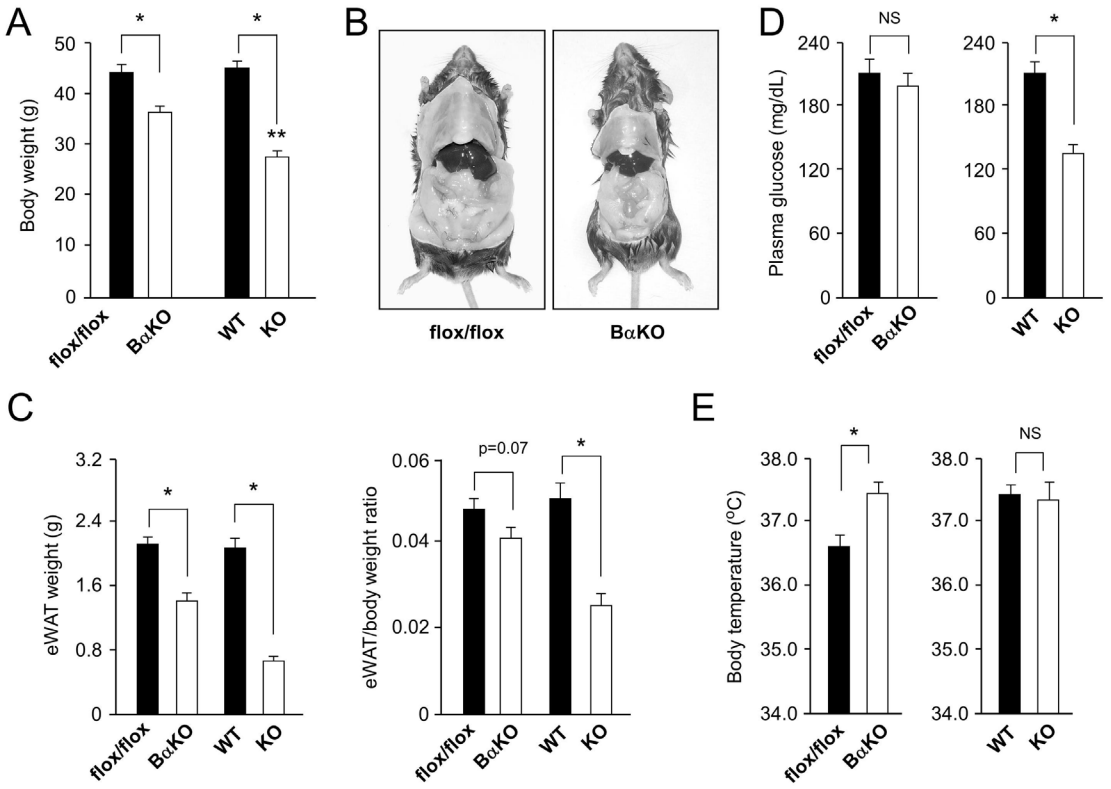

Fig. A.4. CLAMS studies in high-fat diet fed flox/flox and BαKO mice. (A) Food intake in flox/flox and BαKO mice. Data represent food consumption per day following normalization to body weight (left) or on a per mouse basis (right). *p<0.01. (B) Metabolic rate in flox/flox (filled box) and BαKO mice (open box). Shown is oxygen consumption rate as normalized to body weight (left) or lean mass (right). * p<0.05, # p<0.09. (C) Total activity level during night (N) and day (D) phases. Shown are average movement counts for flox/flox (filled box) and BαKO (open box) mice. (D)-(E), Plasma insulin (D) and leptin (E) concentrations in high-fat diet fed flox/flox and BαKO mice. Data represent mean±SEM (n=7-8 per group). * p<0.02.

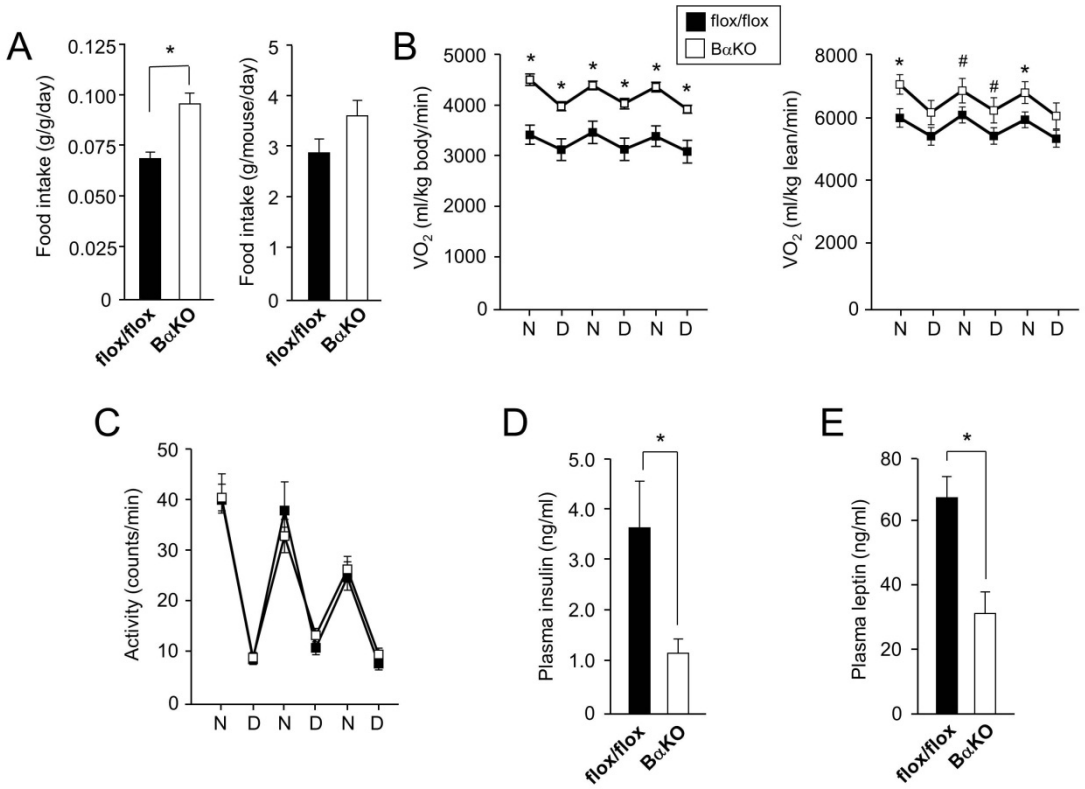

Fig. A.5. Hypothalamic gene expression. (A) qPCR analysis of gene expression in hypothalamus of wild type (WT) and whole body PGC-1α null (KO) mice under fed and fasted conditions. Pooled RNA from 3-5 mice in each group was used in the analyses. Data represent mean±SD. * p<0.005. (B) qPCR analysis of hypothalamic gene expression in flox/flox and BαKO mice under fed and fasted conditions. Pooled RNA from 6-8 mice in each group was used. Data represent mean±SD. * p<0.005.

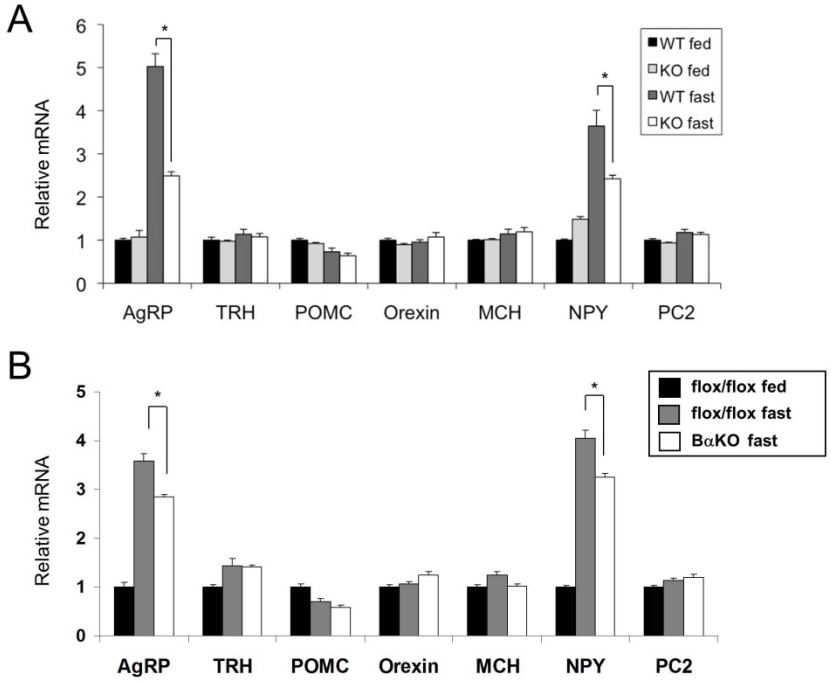

Fig. A.6. Hepatic triglyceride content and gene expression. (A) Liver triglyceride content in control (filled box) and BαKO (open box) mice following ten weeks of high-fat feeding. * p=0.009. (B) H&E (top panel) and Oil Red O staining (lower panel) of liver sections. (C) qPCR analysis of gene expression. Data represent mean±SEM (n=7-8 per group). * p<0.05.

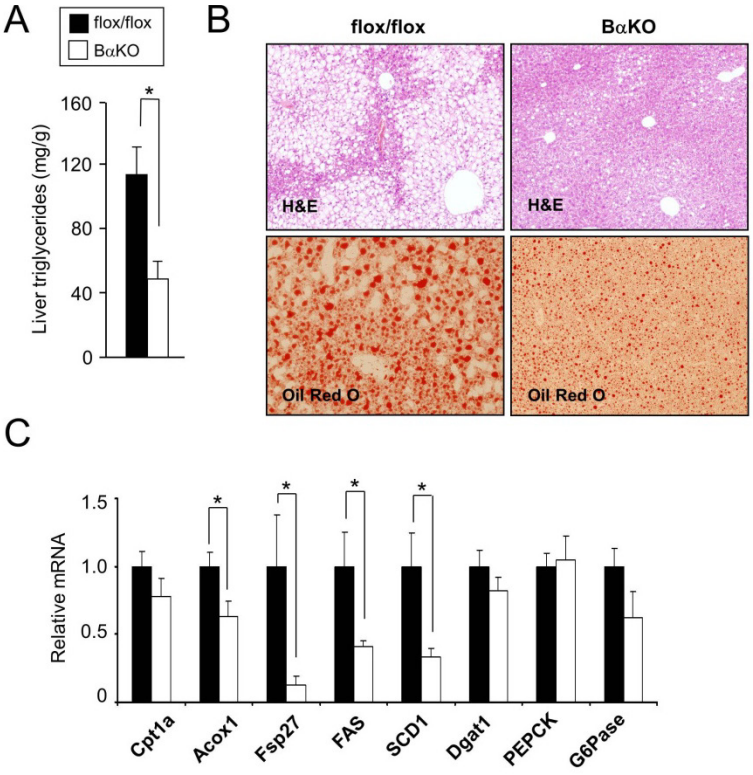

Fig. A.7. H&E staining of brain sections from flox/flox, BαKO, whole body PGC-1α null (KO) mice. Shown are cerebral cortex (cx) and striatum (str) regions. Lower panel, high magnification of striatum sections. Scale bar, 500μm. Note the absence of clear degenerative lesions in flox/flox mouse brain (arrow).

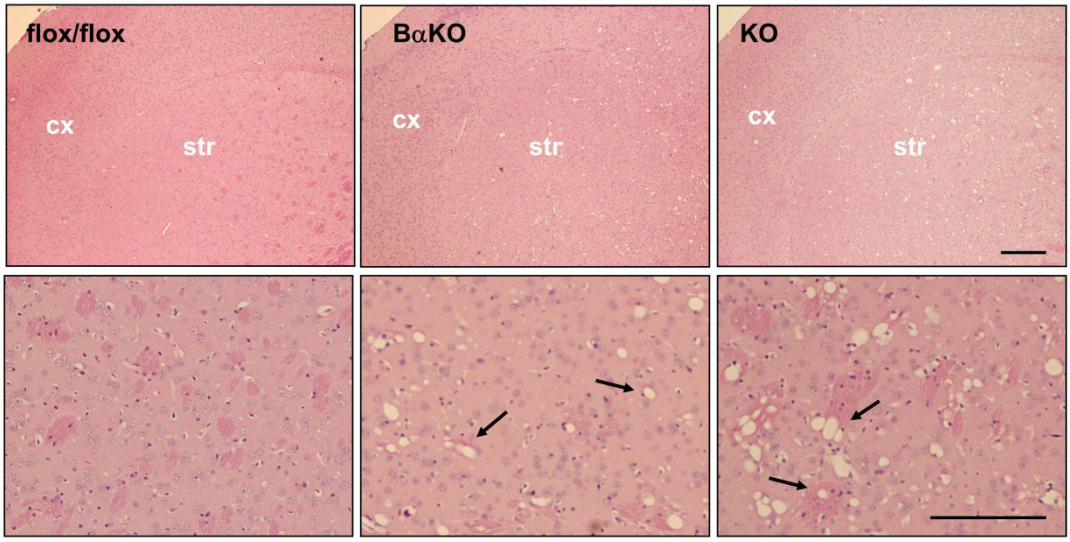

Fig. A.8. Immunohistochemical staining using antibody against neurofilament light chain. Shown are cerebral cortex (cx), corpus callosum(cc) and striatum (str) regions in forebrain sections at low (top) and high (bottom) magnification in flox/flox and BαKO mice. Note the presence of small (arrowhead) and large (arrow) lesions in the striatum (str).

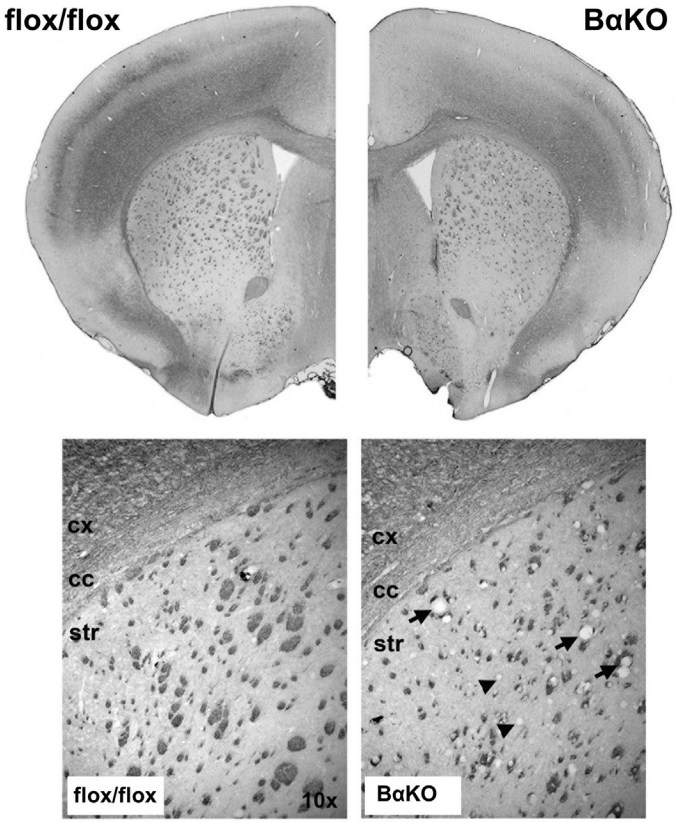

Fig. A.9. Immunoblotting analysis of proteins in the autophagy pathway. Total tissue lysates were prepared from posterior cortex and striatum dissected from wild type (WT), whole body PGC-1α null (KO), flox/flox, and BαKO mice. Immunoblotting was performed using indicated antibodies. Two different exposure times were included for LC3. Ponceau S stain was used as loading control.

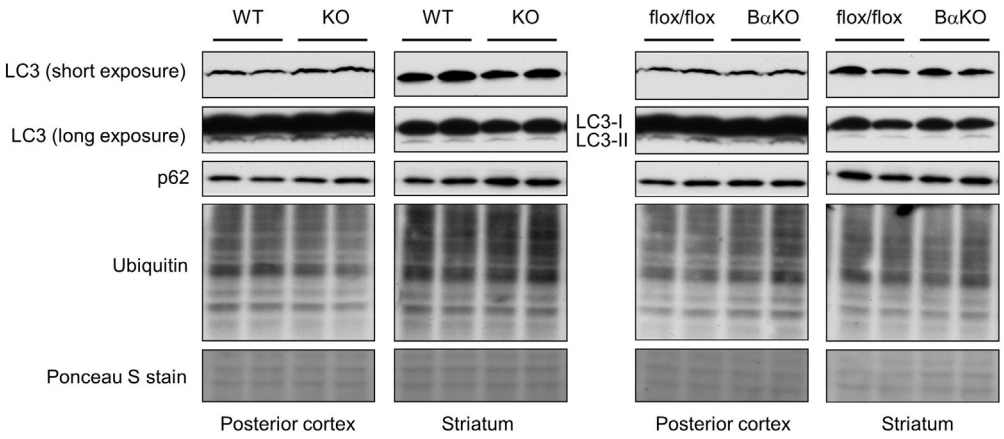

Fig. A.S1. Adaptive hepatic gluconeogenesis in response to starvation and liver morphology. (A) Plasma glucose level of chow fed flox/flox (filled box) and BαKO (open box) mice after starvation for 24 hrs. (B) H&E staining of liver sections from chow fed flox/flox and BαKO mice under fed condition. (C) qPCR analysis on mRNA expression of hepatic gluconeogenesis genes in response to 24-hr fasting. Fed flox/flox (filled box) mice were compared with fasted flox/flox (gray box) and BαKO (open box) mice. * $p<0.05$. Data represent mean±SEM (n=3-4 per group).

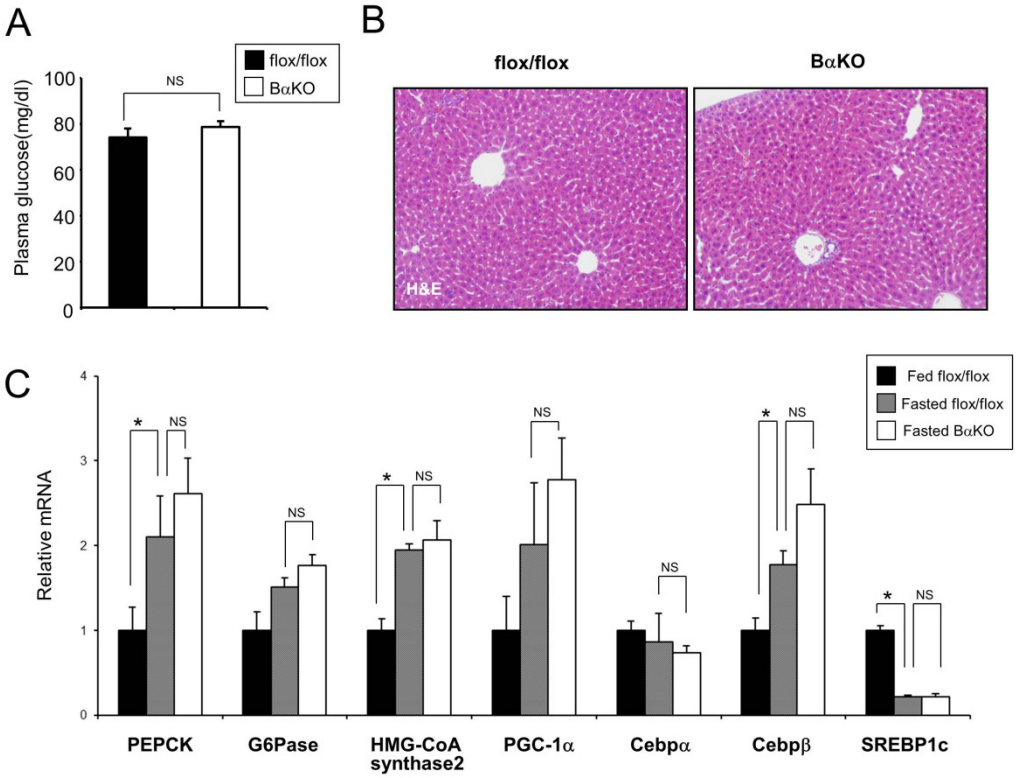

Fig. A.S2. CLAMS study on average activity trace during three days in high-fat fed mice. Data were collected every 10 minutes and averaged for the flox/flox (blue) or BαKO (red) group. Data represent mean±SEM (n=7-8 per group).

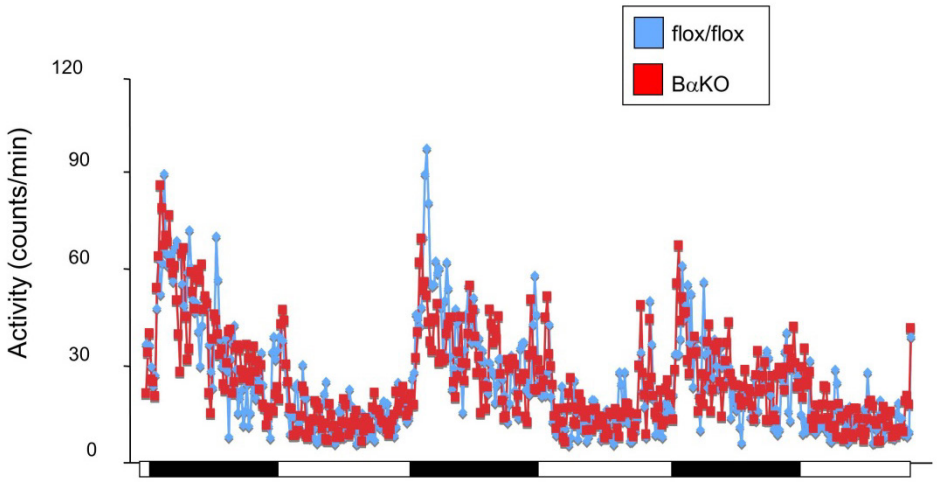

A.7 References

Arany Z, Foo SY, Ma Y, Ruas JL, Bommi-Reddy A, Girnun G, Cooper M, Laznik D, Chinsomboon J, Rangwala SM, Baek KH, Rosenzweig A, Spiegelman BM (2008) HIF-independent regulation of VEGF and angiogenesis by the transcriptional coactivator PGC-1alpha. *Nature* **451:** 1008-1012

Arany Z, He H, Lin J, Hoyer K, Handschin C, Toka O, Ahmad F, Matsui T, Chin S, Wu PH, Rybkin, II, Shelton JM, Manieri M, Cinti S, Schoen FJ, Bassel-Duby R, Rosenzweig A, Ingwall JS, Spiegelman BM (2005) Transcriptional coactivator PGC-1 alpha controls the energy state and contractile function of cardiac muscle. *Cell Metab* **1:** 259-271

Baar K, Wende AR, Jones TE, Marison M, Nolte LA, Chen M, Kelly DP, Holloszy JO (2002) Adaptations of skeletal muscle to exercise: rapid increase in the transcriptional coactivator PGC-1. *Faseb J* **16:** 1879-1886

Beaven SW, Tontonoz P (2006) Nuclear receptors in lipid metabolism: targeting the heart of dyslipidemia. *Annu Rev Med* **57:** 313-329

Casanova E, Fehsenfeld S, Mantamadiotis T, Lemberger T, Greiner E, Stewart AF, Schutz G (2001) A CamKIIalpha iCre BAC allows brain-specific gene inactivation. *Genesis* **31:** 37-42

Chawla A, Repa JJ, Evans RM, Mangelsdorf DJ (2001) Nuclear receptors and lipid physiology: opening the X-files. *Science* **294:** 1866-1870

Cowell RM, Blake KR, Russell JW (2007) Localization of the transcriptional coactivator PGC-1alpha to GABAergic neurons during maturation of the rat brain. *J Comp Neurol* **502:** 1-18

Cui L, Jeong H, Borovecki F, Parkhurst CN, Tanese N, Krainc D (2006) Transcriptional repression of PGC-1alpha by mutant huntingtin leads to mitochondrial dysfunction and neurodegeneration. *Cell* **127:** 59-69

DiMauro S, Schon EA (2008) Mitochondrial disorders in the nervous system. *Annu Rev Neurosci* **31:** 91-123

Draper S, Kirigiti M, Glavas M, Grayson B, Chong CN, Jiang B, Smith MS, Zeltser LM, Grove KL (2010) Differential gene expression between neuropeptide Y expressing neurons of the dorsomedial nucleus of the hypothalamus and the arcuate nucleus: microarray analysis study. *Brain Res* **1350:** 139-150

Erion DM, Shulman GI (2010) Diacylglycerol-mediated insulin resistance. *Nat Med* **16:** 400-402

Feige JN, Auwerx J (2007) Transcriptional coregulators in the control of energy homeostasis. *Trends Cell Biol* **17:** 292-301

Finck BN, Kelly DP (2006) PGC-1 coactivators: inducible regulators of energy metabolism in health and disease. *J Clin Invest* **116:** 615-622

Flier J (2004) Obesity wars: molecular progress confronts an expanding epidemic. *Cell* **116:** 337-350

Frayn KN (1983) Calculation of substrate oxidation rates in vivo from gaseous exchange. *J Appl Physiol* **55:** 628-634

Goto M, Terada S, Kato M, Katoh M, Yokozeki T, Tabata I, Shimokawa T (2000) cDNA Cloning and mRNA analysis of PGC-1 in epitrochlearis muscle in swimming-exercised rats. *Biochem Biophys Res Commun* **274:** 350-354

Handschin C (2009) The biology of PGC-1alpha and its therapeutic potential. *Trends Pharmacol Sci* **30:** 322-329

Handschin C, Lin J, Rhee J, Peyer AK, Chin S, Wu PH, Meyer UA, Spiegelman BM (2005) Nutritional regulation of hepatic heme biosynthesis and porphyria through PGC-1alpha. *Cell* **122:** 505-515

Huss JM, Imahashi K, Dufour CR, Weinheimer CJ, Courtois M, Kovacs A, Giguere V, Murphy E, Kelly DP (2007) The nuclear receptor ERRalpha is required for the bioenergetic and functional adaptation to cardiac pressure overload. *Cell Metab* **6:** 25-37

Kabeya Y, Mizushima N, Ueno T, Yamamoto A, Kirisako T, Noda T, Kominami E, Ohsumi Y, Yoshimori T (2000) LC3, a mammalian homologue of yeast Apg8p, is localized in autophagosome membranes after processing. *EMBO J* **19:** 5720-5728

Kelly DP, Scarpulla RC (2004) Transcriptional regulatory circuits controlling mitochondrial biogenesis and function. *Genes Dev* **18:** 357-368

Kitamura T, Feng Y, Kitamura YI, Chua SC, Jr., Xu AW, Barsh GS, Rossetti L, Accili D (2006) Forkhead protein FoxO1 mediates Agrp-dependent effects of leptin on food intake. *Nat Med* **12:** 534-540

Klionsky DJ, Cuervo AM, Seglen PO (2007) Methods for monitoring autophagy from

yeast to human. *Autophagy* **3:** 181-206

Komatsu M, Waguri S, Chiba T, Murata S, Iwata J, Tanida I, Ueno T, Koike M, Uchiyama Y, Kominami E, Tanaka K (2006) Loss of autophagy in the central nervous system causes neurodegeneration in mice. *Nature* **441:** 880-884

Komatsu M, Waguri S, Koike M, Sou Y-S, Ueno T, Hara T, Mizushima N, Iwata J-I, Ezaki J, Murata S, Hamazaki J, Nishito Y, Iemura S-I, Natsume T, Yanagawa T, Uwayama J, Warabi E, Yoshida H, Ishii T, Kobayashi A et al (2007a) Homeostatic levels of p62 control cytoplasmic inclusion body formation in autophagy-deficient mice. *Cell* **131:** 1149-1163

Komatsu M, Wang QJ, Holstein GR, Friedrich VL, Jr., Iwata J, Kominami E, Chait BT, Tanaka K, Yue Z (2007b) Essential role for autophagy protein Atg7 in the maintenance of axonal homeostasis and the prevention of axonal degeneration. *Proc Natl Acad Sci U S A* **104:** 14489-14494

Koo SH, Satoh H, Herzig S, Lee CH, Hedrick S, Kulkarni R, Evans RM, Olefsky J, Montminy M (2004) PGC-1 promotes insulin resistance in liver through PPAR-alpha-dependent induction of TRB-3. *Nat Med* **10:** 530-534

Kuma A, Hatano M, Matsui M, Yamamoto A, Nakaya H, Yoshimori T, Ohsumi Y, Tokuhisa T, Mizushima N (2004) The role of autophagy during the early neonatal starvation period. *Nature* **432:** 1032-1036

Leone TC, Lehman JJ, Finck BN, Schaeffer PJ, Wende AR, Boudina S, Courtois M, Wozniak DF, Sambandam N, Bernal-Mizrachi C, Chen Z, Holloszy JO, Medeiros DM, Schmidt RE, Saffitz JE, Abel ED, Semenkovich CF, Kelly DP (2005) PGC-1alpha deficiency causes multi-system energy metabolic derangements: muscle dysfunction, abnormal weight control and hepatic steatosis. *PLoS Biol* **3:** e101

Li S, Liu C, Li N, Hao T, Han T, Hill DE, Vidal M, Lin JD (2008) Genome-wide coactivation analysis of PGC-1alpha identifies BAF60a as a regulator of hepatic lipid metabolism. *Cell Metab* **8:** 105-117

Lin J, Handschin C, Spiegelman BM (2005a) Metabolic control through the PGC-1 family of transcription coactivators. *Cell Metab* **1:** 361-370

Lin J, Puigserver P, Donovan J, Tarr P, Spiegelman BM (2002a) Peroxisome proliferator-activated receptor gamma coactivator 1beta (PGC-1beta), a novel PGC-1-related transcription coactivator associated with host cell factor. *J Biol Chem* **277:** 1645-1648

Lin J, Wu H, Tarr PT, Zhang CY, Wu Z, Boss O, Michael LF, Puigserver P, Isotani E, Olson EN, Lowell BB, Bassel-Duby R, Spiegelman BM (2002b) Transcriptional co-activator PGC-1 alpha drives the formation of slow-twitch muscle fibres. *Nature* **418:** 797-801

Lin J, Wu PH, Tarr PT, Lindenberg KS, St-Pierre J, Zhang CY, Mootha VK, Jager S, Vianna CR, Reznick RM, Cui L, Manieri M, Donovan MX, Wu Z, Cooper MP, Fan MC, Rohas LM, Zavacki AM, Cinti S, Shulman GI et al (2004) Defects in adaptive energy metabolism with CNS-linked hyperactivity in PGC-1alpha null mice. *Cell* **119:** 121-135

Lin J, Yang R, Tarr PT, Wu PH, Handschin C, Li S, Yang W, Pei L, Uldry M, Tontonoz P, Newgard CB, Spiegelman BM (2005b) Hyperlipidemic effects of dietary saturated fats mediated through PGC-1beta coactivation of SREBP. *Cell* **120:** 261-273

Lin JD (2009) Minireview: the PGC-1 coactivator networks: chromatin-remodeling and mitochondrial energy metabolism. *Mol Endocrinol* **23:** 2-10

Lin MT, Beal MF (2006) Mitochondrial dysfunction and oxidative stress in neurodegenerative diseases. *Nature* **443:** 787-795

Liu C, Li S, Liu T, Borjigin J, Lin JD (2007) Transcriptional coactivator PGC-1alpha integrates the mammalian clock and energy metabolism. *Nature* **447:** 477-481

Liu XB, Jones EG (1996) Localization of alpha type II calcium calmodulin-dependent protein kinase at glutamatergic but not gamma-aminobutyric acid (GABAergic) synapses in thalamus and cerebral cortex. *Proc Natl Acad Sci U S A* **93:** 7332-7336

Mizushima N (2004) Methods for monitoring autophagy. *Int J Biochem Cell Biol* **36:** 2491-2502

Mizushima N, Yamamoto A, Matsui M, Yoshimori T, Ohsumi Y (2004) In vivo analysis of autophagy in response to nutrient starvation using transgenic mice expressing a fluorescent autophagosome marker. *Mol Biol Cell* **15:** 1101-1111

Mootha VK, Lindgren CM, Eriksson KF, Subramanian A, Sihag S, Lehar J, Puigserver P, Carlsson E, Ridderstrale M, Laurila E, Houstis N, Daly MJ, Patterson N, Mesirov JP, Golub TR, Tamayo P, Spiegelman B, Lander ES, Hirschhorn JN, Altshuler D et al (2003) PGC-1alpha-responsive genes involved in oxidative phosphorylation are coordinately downregulated in human diabetes. *Nat Genet* **34:** 267-273

Mortimore GE, Schworer CM (1977) Induction of autophagy by amino-acid deprivation in perfused rat liver. *Nature* **270:** 174-176

Ouimet CC, McGuinness TL, Greengard P (1984) Immunocytochemical localization of calcium/calmodulin-dependent protein kinase II in rat brain. *Proc Natl Acad Sci U S A* **81:** 5604-5608

Patti ME, Butte AJ, Crunkhorn S, Cusi K, Berria R, Kashyap S, Miyazaki Y, Kohane I, Costello M, Saccone R, Landaker EJ, Goldfine AB, Mun E, DeFronzo R, Finlayson J, Kahn CR, Mandarino LJ (2003) Coordinated reduction of genes of oxidative metabolism in humans with insulin resistance and diabetes: Potential role of PGC1 and NRF1. *Proc Natl Acad Sci U S A* **100:** 8466-8471

Puigserver P, Rhee J, Donovan J, Walkey CJ, Yoon JC, Oriente F, Kitamura Y, Altomonte J, Dong H, Accili D, Spiegelman BM (2003) Insulin-regulated hepatic gluconeogenesis through FOXO1-PGC-1alpha interaction. *Nature* **423:** 550-555

Puigserver P, Wu Z, Park CW, Graves R, Wright M, Spiegelman BM (1998) A cold-inducible coactivator of nuclear receptors linked to adaptive thermogenesis. *Cell* **92:** 829-839

Sandoval H, Thiagarajan P, Dasgupta SK, Schumacher A, Prchal JT, Chen M, Wang J (2008) Essential role for Nix in autophagic maturation of erythroid cells. *Nature* **454:** 232-235

Schon EA, Manfredi G (2003) Neuronal degeneration and mitochondrial dysfunction. *J Clin Invest* **111:** 303-312

Simonson DC, DeFronzo RA (1990) Indirect calorimetry: methodological and interpretative problems. *Am J Physiol* **258:** E399-412

Spiegelman BM, Flier JS (2001) Obesity and the regulation of energy balance. *Cell* **104:** 531-543

St-Pierre J, Drori S, Uldry M, Silvaggi JM, Rhee J, Jager S, Handschin C, Zheng K, Lin J, Yang W, Simon DK, Bachoo R, Spiegelman BM (2006) Suppression of reactive oxygen species and neurodegeneration by the PGC-1 transcriptional coactivators. *Cell* **127:** 397-408

Tritos NA, Mastaitis JW, Kokkotou EG, Puigserver P, Spiegelman BM, Maratos-Flier E (2003) Characterization of the peroxisome proliferator activated receptor coactivator 1 alpha (PGC 1alpha) expression in the murine brain. *Brain Res* **961:** 255-260

Tsien JZ, Chen DF, Gerber D, Tom C, Mercer EH, Anderson DJ, Mayford M, Kandel ER, Tonegawa S (1996) Subregion- and cell type-restricted gene knockout in mouse brain. *Cell*

87: 1317-1326

Wu Z, Puigserver P, Andersson U, Zhang C, Adelmant G, Mootha V, Troy A, Cinti S, Lowell B, Scarpulla RC, Spiegelman BM (1999) Mechanisms controlling mitochondrial biogenesis and respiration through the thermogenic coactivator PGC-1. *Cell* **98:** 115-124

Yoon JC, Puigserver P, Chen G, Donovan J, Wu Z, Rhee J, Adelmant G, Stafford J, Kahn CR, Granner DK, Newgard CB, Spiegelman BM (2001) Control of hepatic gluconeogenesis through the transcriptional coactivator PGC-1. *Nature* **413:** 131-138